UNIVERSITY OF OKLAHOMA

GRADUATE COLLEGE

RIPARIAN NITRATE AND PHOSPHATE REMOVAL UNDER FUTURE CLIMATE SCENARIOS

A THESIS

SUBMITTED TO THE GRADUATE FACULTY

in partial fulfillment of the requirements for the

Degree of

MASTER OF SCIENCE

By

JACOB W. CLEMENTS

Norman, Oklahoma

2024

RIPARIAN NITRATE AND PHOSPHATE REMOVAL UNDER FUTURE CLIMATE SCENARIOS

A THESIS APPROVED FOR

THE SCHOOL OF GEOSCIENCES

BY THE COMMITTEE CONSISTING OF

Dr. Caitlin Hodges, Chair

Dr. Andrew S. Elwood Madden

Dr. Kato T. Dee

Acknowledgments

Oh, the places you'll go! Nothing encapsulates starting and completing this thesis more. However, I could not have gotten to this point without so many wonderful people. First, I would like to thank my parents, Cynthia Hall and John Hood, for their constant support, guidance, and love throughout my entire life. While there are too many scenarios to name in a reasonable amount of space, they have been there for everything, and I am eternally thankful to them. No amount of words can ever truly express this sentiment. Next, I would like to thank Dr. Caitlin Hodges for being such an amazing advisor. She has provided amazing advice, guided me through my research, shared plenty of incredibly funny jokes, helped me describe soil profiles in the midst of snow, and encouraged me to push through and overcome myself, just like the Astros pushed through and overcame the naysayers, the Los Angeles Dodgers, and the Philadelphia Phillies to win **two** World Series championships (2021 was a rough year, though. We don't have to talk about it). I would also like to thank my best friends Matthew Marks, Jacob Thomas, Julian Chenin, Mario Ballinas, and Bronson Baker. Y'all have been amazing friends throughout my time as an undergraduate and graduate student, and I have enjoyed every OU Football game, late-night Whataburger run, Halloween party, and so much more. I would also like to give special thanks to Brittany Moehnke, who is not only a great friend but also a fantastic laboratory group member who helped me sample for my research multiple times in sub-freezing temperatures. Finally, I would also like to thank the amazing people of OU Geosciences, who helped ignite my passion for geosciences.

Table of Contents

Abstract

Riparian buffer zones are specially managed zones that lie between agricultural fields and rivers, lakes, or wetlands. They are crucial for protecting water quality, human health, and ecosystem function. Critical ecosystem services of riparian soils include nitrogen removal via denitrification and phosphorus retention through sorption on mineral surfaces. Soil moisture influences these processes by controlling the rate of oxygen diffusion and, therefore, the soil's redox potential. However, soils are predicted to be drier as climate change progresses, and these changes in soil moisture conditions will alter nitrogen cycle dynamics and phosphorus removal in riparian systems. We conducted a lab experiment to investigate potential changes in riparian ecosystem services brought on by climate change. We hypothesized that climate-induced shifts in moisture dynamics would enhance phosphorus removal but hinder denitrification due to increased oxygen diffusion caused by lower soil moisture conditions. We collected forty-eight soil cores (5 cm diameter, 15 cm height), and we collected additional samples for particle size, bulk density, and powder X-ray diffraction (XRD) analyses. We applied soil treatments in a fully factorial design, considering soil texture (sandy loam versus silty clay loam), antecedent soil moisture (field capacity versus drought), water application (flooding versus capillary rise), and pollutant quantity (simulated agricultural runoff versus deionized water). We primarily performed colorimetric assays on soil porewater and soil samples to determine NO_3^- and PO_4^{3-} availability and movement. We also performed elemental analyses to complement the colorimetric assays. Our porewater chemistry and mass balance results showed significant changes in nitrogen cycle dynamics, showing evidence of denitrification, Dissimilatory Nitrate Reduction to Ammonium (DNRA), nitrogen fixation, and nitrogen mineralization. Statistical analyses of the data, primarily through generalized additive mixed-effects models (GAMMs), indicate significant individual and combined positive and negative effects ($p<0.05$) of the simulated treatments on porewater nitrate, ammonium, and phosphate concentrations, along with porewater pH and ARQ (CO_2/O_2). Critically, Moisture Regime and Water Application, our two climate proxies, both individually and collectively, significantly affected porewater nitrate, ammonium, and phosphate concentrations. Nitrate porewater concentrations are higher in decreased moisture conditions and changing precipitation as predicted under future climate scenarios. Phosphate porewater concentrations were lower in sandier soils, drought conditions, and capillary rise water application. However, phosphate leached out of the soil during simulated intense precipitation, highlighting the complexities of how predicted climate scenarios will be partially beneficial for phosphate sorption. XRD analysis revealed a mixed clay mineralogy, including a mixed-layer illite-montmorillonite, IS70R1. Additionally, clay mineralogy in clay-rich soil plays a statistically significant role in moderating the soil nitrogen cycle. Correlated extractable iron and nitrogen data indicate evidence of the Ferrous Wheel Hypothesis, especially in temporarily anoxic soils flooded by intense precipitation. Our research demonstrates that future climate scenarios affect key riparian biogeochemical processes and should be researched more thoroughly as the average worldwide temperature climbs above 1.5°C.

Plain Language Summary

This study focuses on the impact of climate change on the health of areas next to rivers (riparian buffer zones), which are essential for clean water, human health, and the environment. These zones are particularly good at removing nitrogen and phosphorus from the soil - nitrogen through denitrification and phosphorus by sorbing to minerals in the soil. Soil moisture, which climate change will affect, plays a significant role in these processes. We did a lab experiment to determine how changes in climate, especially in moisture, might affect ecosystem functions like denitrification and phosphorus sorption. We used 48 soil samples with two different soil textures and tested them under different conditions, such as differing soil moisture conditions, water application method, and pollutant level. After creating statistical models, we found that changes in moisture due to climate change can significantly alter how nitrogen and phosphorus are processed in the soil. For instance, in sandy soils or during droughts, phosphorus sorbs to soil better, but intense precipitation causes the phosphorus to leach out of the soil. Nitrogen removal was less efficient in drought and heavy rain conditions. Our study shows that climate change will affect how riparian zones handle nitrogen and phosphorus, which affect water quality and soil health.

Keywords: climate change, riparian buffer zone, denitrification, phosphate sorption, iron redox cycling

1. Background

1.01 Statement of Issue

Riparian buffer zones (RBZs) are strips of land bordering streams, lakes, or wetlands that are managed differently than the surrounding landscape. They protect ecosystems from pollutants derived from land management practices, such as overfertilization. These buffers act as filters, removing agricultural pollutants, trace metals, and other harmful materials from runoff. Riparian buffer zones have been thoroughly researched because they effectively preserve surface water quality. However, this filtration process is rarely straightforward. Factors affecting a riparian buffer's performance include soil properties and site hydrology.

Climate change further complicates our understanding of riparian buffer function as weather patterns change in valuable agricultural regions like the Midwestern United States. According to the International Panel on Climate Change (IPCC), near-future climate change predictions indicate that there will be a change in soil moisture content brought on by less frequent but more intense precipitation events, along with an extended dry season (Figure 1). These changes in soil moisture conditions and precipitation are certain to change runoff volume, frequency of runoff interactions with riparian buffers, and the partitioning of runoff into surface and subsurface flow through the riparian buffer (Rounsevell et al., 1999; Várallyay, 2010; Cahoon et al., 2011; IPCC, 2021).

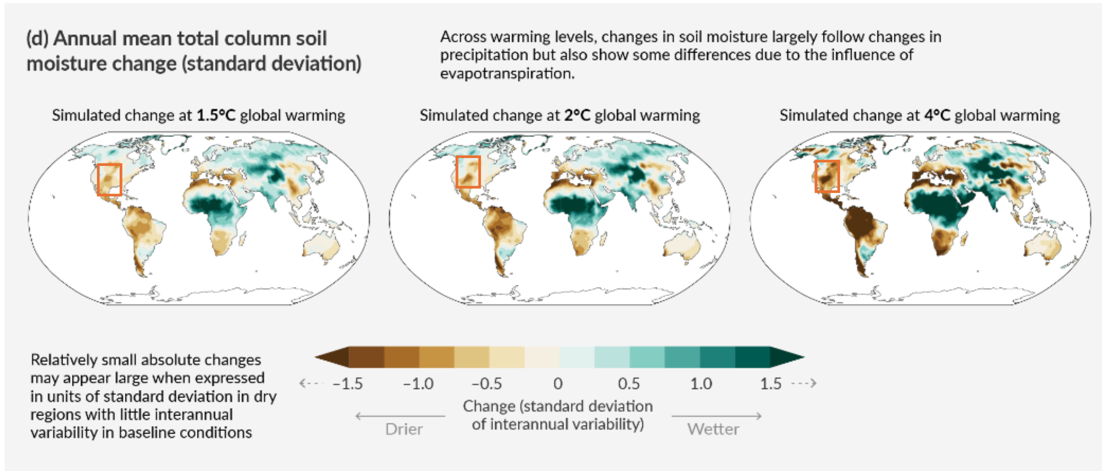

Figure 1: IPCC predicted changes in soil moisture, with the Midwestern United States highlighted (IPCC, 2021).

As soil moisture decreases and precipitation intensity increases, biogeochemical processes that rely on specific soil moisture conditions could be affected. Denitrification, a part of the nitrogen cycle, relies on limited oxygen diffusion through soil pore water brought on by high soil moisture, which could be influenced by drought. Phosphate sorption often relies on redox-active minerals and could change when intense precipitation events temporarily limit oxygen, forcing microbes to reduce Fe(III) to Fe(II). As Fe(III) reduces to Fe(II), the bonds between iron minerals and phosphate will weaken, allowing phosphate to re-enter the solution. These anoxic conditions will allow phosphate to leach out of riparian systems. Climate change, therefore, should affect the nitrogen cycle, phosphorous sorption, and iron redox cycling. Consequently, it is imperative to quantify the impact of these anticipated climate scenarios on riparian buffers to enhance our understanding of these complex processes.

1.02 Nitrogen Cycling in Riparian Buffers

Perhaps no Earth cycle is as important as the N cycle (Figure 2) in governing riparian biogeochemistry. Riparian buffers are often the last line of defense in preventing agricultural runoff from contaminating our limited freshwater supply, and the associated microbially-mediated nitrogen transformations play a crucial role in removing N leached from agricultural fertilizers (Vidon et al., 2018).

Denitrification is a riparian buffer zone's primary and most studied nitrogen removal mechanism (Vidon et al., 2018). Denitrification occurs when soil moisture content is high, with low soil pO_2 and high N availability (Pandey et al., 2020). Complete denitrification, total reduction of NO_3^- to N_2, is favored under specific conditions. First, there must be an anoxic or near-anoxic environment present in the soil due to limited oxygen diffusion. Soil moisture at or above field capacity leads to limited oxygen diffusion and promotes denitrification. Field capacity is where the largest pores in the soil are open, allowing some oxygen diffusion, but the smallest pores are filled with water, allowing denitrification. (Martin et al., 1998; Equations 1-4).

$$1.\ NO_3^- + 2e^- + 2H^+ \rightarrow NO_2^- + H_2O$$

$$2.\ NO_2^- + e^- + 2H^+ \rightarrow NO + H_2O$$

$$3.\ 2NO + 2e^- + 2H^+ \rightarrow N_2O + H_2O$$

$$4.\ N_2O + 2e^- + 2H^+ \rightarrow N_2 + H_2O$$

Equations 1-4: Denitrification reactions

Denitrification can also occur in microsites within soil aggregates when O_2 demand exceeds the diffusion rate. In this case, the physical properties of riparian zones act as primary controls on denitrification. These include clay mineralogy, particle size distribution, and porosity. The absence of free-flowing oxygen allows microbes to complete denitrification, releasing N_2 from the riparian buffer (Burgin & Groffman, 2012). Clay mineralogy can act as a physical control of these anoxic microsites. Notably, smectites, such as montmorillonite, swell during moderate to high moisture and prevent oxygen diffusion into the soil profile, allowing denitrification to proceed to its end reaction. While illites, kaolinites, and chlorites do not swell, they also limit O_2 diffusion when present in high quantities. This occurs because all clay minerals, regardless of expandability, reduce macroporosity and increase microporosity due to their small particle size (Keiluweit et al., 2018).

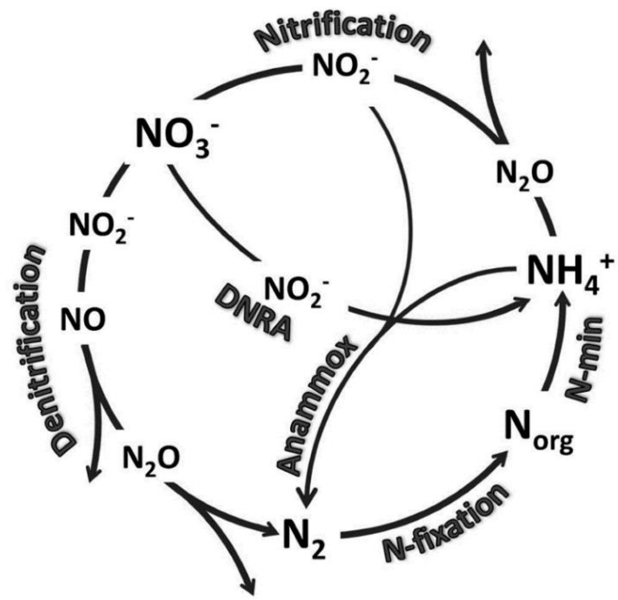

Figure 2: Nitrogen Cycle (Baas et al., 2019)

However, the soil moisture changes caused by climate change threaten the nitrogen cycle's overall function in riparian systems. When soil moisture decreases due to anticipated climate change, the water table lowers, and oxygen can diffuse further into the soil profile. Oxygen can diffuse further into the soil profile because the diffusion rate is orders of magnitude higher in free air than in water. Increased oxygen diffusion leads to a delayed switch in microbe terminal electron acceptors since the preferred terminal electron acceptor, free oxygen, is still present in significant quantities (Cahoon et al., 2011; Burgin & Groffman, 2012; Keiluweit et al., 2018). Under the climate scenarios the IPCC (2021) put forth, decreased soil moisture should impact denitrification and could lead to N_2O being released instead of N_2. N_2O is a potent greenhouse gas and is the result of incomplete denitrification. Oxygen is a more favorable terminal electron acceptor for microbes due to its higher redox potential (E_h) than nitrous oxide. This concept is further explored in the leaky pipe model (Davidson, 1991). When nitrate is denitrified, the ideal goal is to reduce it to N_2. However, pipes have leaks. Leaks in the denitrification pipeline represent incomplete denitrification due to increased oxygen diffusion into the soil profile. In these scenarios, other N species, including nitric oxide (NO) and nitrous oxide (N_2O), are released. So, when soil moisture decreases and oxygen can diffuse further down into the soil, heterotrophs will not use N_2O as a terminal electron acceptor but instead use oxygen. Therefore, N_2O will be the final product of denitrification in increased oxygen conditions, not N_2 (Burgin & Groffman, 2012; Keiluweit et al., 2018).

Furthermore, other processes compete and coexist with denitrification depending on the limiting variables. One of these processes is dissimilatory nitrate reduction to ammonium (DNRA). Dissimilatory nitrate reduction to ammonium competes with and even outcompetes denitrification in tropical soils, limited anaerobic subtropical soils, and wetlands where nitrogen is the limiting variable. Dissimilatory nitrate reduction to ammonium is also influenced by Fe(II) concentrations, total sulfide, soil pH, the NO_2^-/NO_3^- ratio, redox potential, and clay mineralogy (Davis et al., 2008; Fridel et al., 2018; Pandey et al., 2020). By reducing nitrate to bioavailable ammonium, DNRA is a shortcut in the nitrogen cycle and avoids denitrification, fixation, and mineralization (Figure 2, Equation 5). While DNRA has only been studied in limited environments, it is thought to play a critical role in riparian nitrogen cycling (Davis et al., 2008; Fridel et al., 2018; Pandey et al., 2020).

$$NO_3^- + 8e^- + 10H^+ \rightarrow 2NH_4^+ + 3H_2O$$

Equation 5: Dissimilatory Nitrate Reduction to Ammonium (DNRA)

Dissimilatory Nitrate Reduction to Ammonium is also particularly challenging to measure, even in the environments where it is proven to exist. Commonly, measuring DNRA involves measuring ammonium and nitrate pore water concentrations regularly and assessing whether there is a negative correlation between nitrate and ammonium. Potassium chloride (KCl) extractions are also valuable for determining the total change in nitrate and ammonium over a set period. KCl extractions work by using the relatively high concentrations of K^+ ions in solution to displace the NH_4^+ and NO_3^- present in an ion exchange reaction. After supernatant filtration, the K^+ ions remain bonded to the soil particles, and the NH_4^+ and NO_3^- ions are extracted in solution. Using the $^{15}N/^{14}N$ ratio to track the nitrogen cycle through these environments is also possible. Soils are typically depleted in ^{15}N, so by enriching test soils and allowing ^{15}N to replace ^{14}N, it is possible to use an isotope ratio mass spectrometer (IRMS) to “track the nitrogen” (Silver et al., 2001; Pandey et al., 2020).

Fixed ammonium also plays a critical role in the nitrogen cycle in riparian soils. Previous research indicates that some clay minerals act as ammonium hubs, particularly illites and vermiculites. These clay minerals fix and exchange ammonium to help regulate this portion of the nitrogen cycle. While each type of clay mineral fixes different amounts of ammonium, it is likely that soils with high clay content act as ammonium reservoirs and consequently reduce porewater NH_4^+ concentrations (Doram & Evans, 1983)

1.03 Phosphate Sorption in Riparian Buffer Systems

However, the anoxic conditions favoring denitrification and DNRA are a double-edged sword. Phosphate, a typical agricultural fertilizer, requires iron oxides and, consequently, available oxygen to be removed from agricultural runoff. In soils with appreciable concentrations of Fe oxides, phosphate adsorbs onto these oxides and is immobilized. However, this process relies on those iron oxides remaining oxidized. When Fe(III) reduces to Fe(II), the adsorbed PO_4^{+3} can enter the solution, as Fe(II) is water-soluble. Soils at field capacity are just as acceptable for phosphate sorption as for denitrification because the open pores in the soil that do not retain water through capillary action allow enough oxygen to diffuse and preserve the iron oxides that serve as sorption sites for PO_4^{-3} (Pote et al., 1996; Sharpley & Smith, 1996; Sharpley & Smith, 2009; Andersson et al., 2013; Asomaning, 2020).

However, future climate scenarios could threaten this balance. During drought conditions, oxygen should diffuse further into the soil profile since the water table will be lower and diffusion in air is orders of magnitude higher than in water. Therefore, it stands to reason that drought conditions will increase phosphate sorption in riparian soils since oxygen will preserve the Fe oxide sorption sites. However, the less frequent but more intense precipitation events predicted by the IPCC (IPCC, 2021) could significantly impact phosphate concentrations in riparian buffers. While the increased length of drought periods could allow for more phosphate sorption, more intense precipitation events could overwhelm the drought-stricken soils. Water could quickly fill all the available pore space within these soils and cause temporary anoxic conditions. Under these temporary conditions, iron could be reduced, weakening the bonds with phosphate and causing the phosphate to leach out of the soil. Therefore, it is essential to quantify how intense precipitation events impact phosphate sorption in riparian soils.

1.04 Sulfur Dynamics in Riparian Soils

The sulfur cycle (Figure 3) plays a significant role in controlling riparian biogeochemistry and is inextricably linked with climate, nitrogen, phosphorus, and iron in soils. Sulfur mineralization/immobilization and adsorption/desorption depend heavily on the quantity of iron and aluminum oxides, soil pH, organic matter composition, and clay mineralogy (David et al., 1983). Critically, sulfur and iron are linked, particularly in anaerobic soils. In these anaerobic environments, sulfur is typically reduced. Reduced sulfur can abiotically dissolve iron in a reductive dissolution reaction. Therefore, in these anaerobic environments, iron-sulfide minerals undergo multiple transformations (Equations 6-8, Figure 4).

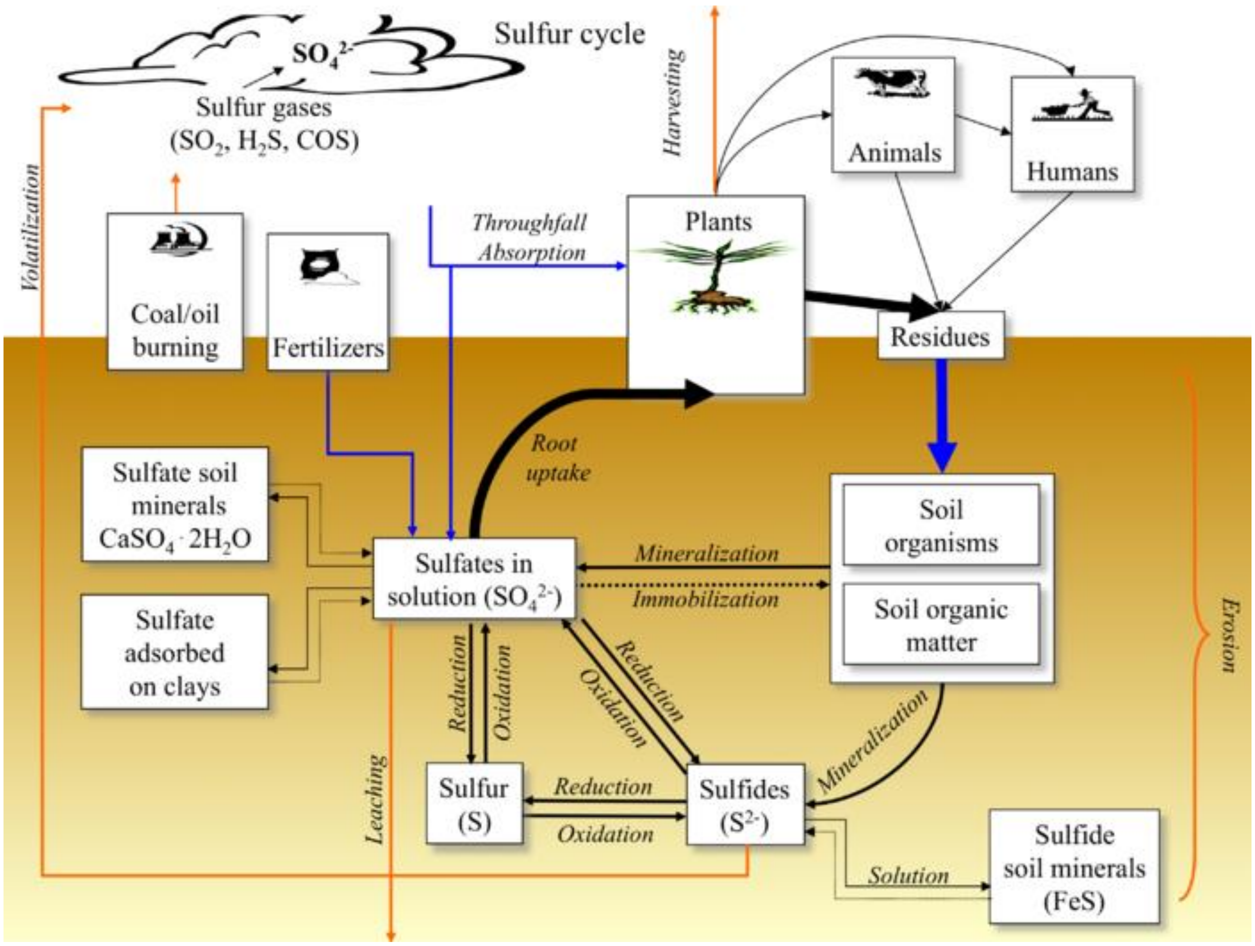

Figure 3: Sulfur Cycle (University of British Columbia, 2023)

6. $HS^- + 2O_2 \rightarrow H^+ + SO_4^{2-}$

7. $2HS^- + FeOOH + H^+ \rightarrow S_0 + FeS + H_2O$

8. $Fe^{2+} + HS^- \leftrightarrows FeS + H^+$

Equations 6-8: Iron-Sulfur Reactions

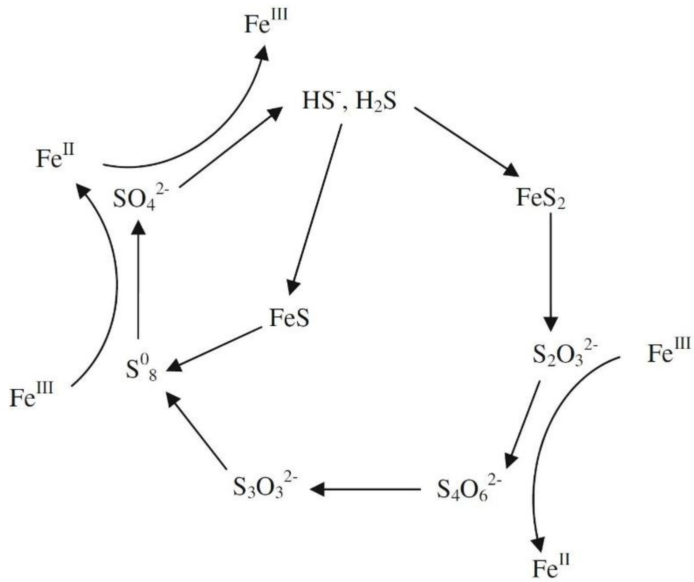

Figure 4: Iron and Sulfur Interactions (Li et al., 2012)

Sulfur also interacts with carbon in riparian buffers. Bioavailable sulfur and organic carbon are frequently linked outside arid environments due to plant uptake of both organic nutrients (Luo et al., 2015). In soils, organic sulfur species are typically treated similarly to bioavailable sulfur since organic sulfur can make up 99% of the S in a system and is more assimilable than inorganic sulfur for plants. Sulfate can be mineralized into ester sulfate or immobilized into carbon-bonded S. However, ester sulfates are typically less stable than carbon-bonded S and usually comprise the bioavailable portion (Figure 5, Scherer, 2009).

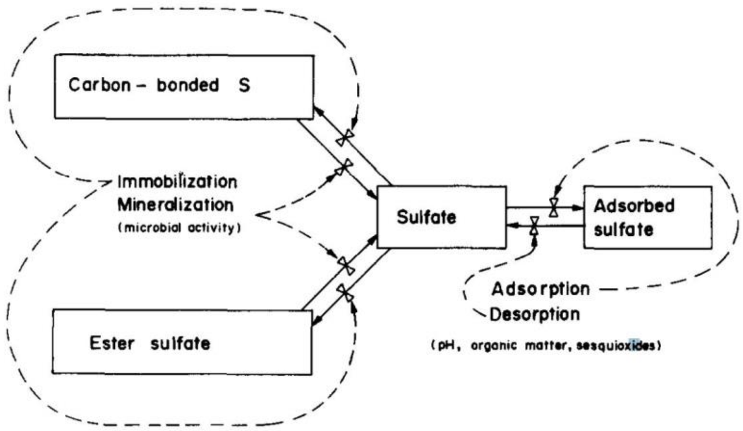

Figure 5: Inorganic and Organic Sulfate Flux (David et al., 1983)

Furthermore, the sulfur cycle in riparian buffers is affected by climate, soil texture, soil pH, and clay mineralogy. Sulfate in the soil leaches out during intense precipitation. The loss of sulfate is more significant in coarser-grained soils, such as sandy loam. Finer particle soils inhibit fluid movement through the soil, preventing sudden, high quantities of water from reaching the sulfate. This effect works with the clay mineralogy of the soil. Depending on the number of edge sites on the clay mineral, sulfur species can adsorb onto the clay minerals. Sulfur preferentially adsorbs onto kaolinites, illites, and smectites (Scherer, 2009). This further prevents sulfur loss in clay-rich soils; the inverse is true for sandier soils. Sulfur adsorption is also dependent on soil pH. Sulfur adsorption is highest at a soil pH of 3, and then as the soil pH increases to a pH greater than 6.5, adsorption reaches zero. This effect occurs because OH^- and SO_4^{2-} compete at this pH range, and OH^- outcompetes sulfate for bonding sites. Additionally, phosphorus compounds are more soluble at this pH range and compete for the edge sites on clays (Scherer, 2009).

1.05 Soil and Pore Water pH

Soil and pore water pH significantly control mineral stability and soil biogeochemical processes. Depending on the pH of both the soil and its pore water, a bevy of soil processes are affected, including, but not limited to, denitrification, phosphorous availability, heavy metal precipitation, organic matter mineralization, and clay mineral stability (Devau et al., 2009; Neina, 2019; Figures 6, 7).

Figure 6: Biogeochemical processes and soil characteristics regulated by soil pH (adapted from (Devau et al., 2009; Neina, 2019)

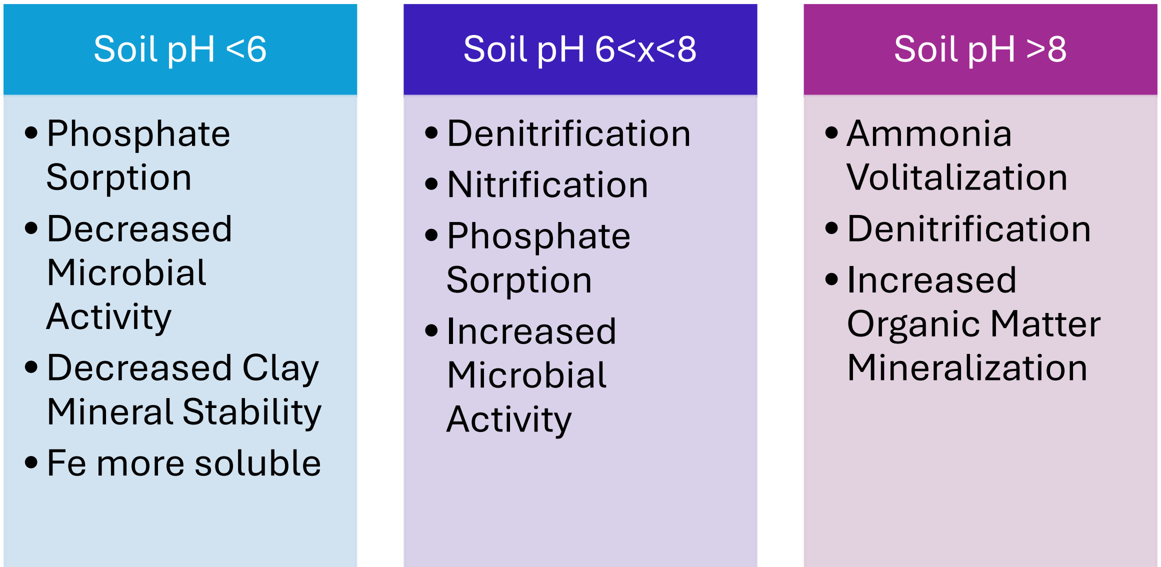

Figure 7: Biogeochemical processes and soil characteristics regulated by soil pH divided by soil pH ranges (adapted from (Devau et al., 2009; Neina, 2019)

Some of the most relevant biogeochemical processes to this work influenced by soil pH are denitrification and nitrification, two essential components of the nitrogen cycle. Other processes, such as ammonia volatilization, require a basic soil pH (>8) and are outside this work's scope. When the soil pH is below 7, nitrous oxide is the most likely product of denitrification, whereas dinitrogen is the more likely product of denitrification at a soil pH above 8. As soil pH decreases from that ideal range, the nitrous oxide reductase enzyme cannot convert the nitrous oxide into dinitrogen, and this microbial population is reduced in size (Neina, 2019). Critically, soil pH also affects nitrification, converting ammonium to nitrate. A soil pH of 6 to 8 is the ideal zone for nitrification, with the nitrification rate decreasing outside of this ideal zone (Neina, 2019).

Soil pH also influences organic matter stability. As mentioned earlier, pH affects microbial populations and, therefore, rates of biogeochemical processes, including the oxidation of soil organic matter. Subsequently, organic carbon, nitrogen, sulfur, and phosphorous are susceptible to changes in soil pH. At a higher soil pH, the rate of organic matter mineralization is higher because the bonds between the organic matter and clay minerals are easier to break (Curtin et al., 1998). This leads to additional inputs of N into the nitrogen cycle and has vast effects on other nutrient availability for plants.

Similar to organic phosphorus, the availability of inorganic phosphorus is controlled by soil pH. Geochemical modeling has shown that different clay minerals contribute to phosphorus adsorption between a soil pH of 5.8 and a soil pH of 7.4. As soil pH increases, the amount of phosphorus sorbed onto illite increases. This also occurs in kaolinite, but to a lesser degree due to kaolinite's lower cation exchange capacity when compared to illite (Devau et al., 2009).

1.06 Iron Redox Reactions in Riparian Systems

Iron redox cycling is a necessary biogeochemical process influencing nutrient cycling, soil carbon, and soil nitrogen cycles. Iron compounds are less desirable terminal electron acceptors and have a lower Gibbs Free Energy than nitrate and manganese compounds. The availability of free oxygen in soil is crucial to moderating iron redox cycling. When aerobic conditions exist in the soil, iron is more likely than not in the form of oxidized Fe(III). However, under anaerobic conditions, microbes must switch to using alternate terminal electron acceptors such as Fe(III)OH (Patrick & Jugsujinda, 1992; Rissmann, 2011; Hodges et al., 2019). Additionally, clay minerals, particularly illites and smectites, can act as terminal electron acceptor hubs and mediate iron redox processes (Shelobolina et al., 2012).

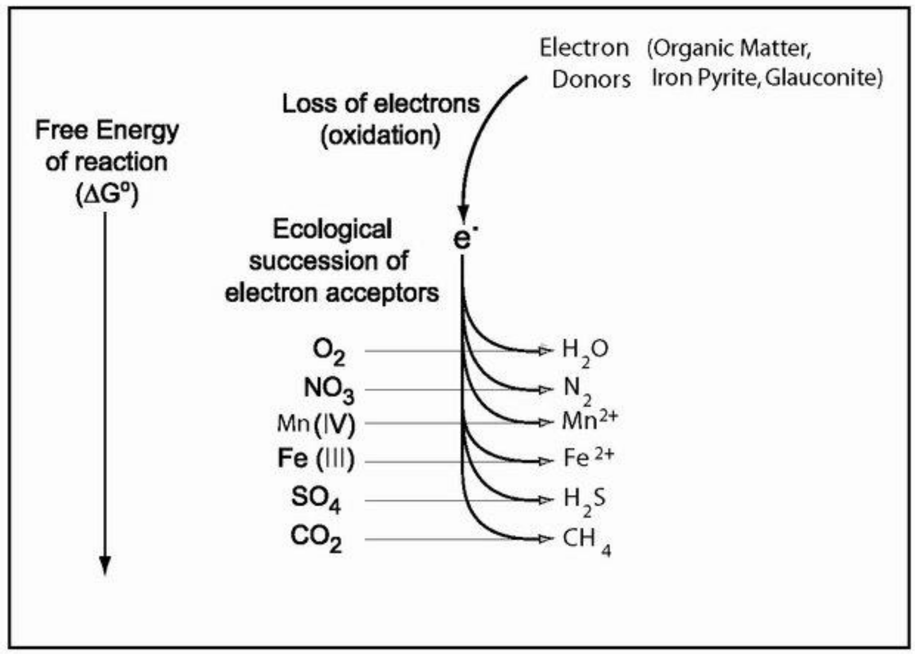

Figure 8: Terminal Electron Acceptors in Soil and Groundwater (Rissmann, 2011)

Iron redox reactions are linked with other biogeochemical processes. High concentrations of Fe(II) have been linked to fueling DNRA in tropical soils through chemoautotrophic processes by reducing the nitrite to ammonium (Pandey et al., 2020). This correlation exists because higher Fe(II) concentrations typically indicate anoxic environments where DNRA activity is favored. Previous research has also found positive correlations between DNRA and Fe(II) concentrations (Hou et al., 2012; Yin et al., 2014; Pandey et al., 2020).

1.07 Powder X-Ray Diffraction (XRD)

Powder X-ray diffraction (XRD) is a powerful tool in Earth materials characterization. It has been a stalwart of geosciences for the past century, helping geoscientists characterize countless rock and soil samples. As regularly ordered, three-dimensional objects, minerals refract light differently based on their composition and structure. Therefore, we can discern information about a sample's mineralogy when X-ray waves are diffracted (Chauhan & Chauhan, 2014; Bunaciu et al., 2015).

However, XRD analysis of soil samples typically varies from XRD analysis of rock samples. Rock samples typically involve whole-rock random and oriented, clay-sized mounts to determine the complete mineralogy of the sample. Soil scientists are often most focused on the mineralogy of the clay-sized fraction, and so typically, many studies into soil mineralogy using XRD only use oriented mounts. Typical treatments for the oriented mounts include air-drying, hydration with ethylene glycol, and heat treatment at 550°C. Combining these treatments forms an analysis, providing information regarding clay mineralogy and quantity, including mixed-layer clay minerals. However, many procedures, treatments, and sample preparation methods exist to analyze the clay-sized fraction in soils, leading to significant ambiguity (Kahle et al., 2002).

1.08 Apparent Respiratory Quotient (ARQ)

The apparent respiratory quotient (ARQ) is critical in measuring soil microbial activity and respiration. The ARQ, when measured in a closed system, is defined as:

$$ARQ=(CO_{2\ measured}\%-CO_{2\ atm}\%)/(20.95\%-O_{2\ measured}\%)$$

Equation 9: Headspace ARQ (adapted from Hodges et al., 2019)

When measuring soil pore gas concentrations directly, ARQ often needs a correction factor to account for the difference in diffusion rates between O_2 and CO_2. However, no diffusion correction is needed when calculating ARQ from headspace gases due to the nature of the closed system. Under typical conditions, the ARQ should be approximately one since oxygen is continuously resupplied and carbon dioxide is continually respired from the system (Angert et al., 2015). Frequently, the ARQ deviates significantly from the ideal conditions, and these changes inform us of critical soil biogeochemical processes in real time. Multiple biogeochemical processes change the ARQ, including anaerobic respiration and oxidation reactions (Hodges et al., 2019a). When the ARQ is above 1, the soil undergoes processes such as anaerobic respiration, organic acid mineralization, and precipitation of carbonates. Additionally, more CO_2 is produced than expected. An ARQ below 1 indicates a bevy of processes, such as carbonate weathering and dissolution of CO_2 gas into soil water. When the ARQ is less than 1, less CO_2 is produced than expected, or more O_2 is consumed than expected (Hodges et al., 2019). Under different anticipated climate regimes, the ARQ can be used to determine what biogeochemical processes are occurring throughout the soil profile and at what rates.

1.09 The Ferrous Wheel Hypothesis

The Ferrous Wheel is a controversial topic in soil biogeochemistry that couples the nitrogen cycle to iron redox reactions. The Ferrous Wheel Hypothesis postulates that ferrous iron facilitates the abiotic reduction of nitrate to nitrite in forest soils. Nitrite then reacts with dissolved organic matter (DOM) in soils through nitration and nitrosation to form dissolved organic nitrogen (DON) (Davidson et al., 2003; Matus et al., 2019). While it is well established in soil biogeochemistry that compounds higher on the redox ladder can facilitate the reduction of compounds lower on the redox ladder, especially with iron and sulfur, these redox reactions are usually biotically mediated.

Previous research has taken issue with the proposed abiotic nature of the ferrous wheel as well as the existence of the ferrous wheel itself (Colman et al., 2008; Schmidt & Matzner, 2009). Proponents of the Ferrous Wheel Hypothesis argue that using ^{15}N can track N incorporation into the DOM with maximum incorporation of 25% of the original pool of ^{15}N (Matus et al., 2019). While it is far outside the scope of this work to consider the abiotic versus the biotic nature of the ferrous wheel, we do argue that it should be possible to provide evidence for nitrate reduction coupled with Fe oxidation by tracking the changes in nitrate, Fe(II), and organic nitrogen.

1.10 Research Purpose

With this study, we seek to quantify how riparian buffer zones will react to future climate scenarios. Riparian buffer zones and their associated ecosystem services are vital to terrestrial and freshwater ecosystems. Therefore, it is essential to understand how predicted climate scenarios will impact riparian biogeochemical cycles. The questions our study attempts to answer are:

1. How does anticipated climate change impact denitrification in riparian buffers?
2. How are phosphorous sorption and iron redox cycling in riparian buffers affected by anticipated climate change?

We hypothesize that riparian soils experiencing drought and intense precipitation will be worse at retaining N due to increased oxygen diffusion into the soil. However, these same soils under the predicted soil moisture conditions could help retain P since oxygen will not be a limiting factor. However, the intense precipitation events should cause P to desorb and leach out of the riparian soils. This work will fill critical knowledge gaps in riparian and wetlands research worldwide by answering these research questions. We also hope to provide new information on riparian biogeochemistry for land managers, biogeochemical modelers, soil health advocates, nanogeochemists interested in clay-sized particles in soils, aqueous geochemists interested in nitrogen cycling, ferrous wheel enthusiasts, and other stakeholders interested in riparian buffers for commercial or sustenance agriculture.

2. Methods

2.01 Site and Soil Characterization

The selected site is in the Lexington Wildlife Management Area (WMA) centered around the Helsel Creek riparian buffer zone at 35°3'9.08"N, 97°10'34.69"W (Figure 9a). The site has floodplain soils, with the Port soil series mapped on both sides of the creek. The Port soil series is a Mollisol, with diagnostic pedogenic carbonates in the B horizon, and a Permian-age sandstone parent material, the Garber Sandstone. The Port soil series taxonomic class is a fine-silty, mixed, superactive Cumulic Haplustoll (National Cooperative Soil Survey, 2023). We collected soil cores (Figure 9b) from a sandy loam (SaLo) (orange circle) and a silty clay loam (SiClLo) (blue circle) (Figure 9a).

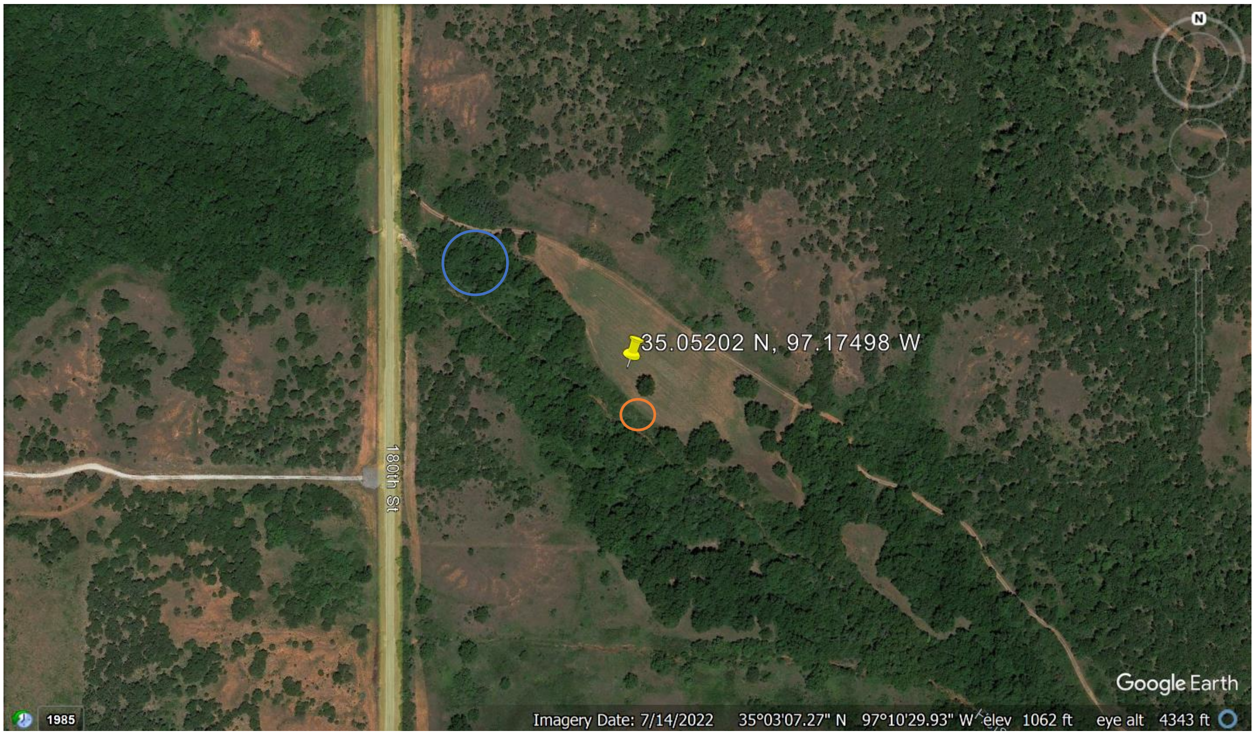

Figure 9a: Google Earth image of the study area within the Lexington WMA.

Figure 9b: Soil core collection in the Silty Clay Loam Riparian Buffer Zone

To quantify the clay mineralogy of the Port soil series, we selected the sample with the highest clay content in the Silty Clay Loam soil profile. Therefore, we conducted a micropipette soil particle size analysis on all horizons in the Silty Clay Loam profile following Miller & Miller (1987). We prepared the samples using a 7:1 mixture of 0.05 M sodium hexametaphosphate and the less than two-millimeter soil fraction. After two hours of shaking and another two hours of settling, only the clay-sized fraction remained suspended at the top of the mixture. We used a pipette to collect a standard volume of 2.5 mL of the suspended clay fraction from each replicate. Each suspended clay sample was then placed in an aluminum pan for drying. We separated the sand from the silt and the remaining clay fractions using a 53-micron sieve. After sieving, we collected and dried the sand and clay samples overnight at $105\ ^{\circ}C$ and weighed them to determine each horizon's total clay, silt, and sand content (Miller & Miller, 1987).

After identifying the horizon with the highest clay content, we made an oriented mount for powder X-ray diffraction (XRD) analysis. We tried various methods, including the standard sonic dismembration, but were unsuccessful in dispersing clay-rich microaggregates. These microaggregates caused further problems when making a filter peel oriented XRD mount since the clays would not lay flat on the slide.

Here, we developed a modified oriented mount preparation method that reduces time and effort for soil mineralogists interested in using XRD for site characterization. Building off the Miller & Miller (1987) soil particle size procedure, we identified clay-rich horizons of interest and made three extra replicates. After treating these samples identically to the particle size samples through settling, we pipetted 2.5 mL of the clay fraction and combined the replicates. After diluting the clay fraction with deionized water to a 10:1 water-to-clay ratio, we vacuum filtered the sample using a 0.2-micron filter to collect the clay-sized minerals. After filtering, we hydrated the clays with two milliliters of 1 M $CaCl_2$ solution. Then, we applied the oriented mount slide to the filter and dried the clay in a 100°C oven for 60 to 90 seconds. Finally, we peeled off the dried filter paper, creating an oriented mount for XRD analysis.

We performed XRD analyses of the oriented mounts using a Rigaku Ultima IV diffractometer. The Rigaku Ultima IV diffractometer uses Cu-K-alpha radiation (40 kV, 44 mA) and a Bragg-Brentano detector. We ran the samples sequentially in air-dried, ethylene glycol, and 550°C heat-treated states. The scanning range for the oriented mount spanned two to thirty degrees 2Θ with a fixed increment of 0.2° per step. Data analysis was completed using Jade MDI Pro with the ICDD (International Centre for Diffraction Data) PDF4+ database (ICDD, 2023).

We also measured soil pH and bulk density of the sandy loam and silty clay loam soil cores. We made a 1:1 solution of two-millimeter sieved soil and 0.01 M $CaCl_2$ consistent with previously established procedures (e.g., Eckert & Sims, 2009). The higher ionic strength of dilute $CaCl_2$ compared to deionized water increases the reproducibility of soil pH measurements, which are otherwise sensitive to differences in the electrical conductivity of the soil solution. After making the slurry, we analyzed the soil pH with the ThermoFisher Orion Star A211 pH probe. Additionally, we collected soil bulk density samples by collecting three replicate cores, five centimeters in diameter and fifteen centimeters in height, using a slide hammer. We weighed the soil cores after drying at 40°C for 30 days to find the average bulk density.

2.02 Incubation Setup

We collected forty-eight soil cores from the Helsel Creek riparian zone to test our research questions regarding the effects of climate change on riparian buffers. Half of these cores have a sandy loam (SaLo) soil texture, while the other half have a silty clay loam (SiClLo) soil texture. The cores were soil stored in PVC liners fifteen centimeters long and five centimeters in diameter, with 3 centimeters left between the top and the soil, allowing headspace gases to accumulate. Each core was capped on both ends. After drying the cores in the oven for thirty days at 40°C, the soil cores were water-free since they maintained a constant mass for the last five days of drying. We applied treatments simulating different moisture regimes, water application points, and water types in a fully factorial design between the two soil textures. Field Capacity represents the soil moisture regime under normal conditions, while Drought represents the soil moisture regime predicted under future climate scenarios. We maintained the mass of Field Capacity cores by adding DI water weekly, while the Drought cores had no water added throughout the experiment. Similarly, we used two water application points to simulate ideal and predicted climate conditions. Allowing water uptake from the bottom of the core simulated Capillary Rise, the ideal water application method. Applying water from the top resulted in Flooding, which is predicted under future climate scenarios. Finally, we used two different water types to simulate input from agricultural systems. We used a simulated agricultural runoff, DI water mixed with NO_3 and PO_4 fertilizers, to simulate input from an agricultural system. We used DI water to simulate ideal conditions without input from an agricultural system. The agricultural runoff has a concentration of 7.23 mmol/L NO_3 and 0.35 mg/L PO_4, consistent with previous core experiments (Tindall et al., 1996) This fully factorial design is shown graphically in

Figure 10, with the replicates for each treatment removed. The abbreviations for each treatment are shown in Supplemental Material T-6.

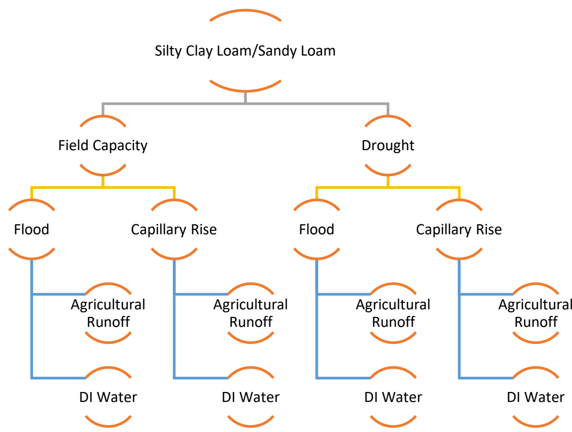

Figure 10: Experimental design specified to treatment level.

We applied 15 mL of agricultural runoff or DI water to each flooding treatment and 10 mL of agricultural runoff or DI water to each capillary rise treatment weekly. This amount is far less than the water needed to maintain field capacity conditions, about 30 mL/week, but enough to ensure we would get a representative porewater sample from each core. One day after the water application, we used rhizons to extract the pore water from each core. We placed the rhizons at the midpoint of the soil in the cores to allow time for the applied water to interact with the soil through flooding and capillary rise. The rhizons have a 0.15-micron filter built in so no sediment can contaminate the pore water. Using vacuum tubes, we collected the pore water from the cores one day after application (Figure 11).

Figure 11: Core experiment setup featuring soil cores, rhizons, and vacuum collection tubes.

2.03 Measurements and Analyses During Incubation

After collecting pore water, we used colorimetric analysis to determine the amount of nitrate, phosphate, and ammonium in the pore water. We used a ThermoFisher MultiSkan SkyHigh microplate UV-Vis analyzer with wavelength scanning capability for these colorimetric analyses. We created microplates based on established colorimetric analysis procedures for nitrate (Doane & Horwath, 2003), phosphate (McConnel, 2020), and ammonium (Ringuet et al., 2011). Additionally, we measured pore water pH directly using the ThermoFisher Orion Star A211 pH probe.

We measured the headspace O_2 and CO_2 and calculated the ARQ weekly to complement our pore water data during the core experiments. At the beginning of the experiment, we installed grey, leakproof septa at the top of each core lid. Before sampling the headspace gases, we capped the cores for twenty-four hours before sampling. We performed O_2 measurements using the Quantek 901 oxygen meter and CO_2 measurements with a LICOR 7815 Trace Gas Analyzer (Hodges et al., 2019b). After measuring these headspace values for each replicate, we combined them into a treatment-level average. We normalized both values to their respective laboratory atmospheric normal values using Equation 14 to calculate the ARQ.

$$ARQ=(CO_{2\ measured}-0.025)/(20.95-O_{2\ measured})$$

Equation 10: Headspace ARQ (Lab Ambient)

2.04 Post-Incubation Measurements and Analyses

Following the conclusion of the core experiments, we determined the amount of nitrogen in each main pool in the nitrogen cycle, including total nitrogen, bioavailable ammonium, and bioavailable nitrate, in the treatment and control samples. We used the Elementar EL Vario Cube to determine each treatment and control sample's total carbon, nitrogen, and sulfur concentrations (Xu et al., 2017).

We also utilized two-molar potassium chloride (2M KCl) extractions to determine the concentration of bioavailable ammonium and nitrate in the treatment and control samples (Keeney & Nelson, 1982). Potassium chloride extractions allow analysis of the bioavailable nitrate and ammonium by displacing nitrate and ammonium with potassium. After the extraction of nitrate and ammonium and supernatant filtration, we used the same colorimetric analyses for the pore water to determine the initial and final nitrate and ammonium concentrations. Integrating these data with the elemental and pore water analyses allows us to determine which nitrogen pools were impacted by the treatments and how these impacts affected the final pore water nitrate concentrations throughout the pore water analyses. Furthermore, we performed a nitrogen cycle mass balance to determine how much nitrogen, if any, each treatment lost. To do this, we used our pre-and post-treatment total N values, the amount of NH_4^+ removed from the system, and the amount of NO_3^- fertilizer we added. We calculated the change in each N pool by using the formula below and converting all N measurements to grams (Formula 11). This involved multiplying the percentage values of total N by the average pre-treatment mass of the cores. Then, we subtracted the pre-treatment N mass from the post-treatment N mass and then subtracted the total amount of NO_3^- that we added during the experiment. Since we did not add ammonium to the system, we did not include it in our calculations.

$$\text{Total N} = NO_3 + NH_4 + SON$$

Formula 11: N Mass Balance Calculation

To test the iron redox reactions occurring in these soils, we used the initial 0.5M HCl-extractable Fe (II) and Fe (III) in the Silty Clay Loam and Sandy Loam soils using the ferrozine-based microplate method (Huang & Hall, 2017). We used the same approach to test the final 0.5M HCl-extractable Fe (II) and Fe (III) content in each core following the conclusion of the denitrification and phosphorous sorption experiments and averaging each replicate to produce a treatment level final average.

2.05 Data Analysis and Figure Creation

Data collection was exclusively conducted through Microsoft Excel v2307. We collected historical imagery through Google Earth (v7.3.6, Alphabet 2023). We used R Statistical Software (v4.1.2; R Core Team 2022) for statistical analyses. Specifically, we used the R mgcv package to create the generalized additive mixed effects models (GAMMs) (v1.9-0, Wood, 2023). We used generalized additive mixed-effects models over the more common generalized linear mixed-effects models (GLMMs) found in the R package nlme (v3.1-163, Pinheiro et al., 2023) and other packages due to the conditional linearity and smoothing terms that GAMMs provide. Utilizing these abilities found in GAMMs enabled more robust and better-fitting models for our continuous time-series data. We verified the accuracy of these models using AIC scores, deviance explained (R^2 for GAMMs), Q-Q plots, plotting the Histogram of Residuals, and plotting the Residuals versus the Fitted Values to examine for heteroscedasticity. We also performed posthoc Wald tests on our GAMMs using the functions found in the R mgcv package and clustered statistically similar comparisons using dendrogram plots found in ggplot2. We also generated boxplots showing the individual and combined treatment effects on porewater chemistry and ARQ measurements using ggplot2. We also examined data correlations with k-means clustering and correlation coefficients using the R dplyr package (v1.1.3, Wickham et al., 2023). For significant results from the models, we used $\alpha=0.1$ due to the various treatments and relatively low number of replicates. We used Microsoft Word v2307 to generate the soil profile tables and other data tables in this work. Additionally, we used the soiltexture R package to create the soil texture triangles (v1.5.1, Moeys et al., 2018). To generate and analyze multiple nonparametric decision trees, we used the R package randomForest (v4.7-1.1, Liaw, 2022). We used Jade MDI Pro to organize and plot all Powder XRD traces onto one figure (v6.5, ICDD 2023). Furthermore, we generated nitrate, ammonium, phosphate, pore water pH, and ARQ plots in Microsoft Excel v2307. We generated our decision tree visualizations, k-means clustering, correlation figures, and model graphs in R using ggplot2 (v3.4.4, Wickham et al., 2023). Finally, we generated our boxplots using the tidyverse R package (v2.0.0, Wickham et al., 2023).

3. Results

3.01 Field Site Characterization

3.01.1 Pedology of Helsel Creek Riparian Buffer Zone

We identified that one of the mapped units (NRCS, 2023), the Port soil series, was the primary soil series in the Helsel Creek riparian buffer zone. However, there were notable differences between the two soil profiles. The silty clay loam profile had significant clayey textures in the A, Bw1, and Bw2 horizons (Figure 12). We observed ferro-manganese nodules in the Ab horizon.

Horizon	Depth	Color	Structure	Field Texture
A	0-7 cm	7.5 YR 3/4	Subangular Blocky	Clay Loam
Bw1	7-26 cm	2.5 YR 4/8	Subangular Blocky	Clay Loam
Bw2	26-34 cm	2.5 YR 5/8	Subangular Blocky	Clay Loam
C	34-81 cm	2.5 YR 4/8	Single Grain/Structureless	Sandy Loam
Ab	81-96 cm	10 YR 2/2	Subangular Blocky	Sandy Clay Loam
2C	96+ cm	2.5 YR 4/6	Single Grain/Structureless	Loamy Sand

Figure 12: Pedological information of the Helsel Creek Riparian Buffer Silty Clay Loam (SiClLo) Topsoil Profile

The sandy loam profile has more sand in the upper horizons, with accompanying granular structures. Additionally, redoximorphic features are present in the Btk1, Btk2, and C horizons, namely manganese nodules (Figure 13).

Horizon	Depth	Color	Structure	Field Texture
Ap	0-24 cm	5 YR 3/4	Granular	Sandy Loam
A	24-50 cm	5 YR 3/4	Subangular Blocky	Sandy Clay Loam
AB	50-68 cm	2.5 YR 3/6	Subangular Blocky	Sandy Clay Loam
Bw	68-110 cm	2.5 YR 4/6	Subangular Blocky	Clay
Btk1	110-128 cm	2.5 YR 4/6	Subangular Blocky	Clay
Btk2	128-165 cm	2.5 YR 4/8	Subangular Blocky	Sandy Clay
C	165+ cm	2.5 YR 5/8	Single Grain/Structureless	Sandy Clay Loam

Figure 13: Pedological information of the Helsel Creek Riparian Buffer Sandy Loam (SaLo) Topsoil Profile

The physiochemical properties of both soils also differed. The SiClLo cores had less initial nitrogen and carbon than the SaLo cores but more initial sulfur. Bioavailable nitrate and ammonium were higher in the sandier soils, along with Fe(III), but the clay-rich soils had more Fe(II). The silty clay loam soil had a higher bulk density and soil pH than the sandy loam soil (Table 1).

Table 1: Initial Physiochemical Properties of the Tested Soils

Core	N Initial %	C Initial %	S Initial %	Bioavailable NO_3^- g/g soil	Bioavailable NH_4^+ mg/g soil	Fe(II) Initial mg/g soil	Fe(III) Initial mg/g soil	Bulk Density g/cm^3	Soil pH
SiClLo	0.0650	0.6750	0.0975	0.004077	0.0916	0.2257	0.7852	1.48	6.08
SaLo	0.0750	0.7700	0.0460	0.006607	0.1383	0.2200	1.4998	1.39	5.51

Micropipette particle size analysis of the SiClLo topsoil profile resulted in textures ranging from silty clay loam in the A and Bw1 horizons to a sandy loam texture in both C horizons (Figure 14). The sandy loam topsoil profile is almost exactly the opposite. The upper horizons have textures ranging from sandy loam to silty loam, while the Bk1, Bk2, and C horizons have silty clay and silty clay loam textures (Figure 15).

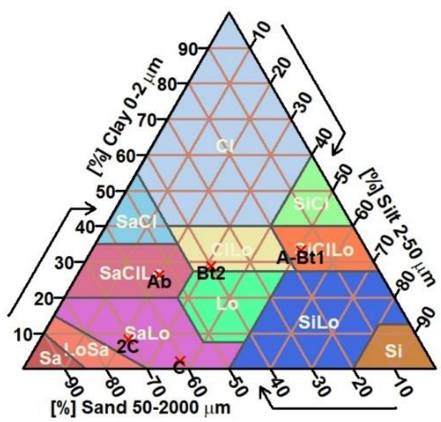

Figure 14: Silty Clay Loam (SiClLo) Topsoil Profile Particle Size Analysis

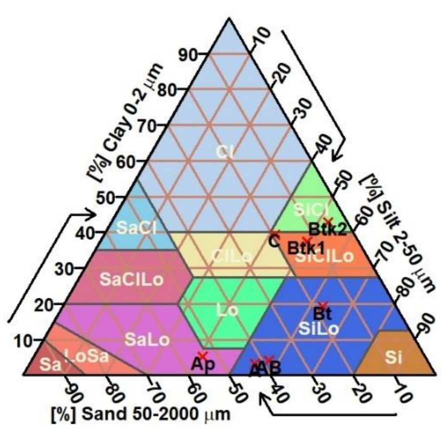

Figure 15: Sandy Loam (SaLo) Topsoil Profile Particle Size Analysis

3.01.2 Powder X-Ray Diffraction (XRD)

Using the SiClLo topsoil allowed the perfect opportunity to analyze the surface clay mineralogy of the Port soil series using XRD. After making the filter peel oriented mount and running it in its three treatments, XRD analysis confirmed the mixed clay mineralogy in the Port soil series description (National Cooperative Soil Survey, 2023). Oriented mount analysis through air drying, glycolation, and heat treatment suggests the presence of kaolinite, illite, smectite, chlorite, and a mixed layer of illite-smectite (Figure 16). Notably, d-spacing differences due to interlayer hydration between the air-dried and glycolated treatments are consistent with smectite and the mixed layer illite-smectite. Further modeling of the mixed layer illite-smectite revealed that it is an IS70R1 clay, consisting of 70% illite and 30% smectite, where the illite layers and smectite layers alternate with short-range ordering.

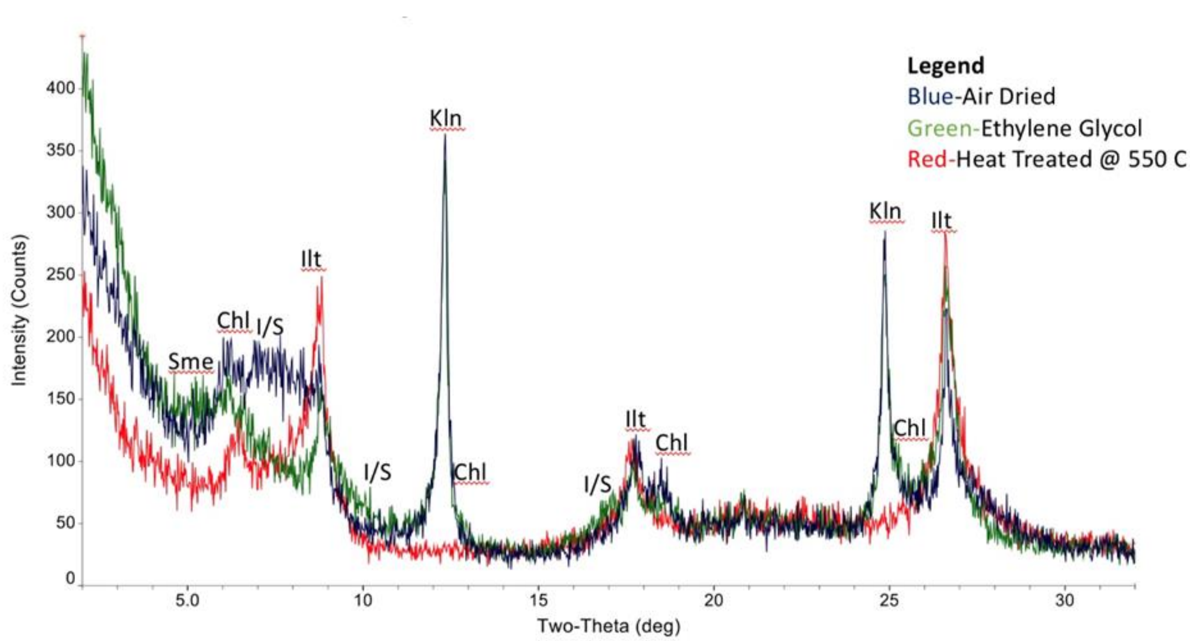

Figure 16: Powder X-Ray Diffraction Treatment Results and Interpretations of Silty Clay Loam (SiClLo) Topsoil

3.02 Porewater Chemistry During Incubations

3.02.1 Porewater pH

Statistical analysis using a GAMM yielded valuable insights into the controls on pore water pH. The interaction of Moisture Regime and Water Type provided the most significant effect (p-value = 0.00265). Conversely, Soil Texture was the least significant factor in controlling pore water pH (p-value = 0.05372) (Table 2, Figure 17). Additionally, there is a negative correlation between ammonium and pore water pH, with correlation values ranging from -0.225 to -0.788. A similar negative correlation exists with nitrate and pore water pH. (Supplemental Material F-1). Furthermore, our climate proxies, Moisture Regime (p-value=0.03335), and Water Application (p-value=0.04659) were individually significant, indicating that our climate proxies are important for predicting porewater pH.

A posthoc Wald test of the GAMM for porewater pH yielded 64 significant comparisons grouped into fourteen statistically different clusters, revealing how decreasing soil moisture and flooding impacted porewater pH throughout the incubations (Supplemental Material F-11, T-4, C-1). These clusters consist of treatment comparisons that are all statistically similar in how changing the treatment factor levels of Moisture Regime, Water Application, and Water Type affected porewater pH. Drought conditions were present in twelve comparisons, and Field Capacity and Flooding conditions were present in nine comparisons. These comparisons include ones such as the silty clay loam soil undergoing simulated drought and flooding with agricultural runoff (SiClLo-D-F-Ag) compared against the silty clay loam soil under the Field Capacity antecedent soil moisture and flooding water application with agricultural runoff applied (SiClLo-FC-F-Ag) (Estimate = 0.6379, SE = 0.2939, p-value = <0.001). This comparison indicates a positive relationship between switching the moisture regime to drought and porewater pH. Drought and capillary rise are the treatments most commonly compared in sandier soils, with eight total comparisons each. The estimates and standard errors (SE) for these comparisons ranged widely, suggesting varying degrees of impact on Porewater pH. This can be seen in a comparison between two sandy loam treatments. When comparing the Drought to the Field Capacity antecedent soil moisture with the same Water Application and Water Type (Capillary Rise and Agricultural Runoff), a significant negative effect on porewater pH exists (Estimate=-0.5581, p-value=<0.001). Similar comparisons exist with different Water Application types (Supplemental Material C-1). Consequently, these results indicate that changing the Moisture Regime from Field Capacity to Drought or changing Water Application from Capillary Rise to Flooding significantly impacts porewater pH values.

Table 2: Pore Water pH Generalized Additive Model Results

Significant Factors Affecting Pore Water pH	F	p-value
Soil Texture	3.783	0.05372
Moisture Regime	4.616	0.03335
Water Application	4.030	0.04659
Water Type	4.362	0.03852
Moisture Regime *x* Water Type	9.356	0.00265
Water Application *x* Water Type	7.656	0.00641

Soil Texture *x* Moisture Regime *x* Water Type	4.241	0.04128
Moisture Regime *x* Water Application *x* Water Type	9.274	0.00277
Model Fit	*R^2=0.545*	*Deviance Explained=63.2%*

Pore water pH exhibited significant variability throughout the experiment, reflecting the dynamic nature of soil biogeochemical processes under different treatment conditions. In the SiClLo soils, pore water pH values ranged from as acidic as pH 5 to as alkaline as pH 8.5, depending on the specific treatment. This wide pH range indicates a complex interplay of biogeochemical reactions influenced by various environmental factors. The agricultural runoff treatments diverged substantially from the deionized (DI) water control. The Field Capacity-Flood, Drought-Flood, and Drought-Capillary Rise treatments, in particular, exhibited the most significant variations in pH. We observed an exception in the Field Capacity-Capillary Rise-DI Water treatment, which experienced a notable drop in pore water pH towards the end of the measurement period. Specifically, the Drought-Flood-Agricultural Runoff treatment maintained a consistently lower pore water pH throughout the experiment than the DI control. Conversely, the Field Capacity-Flood-Agricultural Runoff treatment showed an inverse relationship with the DI control (Supplemental Material F-16). However, the sandy loam pore water pH data indicate a vastly different treatment response. pH values vary between 7.96 and 4.63 across all sandy loam soil treatments, with many readings below a pH of 6. The capillary rise treatments are inversely correlated, with the Field Capacity-Capillary Rise pH measurements indicating that the Agricultural Runoff treatment has a lower pore water pH than its DI control and the Drought-Capillary Rise-Agricultural Runoff treatment possessing higher pore water pH measurements than its

DI control. The sandy loam soils exhibit more drastic changes in pH than their SiClLo counterparts, with rapid fluctuations from a pH of 5 to a pH of almost 8 (Supplemental Material F-17).

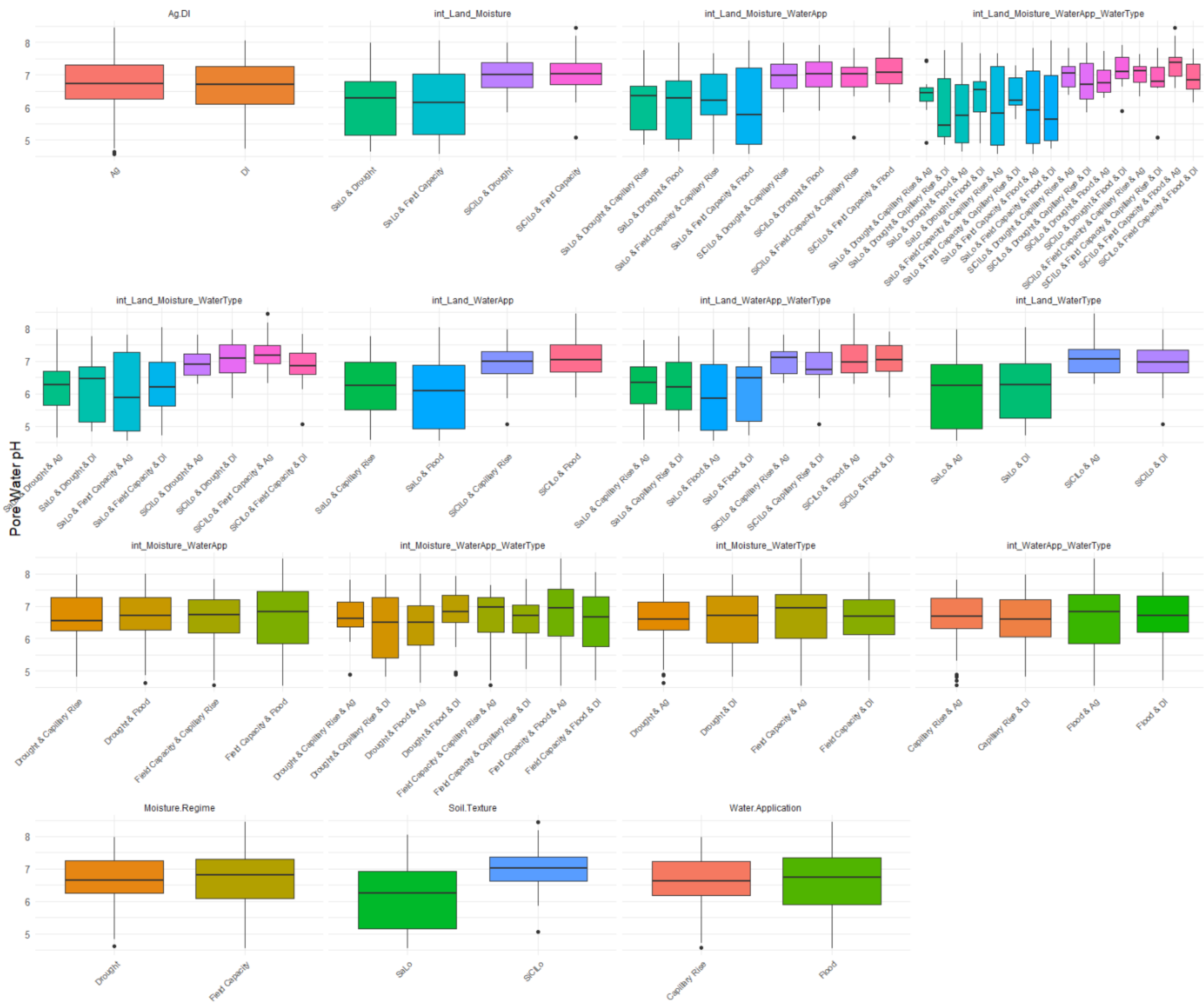

Figure 17: Porewater pH GAMM results showing boxplot comparisons of each treatment level and all treatments' interactions on porewater pH values.

3.02.2 Porewater Nitrate

The GAMM results indicate that soil texture (p-value = 0.04697), antecedent soil moisture (p-value = 0.00389), and runoff delivery (p-value = 0.00296) significantly affected porewater NO_3^- concentrations throughout the incubation experiment. The most significant factors were the interaction of Soil Texture and Water Application and the interaction of Moisture Regime and Water Application with p-values <0.001. Conversely, the interaction of Soil Texture, Moisture Regime, and Water Application provided the least statistically significant effect, with a p-value of 0.0472 (Table 3, Figure 18).

A posthoc Wald test of the porewater nitrate GAMM indicates 59 significant associations between treatments grouped into twelve statistically significant and unique clusters (Supplemental Material F-12, T-1, C-1). These clusters consist of treatment comparisons that are all statistically similar in how changing the treatment factor levels of Moisture Regime, Water Application, and Water Type affected nitrate concentrations. For example, nitrate concentrations were significantly higher in the porewater of sandy loam soils with simulated drought and flooding compared to all other treatments. Among these, the comparison of the Sandy Loam soil under Drought conditions and Capillary Rise water application method with Agricultural Runoff applied (SaLo-D-CR-Ag) against the Sandy Loam soil under Drought conditions and Flooding water application with Agricultural Runoff applied (SaLo-D-F-Ag) showed a negative effect associated with the change of water application from Capillary Rise to Flooding (Estimate = -0.0104, SE = 0.0035, T = -3.0128, p-value = 0.0026). Furthermore, comparisons between the Sandy Loam soil under Drought conditions with Flooding water application and Agricultural Runoff applied (SaLo-D-F-Ag) against the Silty Clay Loam soil under Field Capacity soil moisture conditions with Flooding water application and Agricultural Runoff applied (SiClLo-FC-F-Ag) highlighted significant differences (p-value=0.0025), indicating that changes in the climate proxies of soil moisture and water application significantly affect the RBZ’s capacity to filter N from agricultural runoff.

Table 3: Nitrate Generalized Additive Mixed-Effects Model (GAMM) Results

Significant Factors Affecting Nitrate	F	p-value
Soil Texture	4.001	0.046966
Moisture Regime	8.551	0.003894
Water Application	9.077	0.002959
Water Type	8.513	0.003973
Soil Texture *x* Moisture Regime	7.171	0.008088
Soil Texture *x* Water Application	12.578	0.000497
Moisture Regime *x* Water Application	12.058	0.000645
Soil Texture *x* Water Type	8.198	0.004687
Moisture Regime *x* Water Type	10.344	0.001539
Water Application *x* Water Type	10.370	0.001518
Soil Texture *x* Moisture Regime *x* Water Application	3.991	0.047230
Soil Texture *x* Moisture Regime *x* Water Type	9.029	0.003033
Soil Texture *x* Water Application *x* Water Type	5.824	0.016804
Moisture Regime *x* Water Application *x* Water Type	10.824	0.001204
Soil Texture *x* Moisture Regime *x* Water Application *x* Water Type	6.801	0.009873
Model Fit	R^2=0.787	*Deviance Explained=80.9%*

Porewater nitrate concentrations were higher in the flooding versus the capillary rise treatments, lower in the clay-rich soils, and lower in the soils that remained at field capacity. This is evidenced by the model results (Moisture Regime p-value=0.003894, Water Application p-value=0.002959, Supplemental Material T-1) and the porewater nitrate concentrations. We observed that pore water nitrate concentrations exhibited significant fluctuations in the Silty Clay Loam cores. These ranged from as low as 0.01 g/L to as high as 5.283 g/L, with the Drought-Capillary Rise treatment responsible for these two extremes across all treatments. Such variability points to the complex interplay of environmental factors, such as soil moisture and water application methods influencing nitrogen cycling.

The maximum nitrate values observed in each treatment provide further insights into this variability. The Field Capacity-Flood treatment reached a peak of 4.719 g/L, the Drought-Flood treatment at 5.141 g/L, and the Drought-Capillary Rise treatment showed the highest concentration at 5.283 g/L (Supplemental Material F-18). The Sandy Loam soils have nitrate values that range between 0.01 g/L and 9.11 g/L between all treatments. Maximums for each treatment are 5.103 g/L for the Field Capacity-Flood treatment, 9.112 g/L for the Field Capacity-Capillary Rise treatment, 8.162 g/L for the Drought-Flood treatment, and 3.69 g/L for the Drought-Capillary Rise treatment. Excluding the Drought-Capillary Rise treatment, pore water nitrate values are higher in Sandy Loam soils than in Silty Clay Loam ones (Supplemental Material F-19). These results underscore the critical role of land use and moisture regime in controlling nitrate concentrations, in line with the GAMM's findings. The porewater nitrate concentration data, bolstered by both the GAMM and the posthoc Wald test, provide a comprehensive understanding of nitrate variability in response to predicted climate and management conditions.

Figure 18: Nitrate GAMM results showing boxplot comparisons of each treatment level and all treatments' interactions on porewater nitrate concentrations.

3.02.3 Porewater Ammonium

The GAMM results for porewater ammonium concentrations indicate that two factors influenced ammonium pore water concentrations. Soil Texture was the most significant factor, with a p-value of 0.0223. The interaction of Moisture Regime, Water Application, and Water Type also provided a significant effect, with a p-value of 0.0561 (Table 4, Figure 19). A negative correlation also exists between nitrate and ammonium, with seven out of the eleven weeks of common measurements showing a correlation value between -0.143 and -0.454 (Supplemental Material C-1). A posthoc Wald test of the Ammonium GAMM revealed 54 significant associations in twenty statistically different clusters between the treatments (Supplemental Material F-13, T-2). Particularly noteworthy was the comparison between the Silty Clay Loam soil under Drought conditions with Deionized Water applied through Capillary Rise (SiClLo-D-CR-DI) and the Sandy Loam soil under Field Capacity conditions with Deionized Water applied through Flooding (SaLo-FC-F-DI), which showed a highly significant negative effect when changing soil texture, antecedent soil moisture, and water application method (Estimate = -5.8744, SE = 1.7238, T = -3.4078, p-value = 0.0007). This pattern was consistent across several comparisons, underscoring the intricate relationship between how decreasing soil moisture and more intense precipitation events negatively influence porewater ammonium levels.

Table 4: Porewater Ammonium GAMM Results

Significant Factors Affecting Ammonium	F	p-value
Soil Texture	5.328	0.0223
Moisture Regime *x* Water Application *x* Water Type	3.704	0.0561
Model Fit	R^2*=0.464*	*Deviance Explained=51.6%*

Porewater ammonium concentrations were higher in the flooding versus the capillary rise treatments, lower in the clay-rich soils, and lower in the soils that remained at field capacity. When evaluating all treatments collectively, we found that the Silty Clay Loam ammonium pore water concentrations ranged between 0.096 mg/L and 0.171 mg/L. The flooding treatments consistently showed higher pore water ammonium concentrations than their capillary rise counterparts. Breaking down the results by treatment, the maximum ammonium pore water concentrations were observed as follows: 0.171 mg/L in the Field Capacity-Flood-Agricultural Runoff treatment, 0.113 mg/L in the Field Capacity-Capillary Rise-Agricultural Runoff treatment, 0.143 mg/L in the Drought-Flood-Agricultural Runoff treatment, and 0.128 mg/L in the Drought-Capillary Rise-Agricultural Runoff treatment (Supplemental Material F-20). Sandy Loam pore water ammonium values ranged between 0.04 mg/L and 0.54 mg/L, treatment-dependent. Maximum values for each treatment are 0.32 mg/L for the Field Capacity-Flood treatment, 0.54 mg/L for the Field Capacity-Capillary Rise treatment, 0.26 mg/L for the Drought-Flood treatment, and 0.20 mg/L for the Drought-Capillary Rise treatment. In the Field Capacity-Capillary Rise treatment, a significant spike in ammonium concentrations precedes the spike in pore water nitrate concentrations (Supplemental Material F-21). These variations highlight the influence of changing the moisture regime and water application method on ammonium dynamics within the soil.

Figure 19: Ammonium GAMM results showing boxplot comparisons of each treatment level and all treatments' interactions on porewater ammonium concentrations.

3.02.4 Porewater Phosphate

Statistical analysis of the pore water phosphate concentrations using a GAMM indicates significant treatment effects on the P concentrations in pore water. The interaction of Soil Texture and Water Application provided the most significant effect, with a p-value<0.001. Soil Texture alone provided the least significant effect, with a p-value of 0.0919 (Table 5, Figure 20). Phosphorus also had a significant positive weekly correlation with nitrate, with correlation values ranging between 0.110 and 0.715 for eight weeks and only exhibiting a negative correlation for two weeks. Phosphorus also negatively correlated with ammonium, with most weeks having negative correlation values between -0.09 and -0.288. Phosphorus also positively correlated with pore water pH and ARQ (Supplemental Material C-1).

A posthoc Wald test on the phosphate GAMM yielded 85 significant associations between treatments grouped into eleven statistically different clusters of statistically similar comparisons (Supplemental Material F-14, T-3). The comparisions in these clusters have similar positive and negative effects on porewater phosphate concentrations. These results show various effects across treatment comparisons. For example, the comparison between the sandy loam soil under Field Capacity moisture conditions with DI water applied through Capillary Rise (SaLo-FC-CR-DI) and the silty clay loam soil under Drought conditions with DI water applied through Flooding treatments (SiClLo-D-F-DI) revealed a significant negative effect with a p-value of 0.005. Similarly, other comparisons like the sandy loam soil under drought conditions with agricultural runoff applied through Capillary Rise (SaLo-D-CR-Ag) against the silty clay loam soil under Drought conditions with agricultural runoff applied through simulated Flooding (SiClLo-D-F-Ag) also showed a significant negative effect, with a p-value<0.001. These comparisons suggest substantial differences in phosphorus concentrations between the treatment groups. Conversely, some comparisons indicated positive effects. For instance, the comparison between two silty clay loam soils with agricultural runoff applied through Flooding showed a positive effect of switching from Drought conditions to Field Capacity conditions with a highly significant p-value<0.001. These findings highlight the complex interactions between soil texture, water application, moisture regime, and water type treatments and their impact on phosphorus levels (Supplemental Material F-13, T-3).

Table 5: Porewater Phosphate GAMM Results

Significant Factors Affecting Phosphate	F	p-value
Soil Texture	2.871	0.091932
Moisture Regime	5.745	0.017576
Water Type	12.157	0.000617
Soil Texture *x* Moisture Regime	14.765	0.000169
Soil Texture *x* Water Application	22.815	3.73e-06
Moisture Regime *x* Water Application	3.602	0.059342
Soil Texture *x* Moisture Regime *x* Water Application	14.400	0.000203
Soil Texture *x* Moisture Regime *x* Water Type	7.192	0.008015
Soil Texture *x* Moisture Regime *x* Water Application *x* Water Type	8.353	0.004332
Model Fit	*R^2=0.96*	*Deviance Explained=96.5%*

The varied P porewater concentration results indicate how each soil responded to the treatments. In the Silty Clay Loam soil cores, phosphorus porewater concentrations ranged from 0.07 mg/L to 2.37 mg/L across all treatments. Under the ideal Field Capacity-Capillary Rise treatment, the final P values stayed reasonably constant, consistently below 0.35 mg*L^{-1}/week of applied P. However, the Drought-Capillary Rise treatment had a phosphate porewater concentration of 0.47 mg/L. Flooding also appears to exacerbate this effect, with the Field Capacity-Flood treatment soils showing a porewater concentration of 1.62 mg/L of P on the same observation. The combined impact of flooding and drought released the most P during that measurement, with 2.36 mg/L of P released (Supplemental Material F-22). In the Sandy Loam soils, phosphate concentrations were lower than in the SiClLo soils. Notably, the

Field Capacity-Capillary Rise treatment had the most significant spike with a P porewater concentration of 0.56 mg/L, a substantial difference from its Silty Clay Loam counterpart, which never had P final values that exceeded the applied P that week. Both Sandy Loam drought treatments experienced a spike at the same time as the same Silty Clay Loam treatments. These spikes in the phosphate were much lower in magnitude, with values of 0.38 mg/L for the Drought-Flood treatment and 0.40 mg/L for the Drought-Capillary Rise treatment (Supplemental Material F-23).

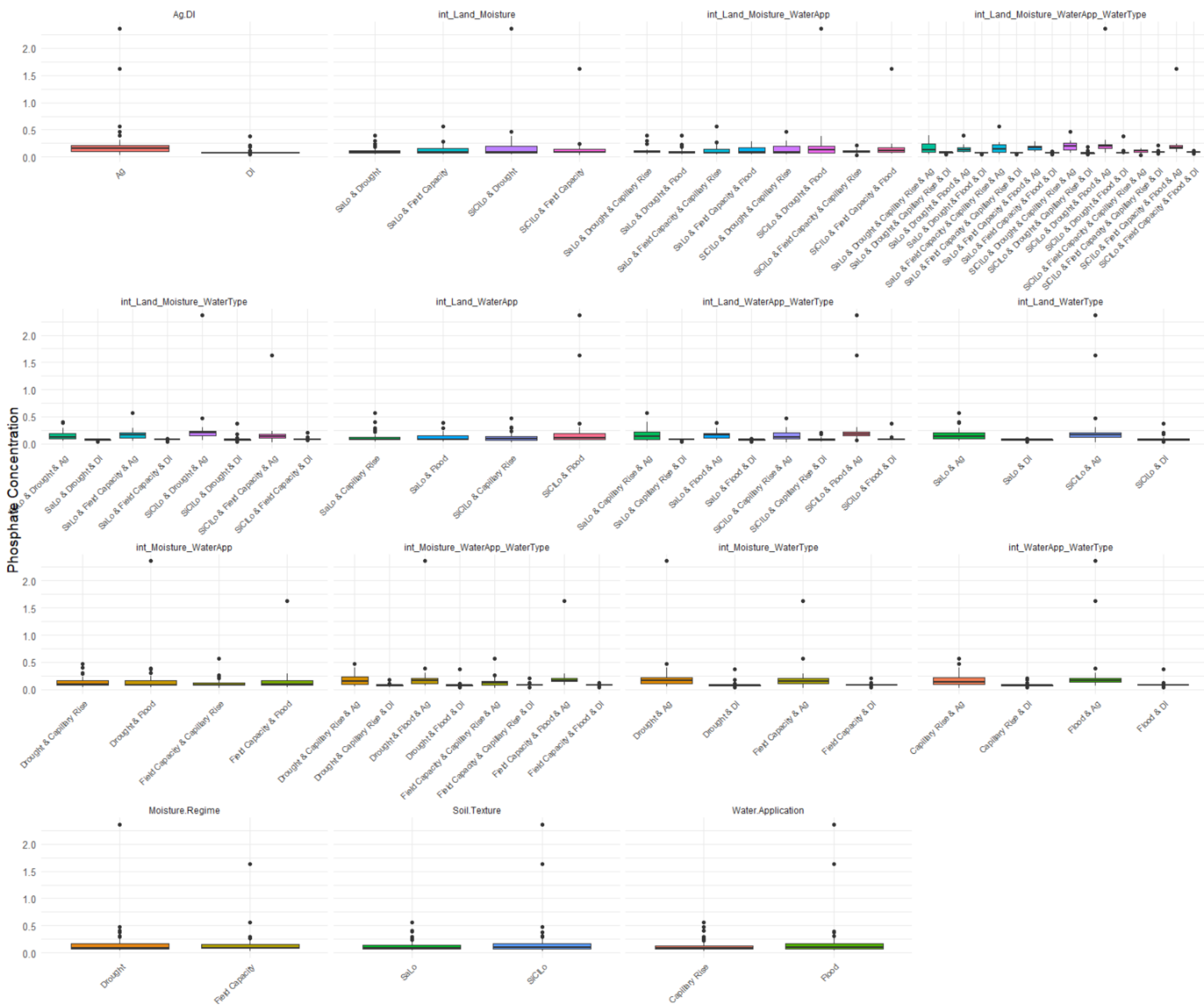

Figure 20: Phosphate GAMM results showing boxplot comparisons of each treatment level and all treatments' interactions on porewater phosphate concentrations.

3.02.5 Apparent Respiratory Quotient, O_2, and CO_2

Critically, statistical analyses of the ARQ values indicate that some treatments significantly affected ARQ. Soil Texture provided the most significant control on ARQ, with a p-value of 0.000381. Water Application had the least statistically significant effect, with a p-value of 0.033 (Table 6, Figure 21). Additionally, ARQ has a negative correlation with nitrate and a positive correlation with ammonium (Supplemental Material C-1).

A posthoc Wald test of the ARQ GAMM yielded 34 highly significant interactions grouped into eight statistically different clusters of statistically similar comparisons, which indicates how our climate proxies affected ARQ values during the incubation. For example, the comparison of two silty clay loam soils under Drought conditions with agricultural runoff applied has a statistically significant negative effect on ARQ by switching water application from Capillary Rise to Flooding (Estimate -0.0686, p-value=0.012). A similar comparison exists between two silty clay loam soils with agricultural runoff applied. This comparison has a significant negative effect by switching from Field Capacity and Capillary Rise to Drought and Flooding (Estimate=-0.0683, p-value=0.0125). Drought conditions appear in twenty-four comparisons, flooding appears in nine, and the combined effect of drought and flooding appears in seven total comparisons (Supplemental Material F-15, T-5, C-1).

Table 6: ARQ Generalized Additive Model Results

Significant Factors Affecting ARQ	F	p-value

Soil Texture	13.108	0.000381
Water Application	4.603	0.033244
Soil Texture *x* Moisture Regime	8.671	0.003655
Soil Texture *x* Water Application	10.903	0.001155
Soil Texture *x* Water Type	4.592	0.033457
Soil Texture *x* Moisture Regime *x* Water Application	11.101	0.001044
Soil Texture *x* Water Application *x* Water Type	10.755	0.001246
Soil Texture *x* Moisture Regime *x* Water Application *x* Water Type	4.773	0.030192
Model Fit	*R^2=0.732*	*Deviance Explained=85.6%*

The apparent respiratory quotient (ARQ) produced clear signals from each climate regime treatment. The ARQ was consistently above the aerobic line after the second measurement in all Silty Clay Loam soils, suggesting anaerobic respiration. The lowest observed ARQ was 0.17, and the highest observed ARQ was 7.24 among treatments. Both flooding treatments and the Field Capacity-Capillary Rise treatment showed strong signals of anaerobic respiration, and the agricultural runoff treatments were higher in ARQ than their DI water counterparts. However, this was not the case with the Drought-Capillary Rise treatment. The Drought-Capillary Rise-Agricultural Runoff treatment was lower than its DI counterpart and had a consistently lower ARQ than the other Silty Clay Loam agricultural runoff treatments, indicating the presence of more oxygen than other treatments. Additionally, the Field Capacity-Agricultural Runoff treatments remained somewhat close to their DI water counterparts, with some covarying peak differences between the agricultural runoff and DI water. This contrasts heavily with the Drought-Agricultural Runoff treatments, which have ARQ values consistently above or below their DI control, depending on the water application method (Supplemental Material F-24).

Conversely, the Sandy Loam ARQ values tell a different story. The minimum and maximum ARQ values are 0.20 and 9.64, respectively, across all treatments. Much like the Silty Clay Loam soils, all Sandy Loam soils exhibited an anaerobic environment after the second measurement, with some treatments showing evidence of anaerobic respiration after the first measurement. In contrast to the Silty Clay Loam soils, the initial spike in ARQ was overall higher in the Sandy Loam samples. The agricultural runoff and DI water cores exhibited similar behavior in the ideal Field Capacity-Capillary Rise treatment. The Field Capacity-Flood-Agricultural Runoff treatment had multiple spikes in ARQ, similar to the Silty Clay Loam soils. However, both drought treatments exhibited initial sharp increases in ARQ and significant decreases, with more minor variations in ARQ over the remainder of the experiment (Supplemental Material F-25).

Figure 21: ARQ GAMM results showing boxplot comparisons of each treatment level and all treatments' interactions on ARQ values.

3.03 Post Incubation Results

3.03.1 Soil pH

Table 7: Soil pH values for the Silty Clay Loam and Sandy Loam Soils

Silty Clay Loam Treatments	Soil pH	pH Standard Error	Change in pH
SiClLo Initial	6.08	-	-
SiClLo-FC-F-Ag	7.32	0.0318	1.24
SiClLo-FC-F-DI	7.26	0.0173	1.18
SiClLo-FC-CR-Ag	7.22	0.0088	1.14
SiClLo-FC-CR-DI	7.27	0.0067	1.19
SiClLo-D-F-Ag	7.26	0.0186	1.18
SiClLo-D-F-DI	7.22	0.0088	1.14
SiClLo-D-CR-Ag	7.22	0.0203	1.14
SiClLo-D-CR-DI	7.22	0.0133	1.14
Sandy Loam Treatments	**Soil pH**	**pH Standard Error**	**Change in pH**
SaLo Initial	5.51	-	-
SaLo-FC-F-Ag	7.27	0.0367	1.76
SaLo-FC-F-DI	7.25	0.0120	1.74
SaLo-FC-CR-Ag	7.21	0.0115	1.70
SaLo-FC-CR-DI	7.28	0.0067	1.77
SaLo-D-F-Ag	7.24	0.0426	1.73
SaLo-D-F-DI	7.25	0.0120	1.74
SaLo-D-CR-Ag	7.27	0.0088	1.76
SaLo-D-CR-DI	7.26	0.0120	1.75

Key: FC-Field Capacity, D-Drought, F-Flooding, CR-Capillary Rise, Ag-Agricultural Runoff, DI-Deionized Water

Random Forest analysis indicates that water application controls soil pH, with Moisture Regime and Water Type also providing equally significant effects. Water Application has the highest increase in node purity, indicating that it has the most significant impact on controlling soil pH. Soil pH is positively correlated with bioavailable nitrate and negatively correlated with bioavailable ammonium (Supplemental Material F-2).

Soil pH varied drastically throughout the core experiments. The initial SiClLo soil pH was 6.08, a neutral soil pH. However, the pH value increased between 1.14 and 1.24 pH units depending on the treatment, with the Field Capacity-Flood-Agricultural Runoff treatment increasing the most and the two capillary rise and agricultural runoff treatments increasing the least. In the Sandy Loam soils, the initial pH was 5.51, a weakly acidic soil. Compared to the Silty Clay Loam soils, however, the pH value of Sandy Loam soils increased between 1.70 and 1.77, reaching soil pH values similar to the Silty Clay Loam soils. Standard errors for Sandy Loam and Silty Clay Loam samples were low (<0.005) (Table 7).

3.03.2 Nitrate and Ammonium KCl Extractions

Random Forest analysis of 500 decision trees indicates that bioavailable nitrate is most affected by Water Application, Water Type, and Moisture Regime, similar to the results of the porewater nitrate GAMM (Supplemental Material F-3). Water Type provides the most significant control on bioavailable nitrate, while Moisture Regime and Water Application also provide significant effects. Similarly, bioavailable ammonium is primarily controlled by water type, which has the highest increase in node purity.

However, our two climate proxies, Moisture Regime and Water Application, were also significant in controlling bioavailable ammonium (Supplemental Material F-4).

The Silty Clay Loam KCl extraction results provide compelling evidence of a shift in nitrogen species from ammonium to nitrate throughout the experiment, a pattern indicative of active nitrification processes in the soil. This shift was observed across all treatments, with nitrate concentrations increasing from an initial value of 0.004077 g/g soil to ranges between 0.0686 g/g and 0.1237 g/g soil. The standard errors for these measurements varied from 0.1596 to 0.2398, indicating a consistent trend despite some variability. Notably, the Field Capacity-Capillary Rise-DI Water treatment exhibited the most significant increase in nitrate, with a change (ΔNO_3) of 0.1196 g/g soil.

Conversely, ammonium concentrations generally decreased throughout the experiment, ranging from reductions of 0.0072 mg/g to 0.0178 mg/g soil, as evidenced in treatments like the Drought-Capillary Rise-DI Water. The standard errors for these decreases were between 2e-4 and 5.2e-3, suggesting a consistent pattern of ammonium depletion across the treatments (Table 8).

Table 8: Silty Clay Loam KCl Extraction Results

Treatment	NO_3 g/g soil	NO_3 Standard Error	ΔNO_3 g	NH_4 mg/g soil	NH_4 Standard Error	ΔNH_4
SiClLo Initial	0.004077	-	-	0.0916	-	-
SiClLo-FC-F-Ag	0.0575	0.1596	0.0534	0.0844	0.0004	-0.0072
SiClLo-FC-F-DI	0.0686	0.1705	0.0645	0.0837	0.0002	-0.0078
SiClLo-FC-CR-Ag	0.0863	0.1598	0.0822	0.0862	0.0014	-0.0054
SiClLo-FC-CR-DI	0.1237	0.2398	0.1196	0.0901	0.0035	-0.0014
SiClLo-D-F-Ag	0.0895	0.2440	0.0854	0.0782	0.0052	-0.0134

SiClLo-D-F-DI	0.0756	0.1902	0.0716	0.0881	0.0021	-0.0034
SiClLo-D-CR-Ag	0.0953	0.1951	0.0913	0.0836	0.0029	-0.0079
SiClLo-D-CR-DI	0.0801	0.1467	0.0760	0.0738	0.0006	-0.0178

Key: FC-Field Capacity, D-Drought, F-Flooding, CR-Capillary Rise, Ag-Agricultural Runoff, DI-Deionized Water

Potassium chloride extractions from the Sandy Loam soils underscore a significant trend similar to that observed in the Silty Clay Loam treatments, yet with notable distinctions. Initially, the SaLo soils had nitrate and ammonium concentrations of 0.006607 g/g and 0.14 mg/g soil, respectively. Ammonium concentrations decreased throughout the experiment, mirroring the trend in Silty Clay Loam soils. However, a critical difference emerged in the nitrate dynamics. In the Sandy Loam soils, changes in nitrate concentrations were more pronounced, ranging from 0.088 g/g soil to 0.1843 g/g soil, with final nitrate levels reaching as high as 0.1909 g/g soil. This contrasted with the Silty Clay Loam soils, where nitrate increases were less extreme. The standard errors for ammonium and nitrate in the Sandy Loam soils ranged between 7e-4 to 9.5e-3 and 0.07 to 1, respectively (Table 9).

Table 9: Sandy Loam Soil KCl Extraction Results

Treatment	NO_3 g/g soil	NO_3 Standard Error	ΔNO_3	NH_4 mg/g soil	NH_4 Standard Error	ΔNH_4
SaLo Initial	0.006607	-	-	0.1383	-	-
SaLo-FC-F-Ag	0.1000	0.1593	0.0934	0.1071	0.0132	-0.0312
SaLo-FC-F-DI	0.1098	0.6232	0.1032	0.0905	0.0015	-0.0478
SaLo-FC-CR-Ag	0.1909	1.0066	0.1843	0.0825	0.0007	-0.0558
SaLo-FC-CR-DI	0.0965	0.1084	0.0899	0.0898	0.0095	-0.0485
SaLo-D-F-Ag	0.1208	0.2109	0.1141	0.0899	0.0062	-0.0484
SaLo	0.0948	0.0407	0.0881	0.0915	0.0060	-0.0468

-D-F-DI						
SaLo-D-CR-Ag	0.1187	0.1025	0.1121	0.0811	0.0029	-0.0572
SaLo-D-CR-DI	0.1103	0.0675	0.1037	0.0725	0.0025	-0.0658

Key: FC-Field Capacity, D-Drought, F-Flooding, CR-Capillary Rise, Ag-Agricultural Runoff, DI-Deionized Water

3.03.3 Iron Redox Cycling

Random Forest analysis also reveals how different factors impact the Fe(II) and Fe(III) concentrations. Fe(II) was most affected by Soil Texture, followed by Water Application, Water Type, and Moisture Regime. Fe(III) was also strongly influenced by Soil Texture but was followed by Water Type, Water Application, and Moisture Regime, which all exhibited similar significance levels (Supplemental Material F-5, F-6). This contrasts with Fe(II), where Water Application provided the second most statistically significant effect. Additionally, K-means clustering analysis (Supplemental Material F-10) confirms that Soil Texture provided the most significant control, with higher Fe(II) concentrations associated with Silty Clay Loam and high Fe(III) concentrations related to SaLo soils (Supplemental Material F-5, F-6).

The iron species data for the Silty Clay Loam soils provide valuable insights into the redox cycling conditions present in the soil. Not only did all treatments indicate a rise in total iron concentration, but there are apparent differences between the treatments. The Field Capacity-Capillary Rise treatments generally experienced the highest increase in Fe(III) and one of the lowest changes in Fe(II). Both Capillary Rise treatments had the lowest increase in Fe(II) concentration from the initial values (0.12 mg/g soil and 0.08 mg/g soil, respectively). In contrast, the Flood treatments experienced the most significant increase in Fe(II) concentration from the initial Fe(II) value. Of the flooding treatments, the Field Capacity-Flood treatments exhibited the highest concentrations of Fe(II) (0.49 mg/g soil and 0.47 mg/g soil, respectively). The same is true of the Field Capacity-Capillary Rise treatments. These treatments have higher total extractable iron, extractable Fe(III), and extractable Fe(II) concentrations than their drought counterparts (Table 10).

Table 10: Silty Clay Loam Iron Redox Cycling Data

Treatment	Fe_{tot} mg/g soil	Fe_{tot} Standard Error	ΔFe_{tot}	Fe(III) mg/g soil	Fe(III) Standard Error	ΔFe(III)	Fe(II)/Fe(III)	Fe(II) mg/g soil	Fe(II) Standard Error	ΔFe(II)
SiClLo Initial	1.0109	-	-	0.7852	-	-	0.2875	0.2257	-	-
SiClLo-FC-F-Ag	2.0413	0.2573	1.0303	1.5525	0.1712	0.7673	0.3148	0.4888	0.0863	0.2630
SiClLo-FC-F-DI	2.0239	0.1835	1.0130	1.2404	0.1105	0.4552	0.6317	0.7835	0.2051	0.5578
SiClLo-FC-CR-Ag	2.2305	0.0885	1.2196	1.8830	0.1840	1.0978	0.1846	0.3475	0.0964	0.1218
SiClLo-FC-CR-DI	2.3525	0.2697	1.3416	1.9498	0.1846	1.1646	0.2066	0.4028	0.1259	0.1770
SiClLo-D-F-Ag	2.2169	0.2642	1.2060	1.7490	0.3942	0.9638	0.2675	0.4679	0.1353	0.2422
SiClLo-D-F-DI	1.9237	0.2531	0.9128	1.3380	0.0625	0.5528	0.4377	0.5857	0.1906	0.3600
SiClLo-D-CR-Ag	1.9131	0.2744	0.9022	1.6023	0.2595	0.8171	0.1940	0.3108	0.0420	0.0851
SiClLo-D-CR-DI	2.1884	0.3640	1.1775	1.8876	0.3659	1.1024	0.1594	0.3008	0.0090	0.0751

Key: FC-Field Capacity, D-Drought, F-Flooding, CR-Capillary Rise, Ag-Agricultural Runoff, DI-Deionized Water

While the amount of total iron also increased similarly to the Silty Clay Loam soils, the Sandy Loam soils were primarily driven by increases in Fe(III). The Fe(II)/Fe(III) ratios are significantly decreased compared to the Silty Clay Loam treatments. For the Field Capacity-Capillary Rise treatment, the negative change in Fe(II) of 14.4 μg/g soil from the initial indicates that some ferrous iron was oxidized into ferric iron. Both Drought treatments also possessed the most significant change in total iron, with the Drought-Capillary Rise treatment experiencing the most significant change in total iron and ferric iron. Other Sandy Loam soils experienced little change in Fe(II) while primarily experiencing changes in Fe(III) (Table 11).

Table 11: Sandy Loam Iron Redox Cycling Data

Treatment	Fe_{tot} mg/g soil	Fe_{tot} Standard Error	ΔFe_{tot}	Fe(III) mg/g soil	Fe(III) Standard Error	ΔFe(III)	Fe(II)/Fe(III)	Fe(II) mg/g soil	Fe(II) Standard Error	ΔFe(II)
SaLo Initial	1.7198	-	-	1.4998	-	-	0.1467	0.2200	-	-
SaLo-FC-F-Ag	3.4890	0.1207	1.7692	3.2130	0.1267	1.7132	0.0859	0.2760	0.0465	0.0560
SaLo-FC-F-DI	3.1331	0.0965	1.4133	2.8983	0.0897	1.3985	0.0810	0.2348	0.0121	0.0148
SaLo-FC-CR-Ag	3.0995	0.1412	1.3797	2.8938	0.1337	1.3940	0.0711	0.2056	0.0113	-0.0144
SaLo-FC-CR-DI	3.4083	0.0662	1.6885	3.2158	0.0748	1.7160	0.0599	0.1925	0.0096	-0.0275
SaLo-D-F-Ag	3.5988	0.1984	1.8790	3.3717	0.1844	1.8719	0.0674	0.2271	0.0140	0.0071
SaLo-D-F-DI	3.0498	0.0626	1.3300	2.7939	0.0848	1.2941	0.0916	0.2559	0.0548	0.0359
SaLo-D-CR-Ag	3.7402	0.0837	2.0204	3.5013	0.0854	2.0015	0.0682	0.2389	0.0159	0.0189
SaLo-D-CR-DI	3.6623	0.1730	1.9425	3.4003	0.1443	1.9005	0.0771	0.2620	0.0292	0.0420

Key: FC-Field Capacity, D-Drought, F-Flooding, CR-Capillary Rise, Ag-Agricultural Runoff, DI-Deionized Water

3.03.4 Elemental Analysis

Random Forest analysis reveals which factors affect total N, C, and S in the Sandy Loam and Silty Clay Loam soils. Total N is affected most by Water Application, then Moisture Regime, Water Type, and Soil Texture. Total C is affected by the same factors, but Water Type is the most significant. Total S is also most affected by Water Application. Soil Texture had the least effect on all these variables (Supplemental Material F-7, F-8, F-9). K-means clustering analysis confirms the Random Forest results, with Water Application as the defining factor in all clusters. Flood treatments in Silty Clay Loam soils are generally higher in total N, C, and S, while capillary rise treatments in Sandy Loam soils are usually higher in these nutrients (Supplemental Material F-7, F-8, F-9).

Elemental analysis of the Silty Clay Loam soil samples, both pre- and post-treatment, yielded valuable insights into the treatments' effects on the soils. The initial weight percent values of carbon, nitrogen, and sulfur are 0.67%, 0.065%, and 0.098%, respectively. Post-treatment analysis revealed a significant increase in the percent carbon in the soils, with values ranging from 0.75% to 2.16%. Notably, the drought and flooding treatments resulted in the most pronounced changes, exemplified by the silty clay loam soil under Drought conditions with DI water applied through Flooding treatment, which recorded a dramatic increase in carbon content to 2.16%, representing a 220% increase from the initial value. This was followed by the silty clay loam soil under Field Capacity conditions with DI water applied through Flooding and the silty clay loam soil under Drought conditions with agricultural runoff applied through Capillary Rise which showed an 84.69% and 59.51% increase in carbon, respectively.

Similarly, nitrogen content exhibited substantial increases, most notably in the silty clay loam soil under Drought conditions with DI water applied through Flooding where nitrogen levels rose by 197.44%. The percent difference in nitrogen across all treatments varied from 69% to 197%, with drought and flooding again causing the highest increases. Sulfur content changes were more varied, with some treatments like the silty clay loam soil under Field Capacity conditions with agricultural runoff applied through Flooding, which had an 82.22% increase. In comparison, others like the silty clay loam soil under Drought conditions with DI water applied through Capillary Rise decreased in sulfur content by 66.50%.

The C/N ratios also changed significantly compared to the initial C/N ratio of 11.19. The range of treatment C/N ratios varied from 5.75 in the silty clay loam soil under Field Capacity conditions with agricultural runoff applied through Flooding to 11.60 in the silty clay loam soil under Drought conditions with DI water applied through. These shifts in C/N ratios indicate a notable impact of the treatments on the nutrient balance in the soil. The analysis underscores the profound effect of changing the Moisture Regime and Water Application, particularly under extreme conditions like drought and flooding, on the soil's elemental composition (Table 12).

Table 12: Silty Clay Loam Elemental Analysis Results

Treatment	%C	%C Standard Error	% Difference C	%N	%N Standard Error	% Difference N	C/N Ratio	%S	%S Standard Error	% Difference S
SiClLo Initial	0.6750	0.0050	-	0.0650	0.0050	-	11.1915	0.0975	0.0185	-
SiClLo-FC-F-Ag	0.7567	0.0775	12.0988	0.1333	0.0067	105.1282	5.7480	0.1777	0.1282	82.2222
SiClLo-FC-F-DI	1.2467	0.0733	84.6914	0.1733	0.0088	166.6667	7.2035	0.0467	0.0030	-52.1368
SiClLo-FC-CR-Ag	1.0767	0.1920	59.5062	0.1167	0.0176	79.4872	9.8220	0.0343	0.0035	-64.7863
SiClLo-FC-CR-DI	1.2233	0.2367	81.2346	0.1133	0.0167	74.3590	10.6884	0.0363	0.0042	-62.7350
SiClLo-D-F-Ag	1.2400	0.3570	83.7037	0.1100	0.0252	69.2308	10.7770	0.0357	0.0058	-63.4188
SiClLo-D-F-DI	2.1600	0.7497	220.0000	0.1933	0.0754	197.4359	11.5976	0.1307	0.0822	34.0171
SiClLo-D-CR-Ag	1.0200	0.4606	51.1111	0.0867	0.0318	33.3333	11.3608	0.0327	0.0032	-66.4957
SiClLo-D-CR-DI	0.9667	0.3598	43.2099	0.0833	0.0260	28.2051	11.1457	0.0337	0.0039	-65.4701

Key: FC-Field Capacity, D-Drought, F-Flooding, CR-Capillary Rise, Ag-Agricultural Runoff, DI-Deionized Water

Meanwhile, the Sandy Loam soil samples indicate the effects of the treatments on soils. The initial values of carbon, nitrogen, and sulfur are 0.77%, 0.075%, and

0.046% respectively. The analysis post-treatment revealed that the percent difference in carbon varied significantly across treatments, ranging from a modest increase of 3.46% in the sandy loam soil under Field Capacity conditions with DI water applied through Capillary Rise to a substantial increase of 228% in the sandy loam soil under Field Capacity conditions with agricultural runoff applied through Capillary Rise, with final carbon values reaching up to 2.38%. Similarly, nitrogen content changes were notable, ranging from an increase of 0.14% in the sandy loam soil under Drought conditions with DI water applied through Flooding to a dramatic increase of 224% in the sandy loam soil under Field Capacity conditions with agricultural runoff applied through Capillary Rise with final nitrogen values peaking at 0.24%.

Sulfur content also exhibited significant variability, with the percent difference ranging from a decrease of 35.51% in the sandy loam soil under Drought conditions with DI water applied through Flooding to an increase of 184% in the sandy loam soil under Drought conditions with DI water applied through Capillary Rise, bringing the final sulfur values to a range between 0.03% and 0.13%. In contrast to the SiClLo soils, the capillary rise treatments, particularly in the SaLo soils, showed the most pronounced increase in total carbon, nitrogen, and sulfur throughout the experiment. For example, the sandy loam soil under Field Capacity conditions with agricultural runoff applied through Capillary Rise not only led to the highest increase in carbon but also in nitrogen and sulfur, suggesting a distinct impact of this treatment on the soil (Table 13).

Table 13: Sandy Loam Elemental Analysis Results

Treatment	%C	%C Standard Error	% Difference C	%N	%N Standard Error	% Difference N	C/N Ratio	%S	%S Standard Error	% Difference S
SaLo Initial	0.7700	0.0400	-	0.0750	0.0050	-	10.3814	0.0460	0.0020	-

SaLo-FC-F-Ag	1.0300	0.2901	33.7662	0.0967	0.0219	28.8889	10.7065	0.0343	0.0038	-25.3623
SaLo-FC-F-DI	1.0233	0.1534	32.9004	0.0933	0.0133	24.4444	10.9616	0.0303	0.0767	-34.0580
SaLo-FC-CR-Ag	2.5267	1.5639	228.1385	0.2433	0.1543	224.4444	10.6521	0.1257	0.0746	173.1884
SaLo-FC-CR-DI	0.7967	0.0441	3.4632	0.0767	0.0067	2.2222	10.4829	0.0320	0.0012	-30.4348
SaLo-D-F-Ag	0.8567	0.0606	11.2554	0.0800	0.0058	6.6667	10.6386	0.0310	0.0012	-32.6087
SaLo-D-F-DI	0.8300	0.1212	7.7922	0.0800	0.0100	6.6667	10.1686	0.0297	0.0032	-35.5072
SaLo-D-CR-Ag	0.9500	0.1332	23.3766	0.0900	0.0100	20.0000	10.5887	0.0350	0.0765	-23.9130
SaLo-D-CR-DI	2.3800	1.3506	209.0909	0.2133	0.1102	0.1383	10.7574	0.1307	0.0847	184.0580

Key: FC-Field Capacity, D-Drought, F-Flooding, CR-Capillary Rise, Ag-Agricultural Runoff, DI-Deionized Water

3.03.5 Nitrogen Mass Balance

Our nitrogen mass balance results provide an indication as to how our two climate proxies, Moisture Regime and Water Application, affect N cycling in riparian soils. Throughout the incubations, we applied 58.53 mg of NO_3^- to the treatments involving simulated agricultural runoff. Increases in Total N were primarily driven by an increase in bioavailable nitrate, which was partially countered by decreases in bioavailable ammonium and soil organic nitrogen (SON). The Sandy Loam treatments experienced greater losses in NH_4^+ than the Silty Clay Loam treatments. Critically, most of the treatments that experienced some form of simulated climate change (drought, flooding, or the combined effect) lost more SON than treatments that were not subjected to simulated climate change. The exception to this is the Silty Clay Loam soil at Field Capacity conditions experiencing Flooding, which had an increase of 5.24 g of SON (Figure 22).

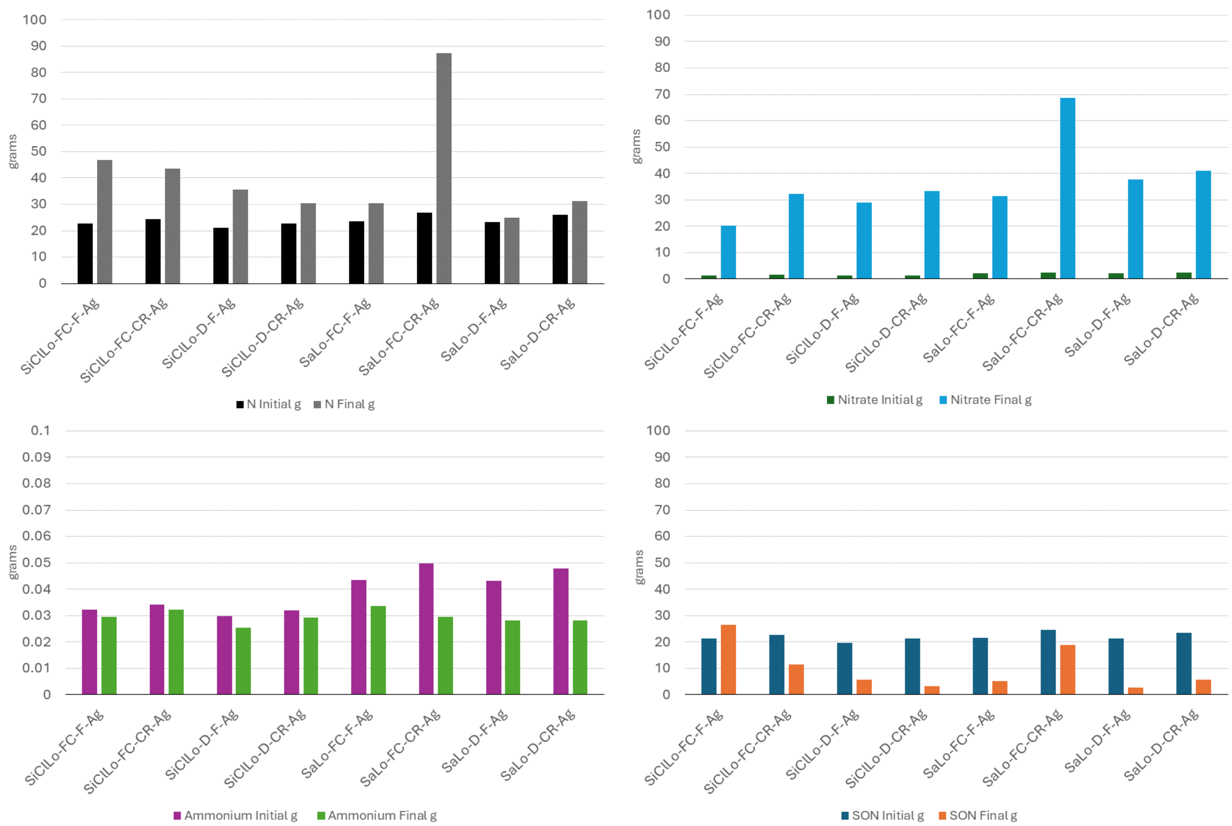

Figure 22: Nitrogen Mass Balance Pre- and Post-Treatment showing changes in each major N pool (Total N, NO_3^-, NH_4^+, Soil Organic Nitrogen) over the course of the experiment.

Key: SiClLo-Silty Clay Loam, SaLo-Sandy Loam, FC-Field Capacity, D-Drought, F-Flooding, CR-Capillary Rise, Ag-Agricultural Runoff, DI-Deionized Water

4. Discussion

4.01 Overview

Our results suggest that riparian soils will be less effective at removing N but better at removing P in the drier climate predicted for much of the Southern Plains of the United States. As drought conditions worsen throughout the region, oxygen can diffuse further into the soil. This will prevent complete denitrification, leading to the production of N_2O, a potent greenhouse gas. However, drought conditions will benefit P removal since oxygen will no longer be a limiting variable in P sorption. Critically, infrequent but intense precipitation events, also predicted under future climate scenarios, can temporarily waterlog riparian soils, which will induce temporary anaerobic conditions. These conditions will force microbial populations to use Fe as a terminal electron acceptor, reducing the iron from Fe(III) to Fe(II) and allowing P to leach to soil pore water. Clay-rich soils will be more efficient at removing N than sandier soils, but sandier soils will be more likely to retain sorbed P during intense precipitation. The clay-rich soils limit oxygen diffusion and retain more water, which favors denitrification. Conversely, the sandier soils allow greater oxygen diffusion, which favors P sorption.

4.02 The Effects of Climate Change on Riparian Denitrification

We analyzed the influence of soil moisture, precipitation, and soil texture on nitrogen cycling within riparian buffer soils. In riparian buffers, denitrification under field capacity scenarios is already a well-researched process (Burgin & Groffman, 2012; Vidon et al., 2018; Pandey et al., 2020). Our results reaffirm that soils at field capacity are the most efficient in removing nitrate due to their optimal moisture content, facilitating microbial processes such as denitrification in the smallest, water-filled pores. However, during drought conditions, the soil's capacity for nitrate removal is reduced due to inhibited denitrification pathways brought on by increased oxygen diffusion into the soil profile. While this change in soil moisture does change when nitrate is leached, it also results in pore water concentrations that are higher in nitrate (Figure 18, Supplemental Material F-18-F-19). The intense precipitation associated with flooding exacerbates nitrate leaching, flushing nitrate from the soil before it can be fully denitrified. Statistical analyses corroborate that Moisture Regime and Water Application, our two climate proxies, were statistically significant in determining nitrate and ammonium concentrations (Tables 3, 4, Supplemental Material F-3, F-4). Therefore, as soil moisture regimes in Oklahoma shift towards drought and precipitation becomes less frequent but more intense, riparian soils should remove less nitrate from surface runoff.

The clay minerals identified in the XRD analysis (Figure 16), primarily smectites and illites, are crucial in controlling nitrogen concentrations. Prior studies have shown that clay minerals limit oxygen diffusion under field capacity conditions, which allows microbes to switch to nitrate as an alternate terminal electron acceptor. (Cahoon et al., 2011; Burgin & Groffman, 2012; Keiluweit et al., 2018). Additionally, 2:1 clay minerals can immobilize ammonium through interlayer cation exchange (Doram & Evans, 1983). Our data show that clay content significantly controls nitrate and ammonium pore water concentrations (Figures 18-19; Supplemental Material F-18-F-21; Tables 3, 4). This control on nitrogen concentrations occurs through the interlayer cation exchange capacity for ammonium, coupled with clay minerals’ ability to restrict oxygen diffusion—thereby facilitating nitrate reduction under low-oxygen conditions.

Our data also demonstrate that sandier soils, consistent with previous cultivation, result in soils that are increasingly unable to regulate nitrate and ammonium concentrations, a phenomenon that is notably more pronounced during drought (Supplemental Material F-19, F-21; Tables 3, 4). Therefore, restored riparian buffers, although beneficial, do not function with the same efficacy as their untouched counterparts.

Additionally, our results present limited evidence consistent with dissimilatory nitrate reduction to ammonium (DNRA). Previous findings on DNRA support that it can occur within riparian buffers in tropical environments (Davis et al., 2008; Fridel et al., 2018; Pandey et al., 2020). However, our results indicate that DNRA may also be necessary for N cycling in subtropical environments. We observed significant decreases in nitrate concentrations and subsequent immediate increases in ammonium concentrations, with differences by climate regime. However, the difference between nitrate and ammonium porewater concentrations were four orders of magnitude apart, with around 1 mg/L of ammonium for every 1 g/L of nitrate. Specifically, the Silty Clay Loam soils undergoing Flooding with Agricultural Runoff and the Sandy Loam Soils under Field Capacity moisture conditions with Agricultural Runoff applied through Capillary Rise treatments exhibit decreases in porewater nitrate and subsequent increases in porewater ammonium (Figures 19-22). Additionally, post hoc Wald tests indicate that ammonium concentrations are partially dependent on Water Type, which also lends credence to the existence of DNRA as we did not add ammonium fertilizer to our simulated agricultural runoff. Our results also indicate a smaller decline in bioavailable ammonium levels than the significant increase in bioavailable nitrate after KCl extractions (Tables 8, 9). The ammonium must have another source since the agricultural runoff only contained nitrate and phosphate fertilizers. We propose that ammonium is replenished from the soil organic nitrogen pool and through DNRA derived from the nitrate in the simulated runoff. This effect is further corroborated by the high ARQ values (Supplemental Material F-23, F-24), consistent with anaerobic respiration and soil organic matter mineralization. However, this process occurs to a lesser extent under drought conditions and in sandier soils due to increased oxygen diffusion, which disrupts the low-oxygen environment typically needed for effective denitrification.

Elemental analysis indicates that under drought conditions, less nitrogen is fixed compared to field capacity samples, influencing the amount of soil organic nitrogen (SON) and inorganic nitrogen available for the conversion to ammonium. (Figure 22; Tables 12, 13; Equations 6-8). These reactions are consistent with the weakly acidic soil and pore water pH levels observed during the experiment (Tables 2, 3, 7; Figure 6; Supplemental Material F-16, F-17).

Consequently, nitrogen cycling in riparian buffers will be affected by changes in moisture regime and water application brought on by anthropogenic climate change. The intricate interplay between soil physical properties, microbial activity, and environmental conditions shapes the efficiency of nitrate removal processes. Notably, under varying moisture regimes, the capacity of riparian soils to regulate nitrogen concentrations is affected, with diminished efficacy during Drought conditions and intense precipitation events for the silty clay loam soils. Sandier soils, however, have diminished nitrogen removal capacity during Field Capacity and Capillary Rise conditions (Figure 22). These findings highlight the importance of preserving soil structures and carefully considering land-use practices in managing riparian buffers. As climate change continues to alter precipitation patterns and soil moisture regimes, understanding and adapting to these changes will be essential for maintaining these critical systems' ecological integrity and functionality. Our research contributes valuable insights into these dynamics, offering a foundation for future studies and strategies to enhance riparian buffer efficiency in the face of evolving environmental challenges.

4.03 The Effects of Climate Change on Riparian Phosphorus Sorption

Oxygen diffusion rates, clay mineral content, and short-range order (SRO) iron and aluminum oxides influence phosphorus sorption in soils. Our study aligns with existing research (Pote et al., 1996; Sharpley & Smith, 1996; Sharpley & Smith, 2009; Andersson et al., 2013; Asomaning, 2020), which suggests that the increased oxygen diffusion and intense flooding events predicted in future climate scenarios significantly impact phosphorus cycling in soils. In drought conditions, phosphorus sorption is enhanced due to increased oxygen diffusion, which facilitates binding to clays and metal oxy(hydr)oxides. This observation confirms that drier soil conditions predicted in future climate scenarios are more conducive to phosphate retention.

Interestingly, our data also show that the clay-rich soils generally exhibit good phosphorus sorption capacity with their soil texture, confirmed by statistical analyses (Figure 20; Table 5; Supplemental Material F-22, F-23). However, their performance notably diminishes during flooding events, where significant amounts of pore water phosphate are present (Supplemental Material F-22). The intense flooding allowed phosphorus sorbed onto the edges of clay minerals and SRO oxides to re-enter the solution in an anaerobic environment (Supplemental Material F-24, F-25) and leach out of the soil. During these events, phosphate leaching from SRO oxides and clay minerals highlights a critical vulnerability. With climate change increasing flooding intensity, there is a high risk of escalated phosphate contamination in surface waters.

The texture of these sandier soils also differs significantly from the clay-rich soils, primarily due to the reduced presence of clay minerals. In the context of phosphorus cycling, the fewer clay minerals in the sandier soils impact how phosphorus interacts with the soil. Despite the decrease in these minerals, their role remains pivotal in phosphorus sorption. However, short-range order (SRO) iron and aluminum oxides do compensate for these soils' limited clay minerals, as evidenced by the higher increases in 0.5 M HCl-extractable Fe (II) and Fe(III) in the sandier soils (Tables 10, 11). These oxides can effectively bind phosphorus, even in small quantities, reducing its mobility in soil pore water. Although these sandier soils contain fewer clay minerals, the increased oxygen diffusion brought on by increased macroporosity and drought compensates by facilitating more efficient phosphorus sorption in the sandier soils (Supplemental Material F-24, F-25; Table 5).

In our study, soils at field capacity, considered ideal for many soil functions, performed poorly regarding phosphorus sorption. This is likely due to limited oxygen diffusion in these conditions, which hampers phosphorus binding to soil particles (Supplemental Material F-22, F-24, F-25). Furthermore, flooding exacerbated phosphorus release, producing higher phosphate concentrations in the solution. This aligns with the observed tendency of flooded soils to release bound nutrients. This factor becomes increasingly important considering the impacts of predicted climate scenarios, changes in moisture regime, and water application on soil phosphorus availability (Supplemental Material F-22, F-23). Statistical analyses support this, with the interaction of Land Use and Water Application providing the most significant effect on the sandy and clay-rich soils (Table 5). These findings are significant because high phosphate concentrations could leach out of soil depending on the rainfall during these flooding events.

4.04 The Effects of Climate Change on Riparian Iron Redox Cycling

Iron cycling through oxidation and reduction is an essential biogeochemical process that plays a significant role in soil's cycling of nutrients, carbon, and nitrogen, even under future climate scenarios. Their Gibbs Free Energy indicates that iron-based compounds are less favored as terminal electron acceptors than nitrate and manganese compounds, offering lower energy yields. (Patrick & Jugsujinda, 1992; Rissmann, 2011; Hodges et al., 2019b). Iron and sulfur are also biogeochemically linked since sulfur can act as a reducing agent for iron in anaerobic soils (Li et al., 2012). Additionally, previous research has identified that high concentrations of Fe(II) are linked with increasing rates of DNRA in anaerobic soils (Pandey et al., 2020). Clay minerals are also hubs for iron redox cycling, particularly 2:1 clay minerals like smectites and illites (Shelobolina et al., 2012).

However, the predicted changes in soil moisture and water application should affect iron redox cycling, like other biogeochemical cycles. Our data indicate that decreased soil moisture favors the formation of extractable Fe(III) over extractable Fe(II) due to increased oxygen diffusion brought on by drought, which lowers ARQ (Tables 10, 11; Figures 25, 26). Conversely, field capacity and flooded and clay-rich samples favor the formation of Fe(II) over Fe(III) due to the reduced oxygen diffusion rate in water and clay minerals. These data are consistent with other research on anoxic soils, indicating that the riparian zone exhibits reducing conditions under these climate proxies.

Further expanding on the role of iron, our research has revealed that higher concentrations of 0.5 M HCl-extractable Fe(II) are consistently found in clay-rich soils experiencing drought and flooding conditions. This observation provides additional support for a potential link between extractable Fe(II) prevalence and the process of dissimilatory nitrate reduction to ammonium (DNRA), as suggested by Pandey et al. (2020). Increased extractable Fe(II) concentrations and ARQ values (Tables 10, 11; Supplemental Material F-24, F-25) in the flooded and field capacity soils indicate a reducing, anaerobic environment favoring DNRA activity. These findings highlight the intricate relationship between soil conditions, iron redox cycling, and nitrogen transformations.

Therefore, iron redox cycling, like other biogeochemical cycles, is susceptible to changes in soil moisture and water application patterns, as predicted under future climate scenarios. Our data show that reduced soil moisture conditions, often associated with drought, promote the formation of Fe(III) over Fe(II) due to increased oxygen diffusion. This aligns with previous work, which states that extractable Fe(II) content increases as precipitation amounts increase (Hodges et al., 2019b). In contrast, field capacity and flooded and clay-rich soils favor the formation of Fe(II) over Fe(III), which is attributable to the reduced rate of oxygen diffusion in temporarily water-saturated and clay-rich environments.

4.05 The Ferrous Wheel Hypothesis

The Ferrous Wheel Hypothesis is a controversial hypothesis that states that nitrate is abiotically reduced to nitrite by Fe(II) oxidizing to Fe(III). Fe(III) then acts as an oxidizing agent for organic carbon, and the cycle repeats (Davidson et al., 2003). This hypothesis is heavily debated, with some research arguing that it exists strictly as an abiotic mechanism (Matus et al., 2019) and some research arguing that it simply does not exist (Colman et al., 2008; Schmidt & Matzner, 2009). Using our bioavailable nitrate and iron redox cycling data, we provide evidence for the Ferrous Wheel Hypothesis outside the stable isotope analyses used in other studies.

Our Silty Clay Loam soil samples with Capillary Rise water application indicate some evidence for the Ferrous Wheel Hypothesis, the reduction of nitrate to nitrite coupled with Fe(II) oxidation. These samples have relatively high concentrations of extractable Fe(II) and nitrate but low concentrations of extractable Fe(III) (Tables 10, 11). As our ARQ data, which is consistently above 1, signifying there is more CO_2 present than O_2 (Supplemental Material F-24, F-25) indicates, anaerobic respiration is occurring, suggesting that any present extractable Fe (III) must have been oxidized from Fe(II) by the slightly less energetically favorable, but more plentiful terminal electron acceptor, nitrate. This is consistent with the previously established Ferrous Wheel pathways (Matus et al., 2019). Under drought conditions, the amount of extractable Fe(II) is lower compared to field capacity conditions, but the trends are still the same (Supplemental Material F-5, F-6). Similar trends under different moisture regimes indicate that if the Ferrous Wheel exists, it is only slightly affected by changes in the moisture regime. However, a change in water application does appear to eliminate the Ferrous Wheel. Changes in nitrate leaching brought on by flooding prevent nitrate from remaining in the soil long enough to be reduced to nitrite by Fe(II). This correlates with our denitrification data, where complete denitrification to N_2 cannot occur due to the increased precipitation leaching nitrate more frequently.

However, our work has some critical limitations related to the Ferrous Wheel Hypothesis. Since we did not use ^{18}O and ^{15}N isotope measurements, we cannot calculate the direct amount of oxygen from nitrate incorporated into $Fe(OH)_3$ and how much nitrogen is incorporated into the dissolved organic nitrogen (DON) pool. Regardless, our data indicate some evidence for the existence of the Ferrous Wheel Hypothesis as an abiotic or biotic mechanism.

5. Conclusions, Implications & Future Directions

Our results indicate that predicted changes in soil moisture and water application affect vital biogeochemical cycles, namely the nitrogen, phosphorus, and iron redox cycles. Drought and flooding conditions cause significant increases in nitrate in soil pore water during leaching events, particularly in previously cultivated riparian zones. Denitrification capacity is reduced under drought conditions due to increased oxygen diffusion. Clay minerals in clay-rich soils also help mediate ammonium concentrations in soil pore water. However, phosphorus sorption improves under the predicted drought conditions. This effect is due to the increased oxygen diffusion present in drought conditions. Clay minerals also drive phosphorus sorption in clay-rich soils, while oxygen diffusion and SRO oxides are the primary drivers of phosphorus sorption in sandier soils. Phosphorus is primarily released through leaching events caused by flooding, especially in Silty Clay Loam soils. Additionally, drought conditions favor the formation of extractable Fe(III) over Fe(II) due to increased oxygen diffusion. Finally, our data indicate limited evidence for the Ferrous Wheel Hypothesis based on the amount of Fe(III) present in anaerobic conditions in clay-rich soils based on the ARQ, nitrate, and ammonium data we collected.

These data and findings provide wide-ranging implications for riparian buffer research. While some studies have investigated how soils will be affected by climate change and other studies have investigated riparian biogeochemical cycling, this research provides a unique perspective on how biogeochemical cycles in riparian buffers will function under the predicted changes in climate. By exploring this intersection, we have provided strong evidence that the predicted changes in climate will result in more nitrate entering surface waters but could decrease the amount of phosphate entering the same surface waters. Furthermore, our data indicate that DNRA occurs in subtropical soils. Additionally, our data that support the Ferrous Wheel Hypothesis further link the biogeochemical cycles of nitrogen and iron. Our data and conclusions will help biogeochemical modelers refine riparian, agricultural, and wetland models and incorporate future climate scenarios into those models. Likewise, our research adds to the growing bodies of literature regarding riparian buffer zones and the effects of future climate scenarios on soils. Our research underscores how critical riparian buffers are to soil health and water quality, even in future climate scenarios.

These findings also present numerous future directions to build upon this research. Future work should ideally focus on transforming the lab-based experiment found here into a field-based experiment. Moving to a field-based experiment will help evaluate the intersection of seasonality, changes in soil moisture, and water application. Furthermore, a field-based experiment would help determine which lab-based scenario most accurately represents current field conditions. Additionally, testing predicted temperature increases and changes in soil moisture and water application in a lab-based experiment could yield more insights into how predicted climate scenarios will affect the riparian biogeochemical cycles tested here. Finally, future work could focus on additional proof for the Ferrous Wheel Hypothesis. By recreating this lab-based experiment and using ^{18}O and ^{15}N stable isotope measurements, future work can determine how much Fe(II) is reducing nitrate based on the subsequent inclusion of ^{18}O into $Fe(OH)_3$. Furthermore, ^{15}N measurements can help determine how much NO_3-N is recycled through DNRA.

6. Acknowledgements & Declaration of Competing Interest

This research was funded through USDA Grant #2020-67034-31716 and the University of Oklahoma Mewbourne College of Earth and Energy. We want to thank Brittany Moehnke and Tiffany Legg for their assistance in sampling this research. We would also like to thank Dr. Andrew Elwood-Madden, who assisted with the Powder XRD portion of this research and reviewed this manuscript, and Dr. Kato Dee, who also reviewed this manuscript. Additionally, we would like to thank Dr. Claire Curry for her advice regarding statistical models and Joseph Nabonne for permission to use the Lexington WMA. We declare no competing interests.

7. References

Abbas, F., Hammad, H., Ishaq, W., Farooque, A., Bakhat, H., Zia, Z., . . . Cerdà, A. (2020). A review of soil carbon dynamics resulting from agricultural practices. *Journal of Environmental Management*.

Aguiar Jr., T., Raseraa, K., Parronc, L., Brito, A., & Ferreira, M. (2015). Nutrient removal effectiveness by riparian buffer zones in rural temperate watersheds: The impact of no-till crops practices. *Agricultural Water Management*, 74-80.

Andersson, H., Bergström, L., Djodjic, F., Ulén, B., & Kirchmann, H. (2013). Topsoil and Subsoil Properties Influence Phosphorus Leaching from Four Agricultural Soils. *Journal of Environmental Quality*, 455-463.

Angert, A., Yakir, D., Rodeghiero, M., Preisler, Y., Davidson, E., & Weiner, T. (2015). Using O2 to study the relationships between soil CO2 efflux and soil respiration. *Biogeosciences*, 2089-2099.

Asomaning, S. (2020). Processes and Factors Affecting Phosphorus Sorption in Soils. In G. a. Kyzas, *Sorption in 2020s*. InTechOpen.

Baas, P., Knoepp, J., & Mohan, J. (2019). Well-Aerated Southern Appalachian Forest Soils Demonstrate Significant Potential for Gaseous Nitrogen Loss. *Forests*.

Bunaciu, A., UdriŞTioiu, E., & Aboul-Enein, H. (2015). X-Ray Diffraction: Instrumentation and Applications. *Critical Reviews in Analytical Chemistry*.

Burgin, A., & Groffman, P. (2012). Soil O2 controls denitrification rate and N2O yield in a riparian wetland. *Journal of Geophysical Research-Atmospheres*.

Cahoon, D., Perez, B., Segura, B., & Lynch, J. (2011). Elevation trends and shrink–swell response of wetland soils to flooding and drying. *Estuarine, Coastal and Shelf Science*, 463-474.

Change, I. P. (2021). *Climate Change 2021: The Physical Science Basis*. Geneva: United Nations.

Chauhan, A., & Chauhan, P. (2014). Powder XRD Technique and its Applications in Science and Technology. *Journal of Analytical and Bioanalytical Techniques*.

Colman, B., Fierer, N., & Schimel, J. (2008). Abiotic nitrate incorporation, anaerobic microsites, and the ferrous wheel. *Biogeochemistry*, 223-227.

Curtin, D., Campbell, C., & Jalil, A. (1998). Effects of acidity on mineralization: pH-dependence of organic matter mineralization in weakly acidic soils. *Soil Biology and Biochemistry*, 57-64.

Data, I. C. (2023). JADE Pro. Livermore, California.

David, M., Schindler, S., Mitchell, M., & Strick, J. (1983). Importance of organic and inorganic sulfur to mineralization processes in a forest soil. *Soil Biology and Biochemistry*, 671-677.

Davidson, E., Chorover, J., & Dail, D. (2003). A mechanism of abiotic immobilization of nitrate in forest ecosystems: the ferrous wheel hypothesis. *Global Change Biology*.

Davis, J., Griffith, S., Horwath, W., Steiner, J., & Myrold, D. (2008). Denitrification and Nitrate Consumption in an Herbaceous Riparian Area and Perennial Ryegrass Seed Cropping System. *Soil Science Society of America Jorunal*, 1299-1310.

Devau, N., Le Cadre, E., Hinsinger, P., Jaillard, B., & Gerard, F. (2009). Soil pH controls the environmental availability of phosphorus: Experimental and mechanistic modelling approaches. *Applied Geochemistry*, 2163-2174.

Doane, T., & Horwath, W. (2003). Spectrophotometric Determination of Nitrate with a Single Reagent. *Analytical Letters*.

Eckert, D., & Sims, J. (2009). Recommended Soil pH and Lime Requirement Tests. *Recommended Soil Testing Procedures for the Northeastern United States*.

Friedl, J., De Rosa, D., Rowlings, D., Grace, P., Müller, C., & Scheer, C. (2018). Dissimilatory nitrate reduction to ammonium (DNRA), not denitrification dominates nitrate reduction in subtropical pasture soils upon rewetting. *Soil Biology and Biochemistry*, 340-349.

Gates-Rector, S., & Blanton, T. (2019). The powder diffraction file: a quality materials characterization database. *Powder Diffraction*, 352-360.

Hodges, C., Kim, H., Brantley, S. L., & Kaye, J. (2019a). Soil CO2 and O2 Concentrations Illuminate the Relative Importance of Weathering and Respiration to Seasonal Soil Gas Fluctuations. *Soil Science Society of America Journal*, 1167-1180.

Hodges, C., Mallard, J., Markewitz, D., Barcellos, D., & Thompson, A. (2019b). Seasonal and spatial variation in the potential for iron reduction in soils of the Southeastern Piedmont of the US. *Catena*.

Hou, L., Liu, M., Carini, S., & Gardner, W. (2012). Transformation and fate of nitrate near the sediment–water interface of Copano Bay. *Continental Shelf Research*.

Huang, W., & Hall, S. (2017). Optimized high-throughput methods for quantifying iron biogeochemical dynamics in soil. *Geoderma*.

Kahle, M., Kleber, M., & Jahn, R. (2002). Predicting carbon content in illitic clay fractions from surface area, cation exchange capacity and dithionite-extractable iron. *European Journal of Soil Science*.

Keeney, D., & Nelson, D. (1982). Nitrogen-inorganic forms. *Methods of soil analysis: Part 2. Chemical and microbiological properties. ASA Monograph Number 9.*, 643-698.

Keiluweit, M., Gee, K., Denney, A., & Fendorf, S. (2018). Anoxic microsites in upland soils dominantly controlled by clay content. *Soil Biology and Biochemistry*, 42-50.

Li, Y., Yu, S., Strong, J., & Wang, H. (2012). Are the biogeochemical cycles of carbon, nitrogen, sulfur, and phosphorus driven by the “Fe(III)–Fe(II) redox wheel” in dynamic redox environments? *Journal of Soils and Sediments*, 683-693.

Liaw, A. (2022). Breiman and Cutler's Random Forests for Classification and Regression. Retrieved from https://cran.r-project.org/web/packages/randomForest/randomForest.pdf

Luo, W., Dijkstra, F., Bai, E., Feng, J., Tao-Lu, X., Wang, C., . . . Yong, J. (2015). A threshold reveals decoupled relationship of sulfur with carbon and nitrogen in soils across arid and semi-arid grasslands in northern China. *Biogeochemistry*, 141-153.

Martin, T. K. (1999). Review: Denitrification in Temperate Climate Riparian Zones. *Water, Air, and Soil Pollution*, 171-186.

Matus, F., Stock, S., Eschenbach, W., Dyckmans, J., Merino, C., Nájera, F., . . . Dippold, M. (2019). Ferrous Wheel Hypothesis: Abiotic nitrate incorporation into dissolved organic matter. *Geochimica et Cosmochimica Acta*, 514-524.

McConnell, C. A., Kaye, J. P., & Kemanian, A. R. (2020). Reviews and syntheses: Ironing out wrinkles in the soil phosphorus cycling paradigm. *Biogeosciences*.

Miller, W., & Miller, D. (1987). A micro-pipette method for soil mechanical analysis. *Communications in Soil Science and Plant Analysis*.

Moeys, J., Shangguan, W., Petzold, R., Minasny, B., Rosca, B., Jelinski, N., . . . ten Caten, A. (2018). soiltexture: Functions for Soil Texture Plot, Classification and Transformation. Retrieved from https://cran.r-project.org/web/packages/soiltexture/index.html

Mohammadi, M., Naghibi, S., Motevalli, A., & Hashemi, H. (2022). Human-induced arsenic pollution modeling in surface waters - An integrated approach using machine learning algorithms and environmental factors. *Journal of Environmental Management*, 1-12.

National Cooperative Soil Survey, United States Department of Agriculture. (2023). Port Soil Series-Official Series Description.

Neilen, A. C. (2017). Differences in nitrate and phosphorus export between wooded and grassed riparian zones from farmland to receiving waterways under varying rainfall conditions. *Science of the Total Environment*, 188-197.

Neina, D. (2019). The Role of Soil pH in Plant Nutrition and Soil Remediation. *Applied and Environmental Soil Science*.

Pandey, C., Kumar, U., Kaviraj, M., Minick, K., Mishra, A., & Singh, J. (2020). DNRA: A short-circuit in biological N-cycling to conserve nitrogen in terrestrial ecosystems. *Science of the Total Environment*.

Patrick Jr., W., & Jugsujinda, A. (1992). Sequential Reduction and Oxidation of Inorganic Nitrogen, Manganese, and Iron in Flooded Soil. *Soil Science Society of America Journal*.

Pinheiro J, B. D., & Team, R. C. (2023). nlme: Linear and Nonlinear Mixed Effects Models. Retrieved from https://CRAN.R-project.org/package=nlme

Pote, D., Daniel, T., A.N., S., Moore, J. P., Edwards, D., & Nichols, D. (1996). Relating Extractable Soil Phosphorus to Phosphorus Losses in Runoff. *Soil Science Society of America Journal*, 855-859.

R Core Team. (2022). R: A language and environment for statistical. Vienna, Austria.

Ringuet, S., Sassano, L., & Johnson, Z. (2011). A suite of microplate reader-based colorimetric methods to quantify ammonium, nitrate, orthophosphate and silicate concentrations for aquatic nutrient monitoring. *Journal of Environmental Monitoring*.

Rissman, C. (2011). *Regional Mapping of Groundwater Denitrification Potential and Aquifer Sensitivity.* Environment Southland.

Rounsevell, M., Evans, S., & Bullock, P. (1999). Climate Change and Agricultural Soils: Impacts and Adaptation. *Climactic Change*, 683-709.

Scherer, H. (2009). Sulfur in soils. *Journal of Plant Nutrition and Soil Science*.

Schmidt, B., & Matzner, E. (2009). Abiotic reaction of nitrite with dissolved organic carbon? Testing the Ferrous Wheel Hypothesis. *Biogeosciences*.

Sharpley, A., & Smith, S. (1989). Prediction of Soluble Phosphorous Transport in Agricultural Runoff. *Journal of Environmental Quality*, 313-316.

Sharpley, A., Smith, S., & R.G., M. (2009). Phosphorous Dynamics in Agricultural Runoff and Reservoirs in Oklahoma. *Lake and Reservoir Managment*, 75-81.

Shelobolina, E., Konishi, H., Xu, H., Benzine, J., Yia, M., Wu, X., . . . Roden, E. (2012). Isolation of phyllosilicate–iron redox cycling microorganisms from an illite–smectite rich hydromorphic soil. *Microbiology: Microbiological Chemistry and Geomicrobiology*.

Silver, W., Herman, D., & Firestone, M. (2001). DISSIMILATORY NITRATE REDUCTION TO AMMONIUM IN UPLAND TROPICAL FOREST SOILS. *Ecology*.

Tindall, J., Petrusak, R., & McMahon, P. (1996). Nitrate transport and transformation processes in unsaturated porous media. *Journal of Hydrology*.

University of British Columbia. (2023). The Sulfur Cycle.

Valiente, N., Jirsa, F., Hein, T., Wanek, W., Prommer, J., Bonin, P., & Gómez-Alday, J. (2022). The role of coupled DNRA-Anammox during nitrate removal in a highly saline lake. *Science of the Total Environment*.

Várallyay, G. (2010). The impact of climate change on soils and on their water management. *Agronomy Research*, 385-396.

Vidon, P. W. (2018). Twenty Years of Riparian Zone Research (1997–2017): Where To Next? . *Journal of Environmental Quality*, 248-260.

Wickham, H. (2016). ggplot2: Elegant Graphics for Data Analysis. Springer-Verlag New York. Retrieved from https://ggplot2.tidyverse.org

Wickham, H. (2023). tidyverse: Easily Install and Load the 'Tidyverse'. Retrieved from https://cran.r-project.org/web/packages/tidyverse/index.html

Wickham, H., François, R., Henry, L., Müller, K., Vaughan, D., & Posit Software, P. (2023). dplyr: A Grammar of Data Manipulation. Retrieved from https://CRAN.R-project.org/package=dplyr

Wood, S. (2023). mgcv: Mixed GAM Computation Vehicle with Automatic Smoothness. Retrieved from https://cran.r-project.org/web/packages/mgcv/mgcv.pdf

Xu, Y., Fan, J., Ding, W., Gunina, A., Chen, Z., Bol, R., . . . Bolan, N. (2017). Characterization of organic carbon in decomposing litter exposed to nitrogen and sulfur additions: Links to microbial community composition and activity. *Geoderma*.

8. Supplemental Material

8.01 Supplemental Material-Figures

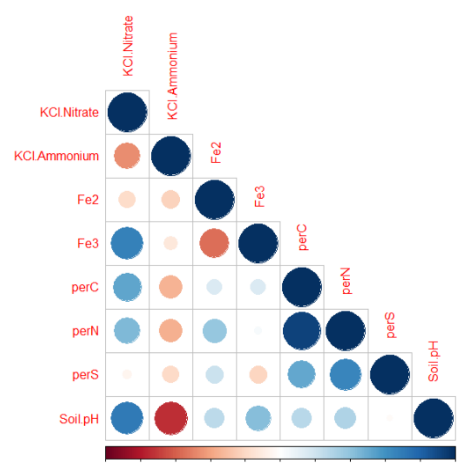

Supplemental Material F-1: Correlation Plot of Post-Incubation Data showing significant positive and negative correlations.

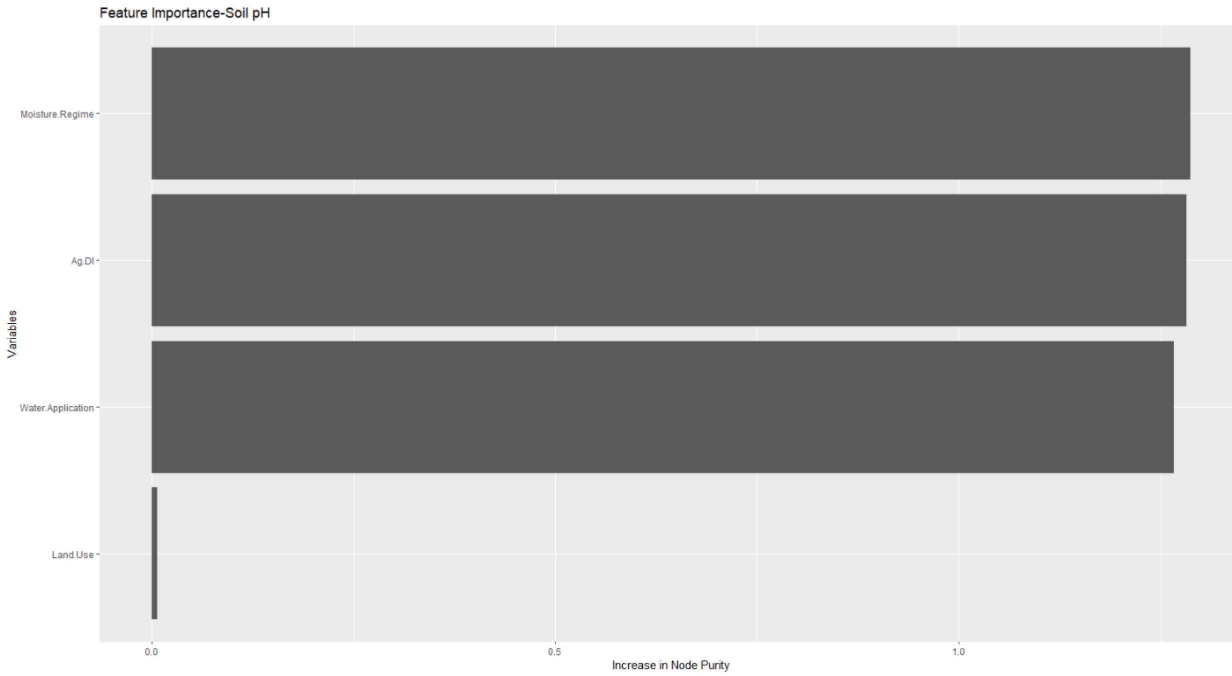

Supplemental Material F-2: Random Forest Plot of Variables Important in Predicting Soil pH as sorted by Increase in Node Purity

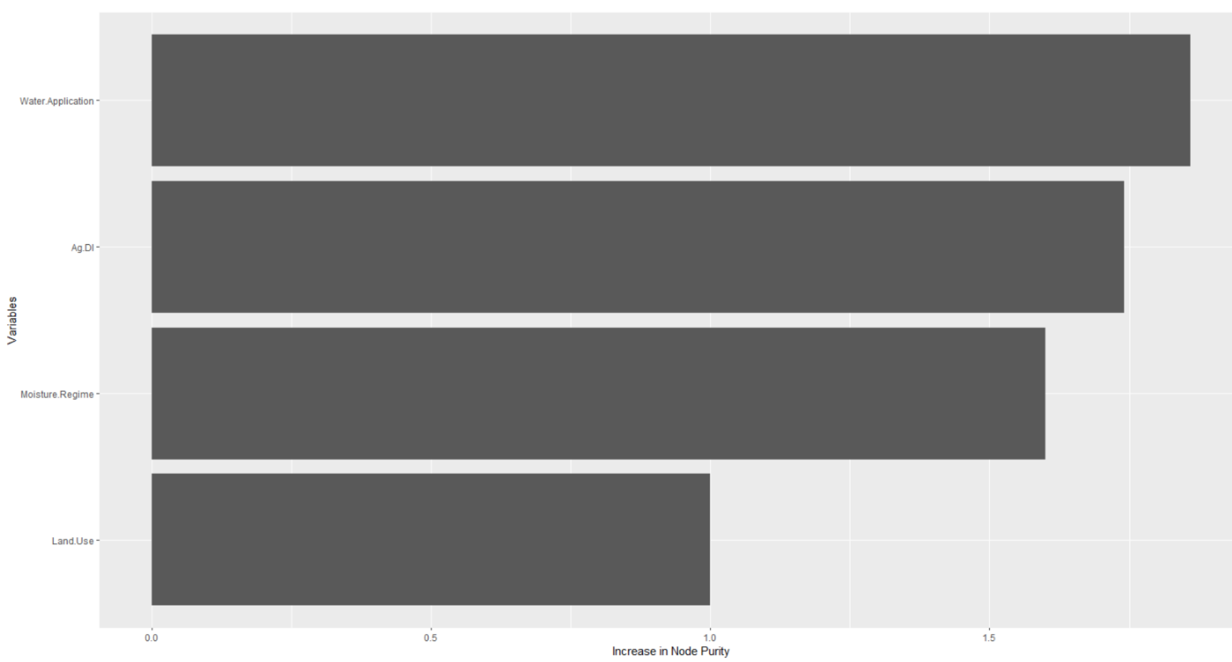

Supplemental Material F-3: Random Forest Plot of Variables Important in Predicting Bioavailable Nitrate as sorted by Increase in Node Purity

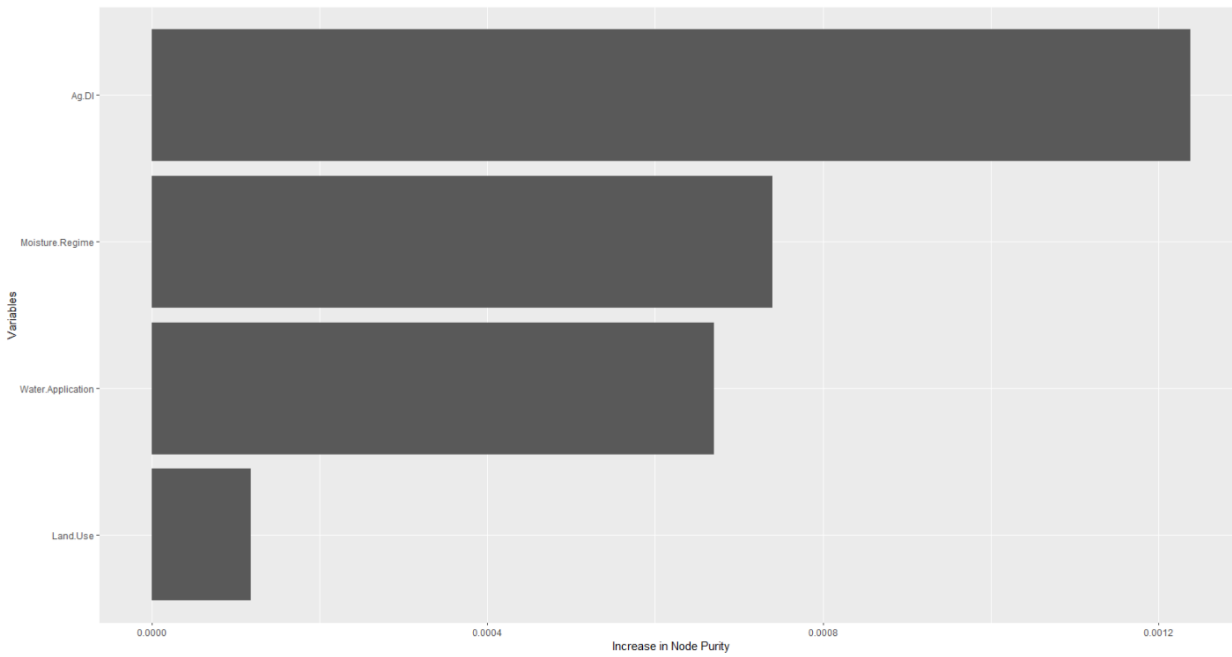

Supplemental Material F-4: Random Forest Plot of Variables Important in Predicting Bioavailable Ammonium as sorted by Increase in Node Purity

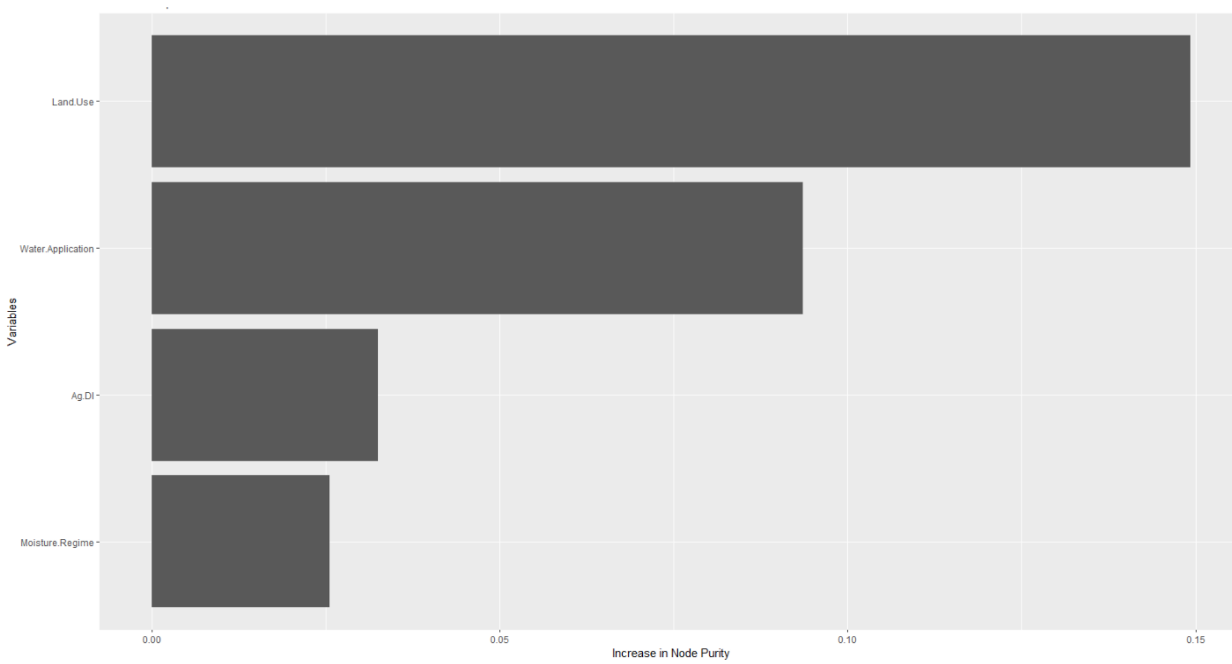

Supplemental Material F-5: Random Forest Plot of Variables Important in Predicting Fe(II) concentrations as sorted by Increase in Node Purity

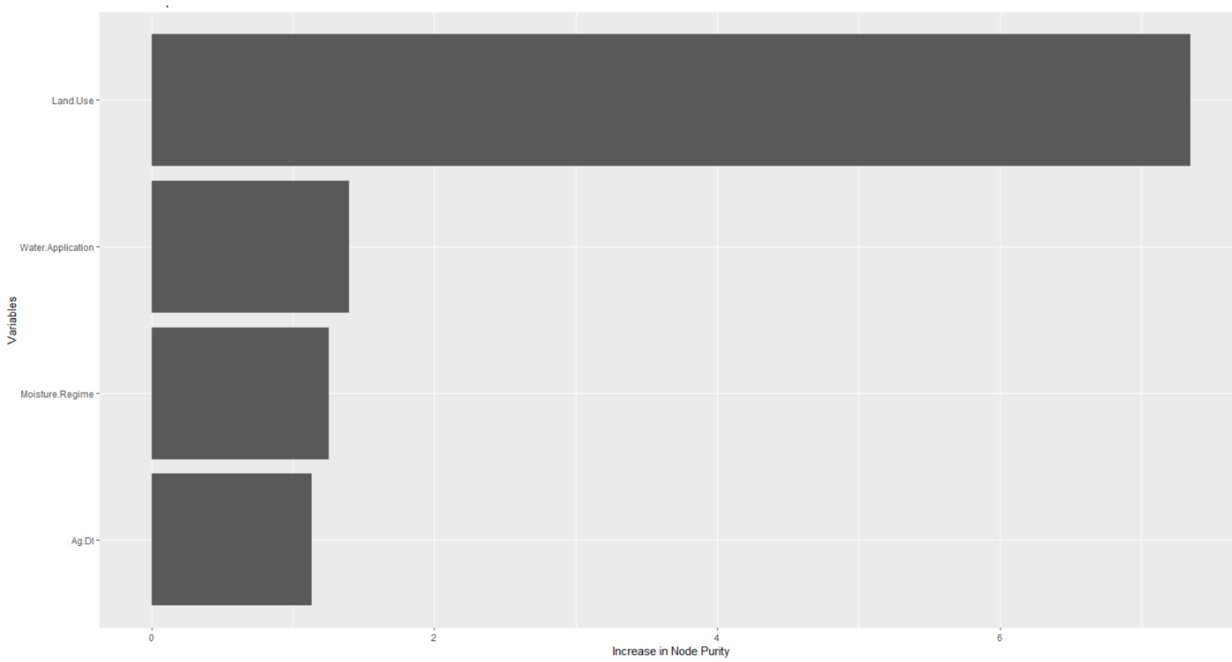

Supplemental Material F-6: Random Forest Plot of Variables Important in Predicting Fe(III) concentrations as sorted by Increase in Node Purity

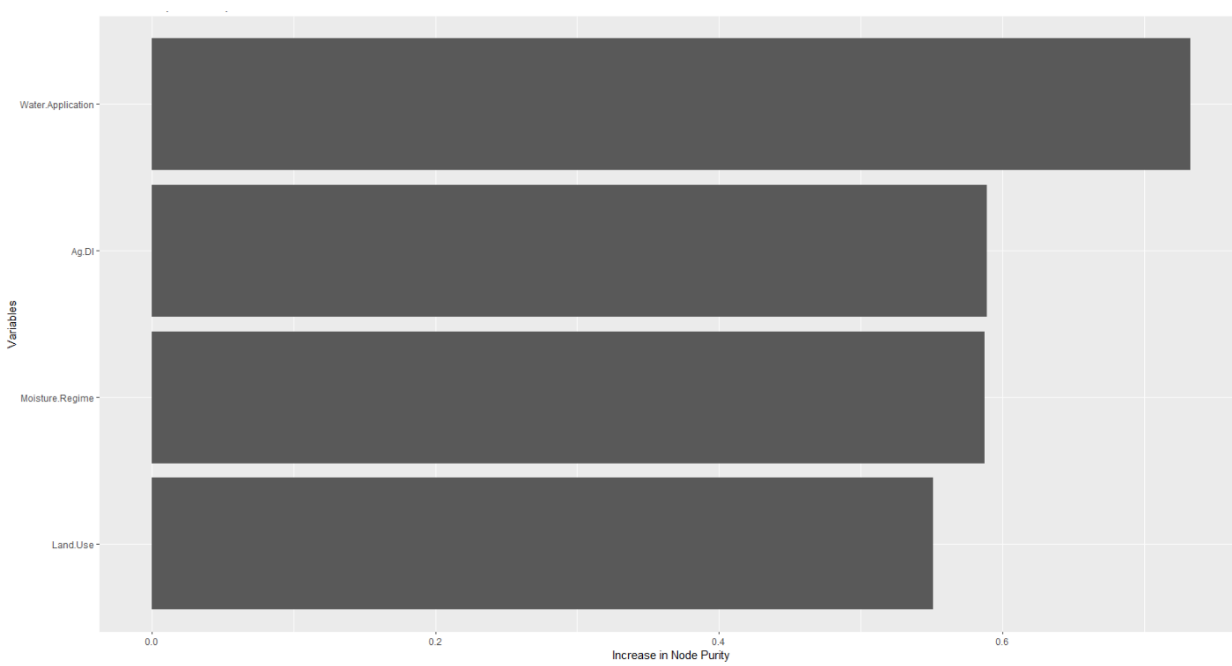

Supplemental Material F-7: Random Forest Plot of Variables Important in Predicting Total Carbon as Sorted by Increase in Node Purity

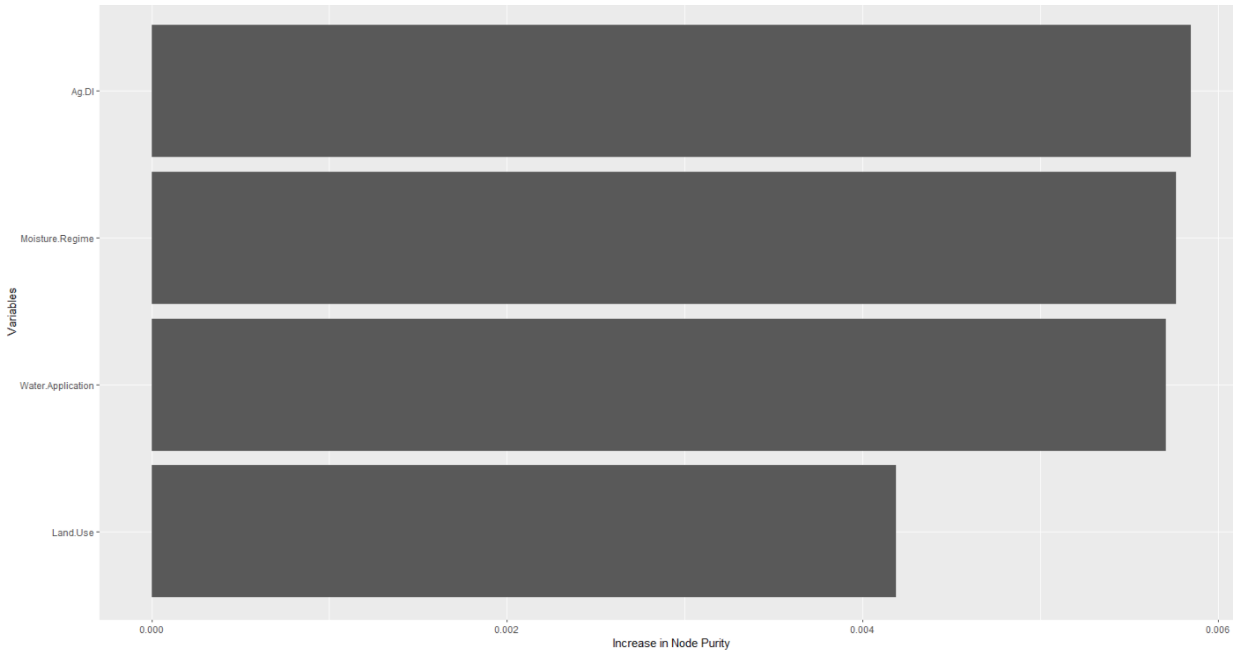

Supplemental Material F-8: Random Forest Plot of Variables Important in Predicting Total Nitrogen as Sorted by Increase in Node Purity

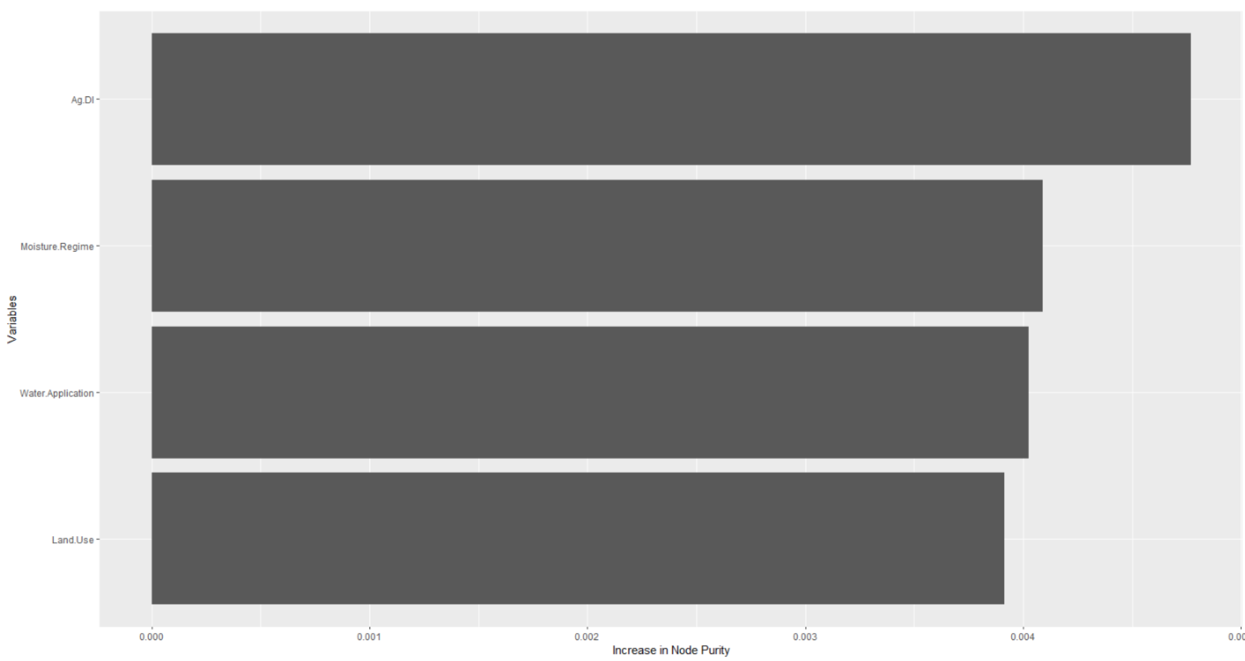

Supplemental Material F-9: Random Forest Plot of Variables Important in Predicting Total Sulfur as Sorted by Increase in Node Purity

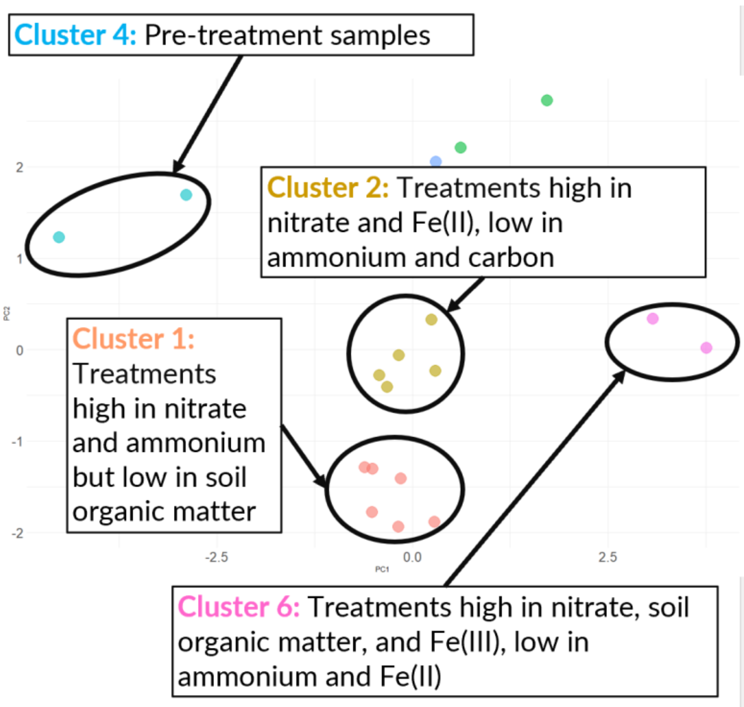

Supplemental Material F-10: Annotated K-means clustering plot of post-incubation data with PC1 and PC2 explaining 63.2% of total variance.

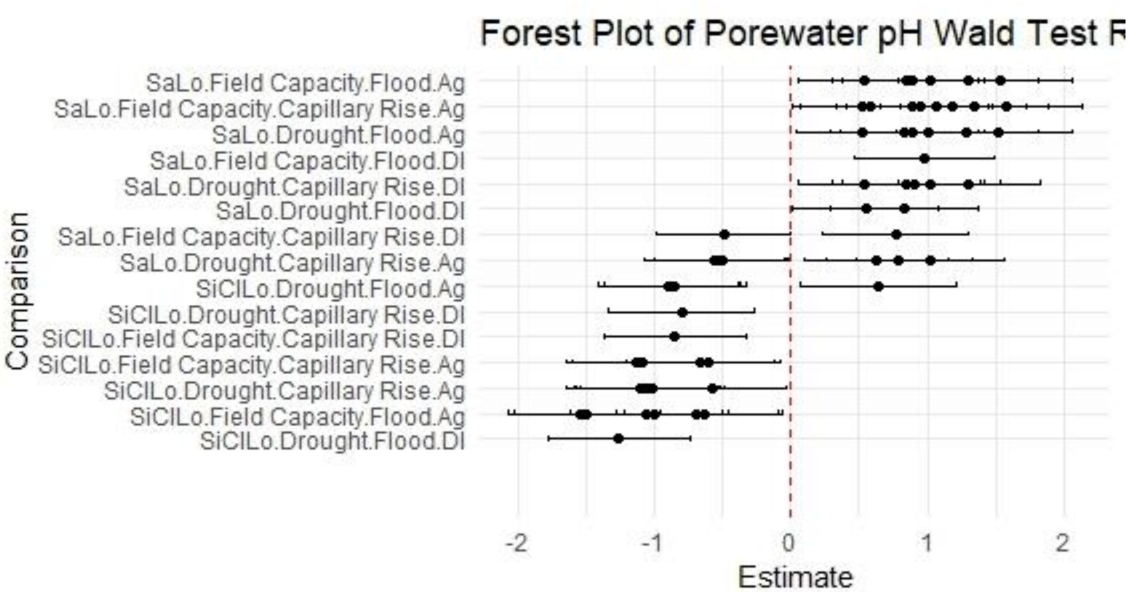

Supplemental Material F-11: Forest Plot of Significant Wald Test Results for Porewater pH. The red line indicates the line of non-significance β=0. Points indicate how many comparisons have this treatment. The lines represent 95% confidence intervals for each comparison. A negative estimate indicates that treatment has a negative effect, while a positive estimate indicates that treatment has a positive effect. If a treatment confidence interval crosses this line, the treatment and all comparisons involving this treatment are not statistically significant in determining Porewater pH.

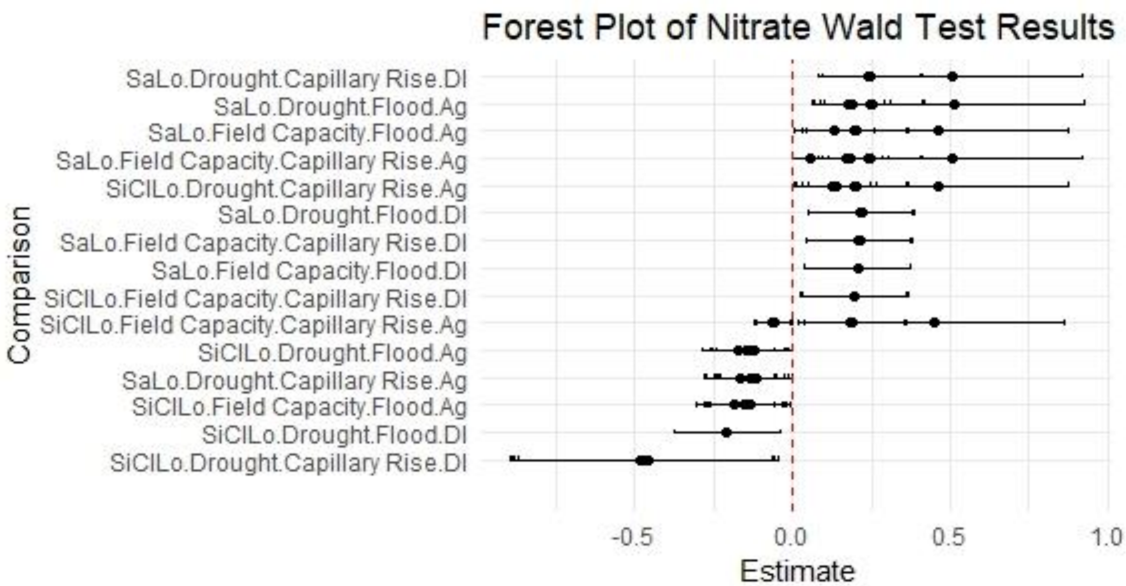

Supplemental Material F-12: Forest Plot of Significant Wald Test Results for Porewater Nitrate concentrations. The red line indicates the line of non-significance β=0. Points indicate how many comparisons have this treatment. A negative estimate indicates that treatment has a negative effect, while a positive estimate indicates that treatment has a positive effect.The lines represent 95% confidence intervals for each comparison. If a treatment confidence interval crosses this line, the treatment and all comparisons involving this treatment are not statistically significant in determining porewater nitrate.

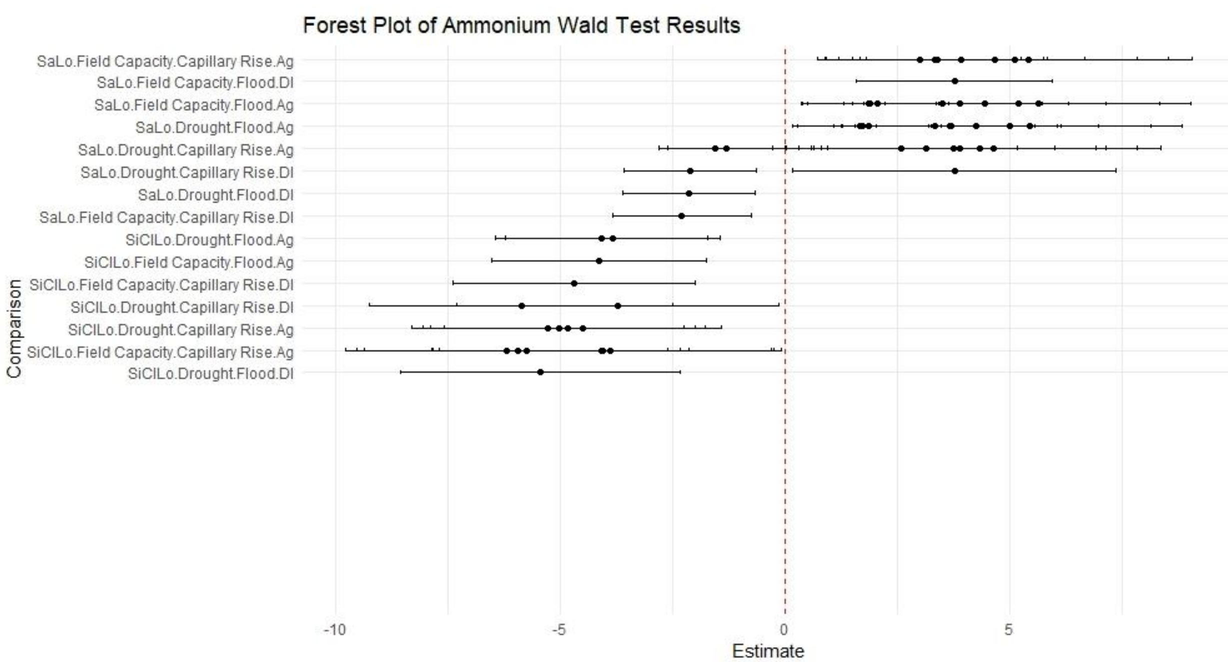

Supplemental Material F-13: Forest Plot of Significant Wald Test Results for Porewater Ammonium concentrations. The red line indicates the line of non-significance β=0. Points indicate how many comparisons have this treatment. A negative estimate indicates that treatment has a negative effect, while a positive estimate indicates that treatment has a positive effect.The lines represent 95% confidence intervals for each comparison. If a treatment confidence interval crosses this line, the treatment and all comparisons involving this treatment are not statistically significant in determining porewater ammonium.

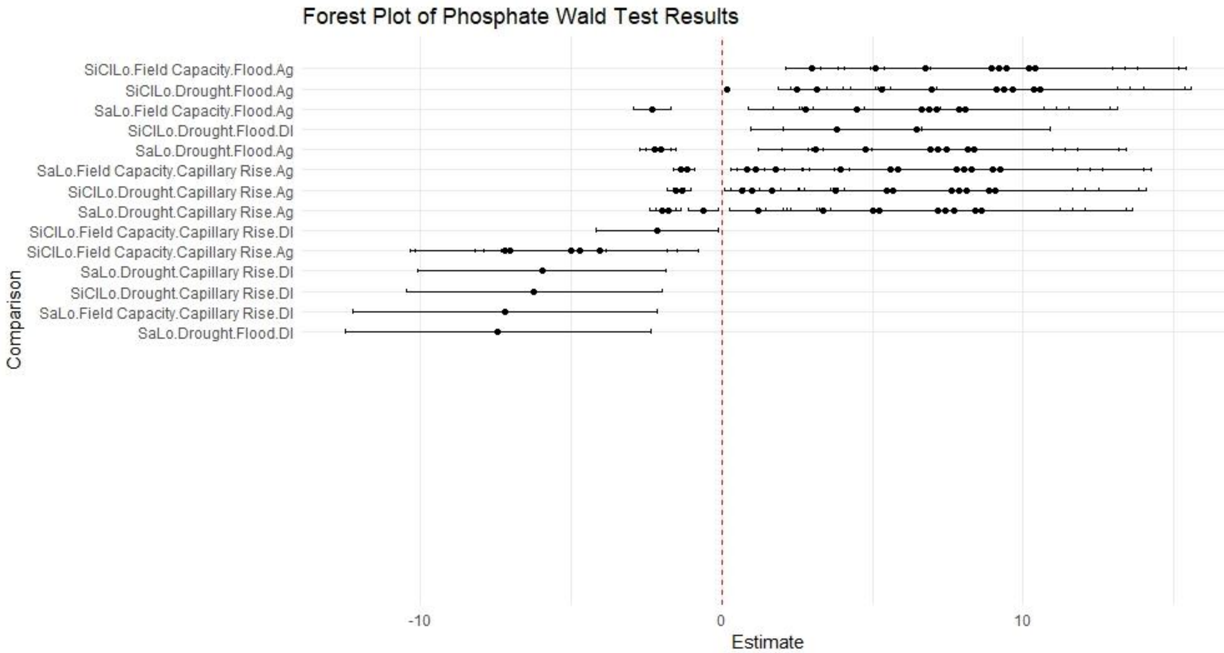

Supplemental Material F-14: Forest Plot of Significant Wald Test Results for Porewater Phosphate concentrations. The red line indicates the line of non-significance β=0. Points indicate how many comparisons have this treatment. The lines represent 95% confidence intervals for each comparison. A negative estimate indicates that treatment has a negative effect, while a positive estimate indicates that treatment has a positive effect. If a treatment confidence interval crosses this line, the treatment and all comparisons involving this treatment are not statistically significant in determining porewater phosphate concentrations.

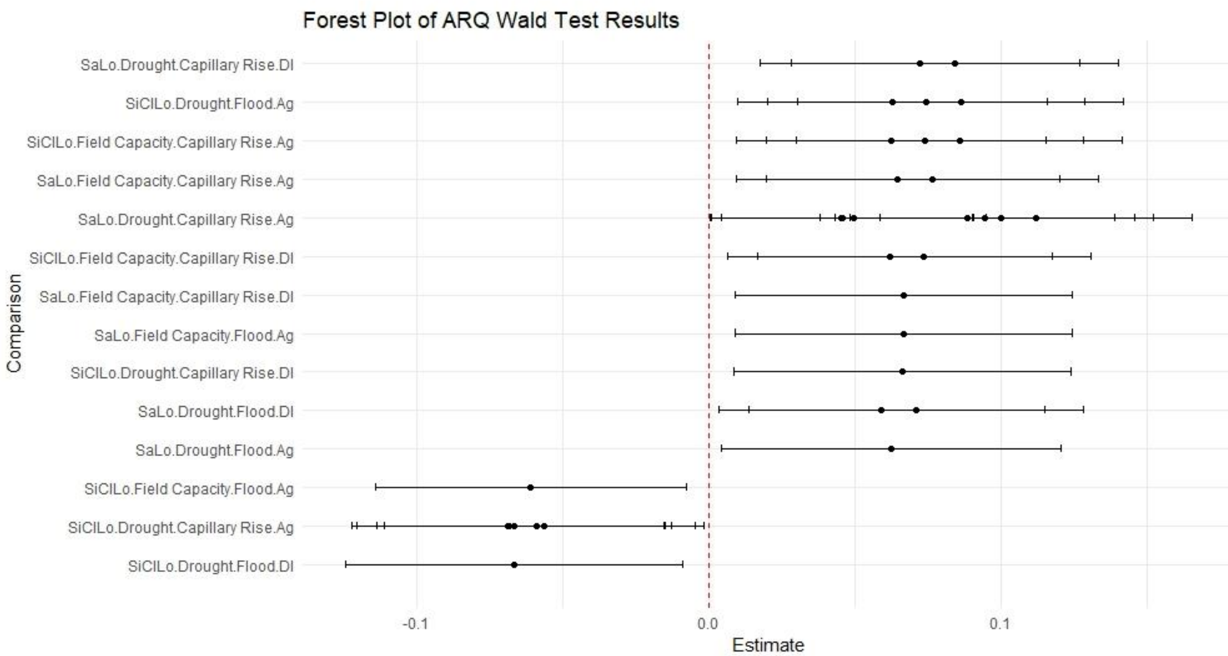

Supplemental Material F-15: Forest Plot of Significant Wald Test Results for the ARQ. The red line indicates the line of non-significance β=0. Points indicate how many comparisons have this treatment. The lines represent 95% confidence intervals for each comparison. A negative estimate indicates that treatment has a negative effect, while a positive estimate indicates that treatment has a positive effect. If a treatment confidence interval crosses this line, the treatment and all comparisons involving this treatment are not statistically significant in determining ARQ.

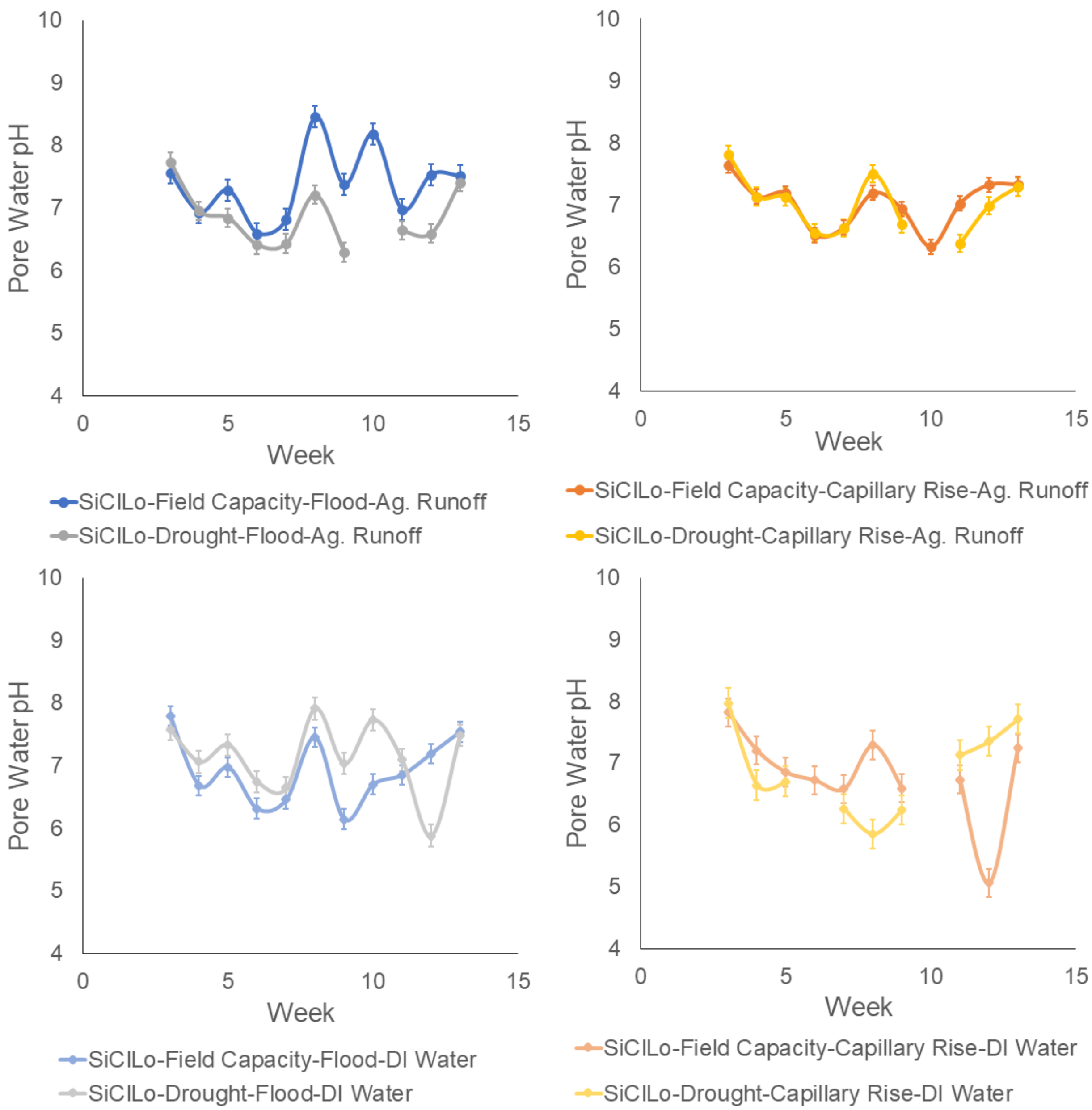

Supplemental Material F-16: Weekly Silty Clay Loam Porewater pH Concentrations

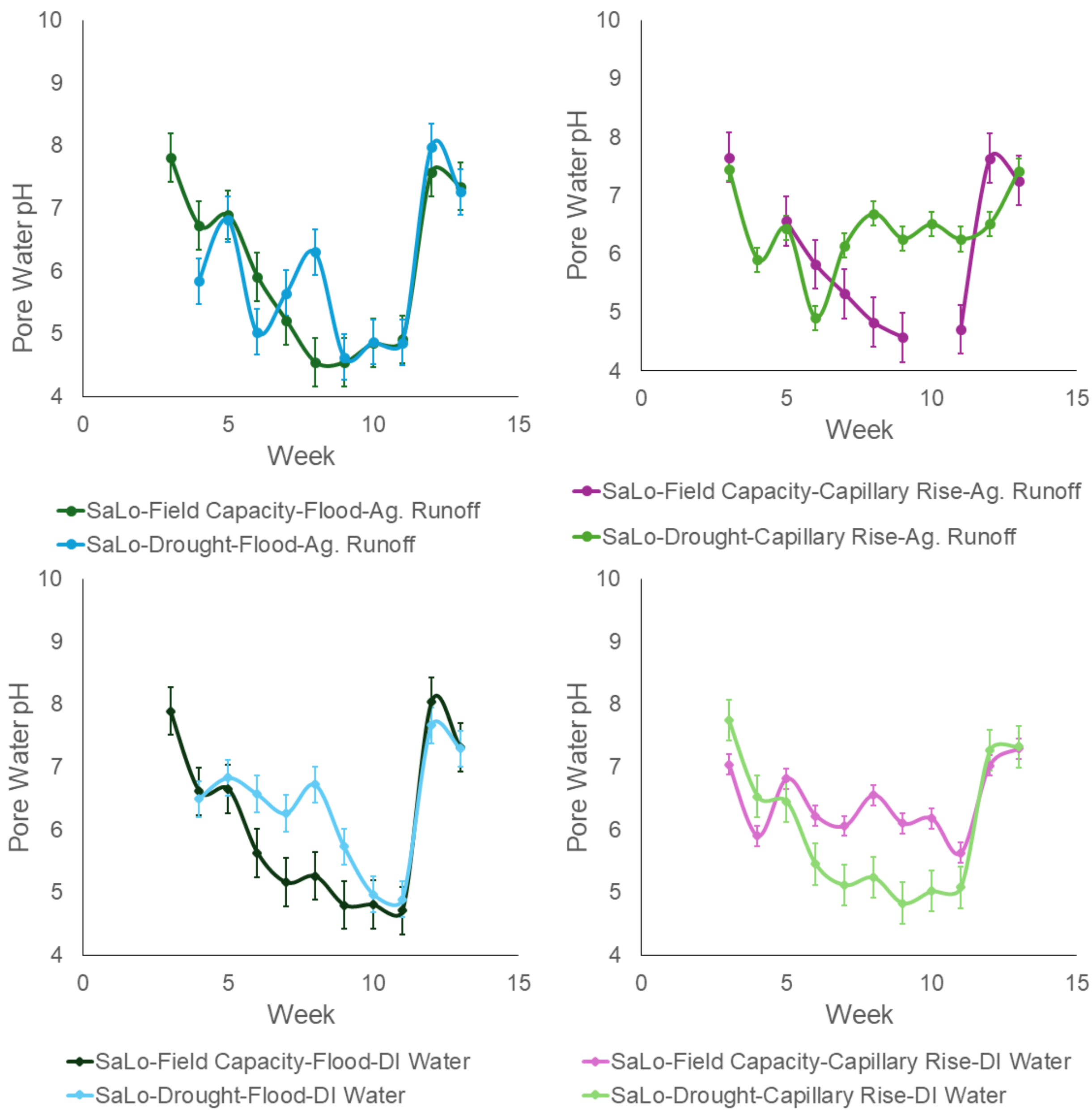

Supplemental Material F-17: Weekly Sandy Loam Porewater pH Concentrations

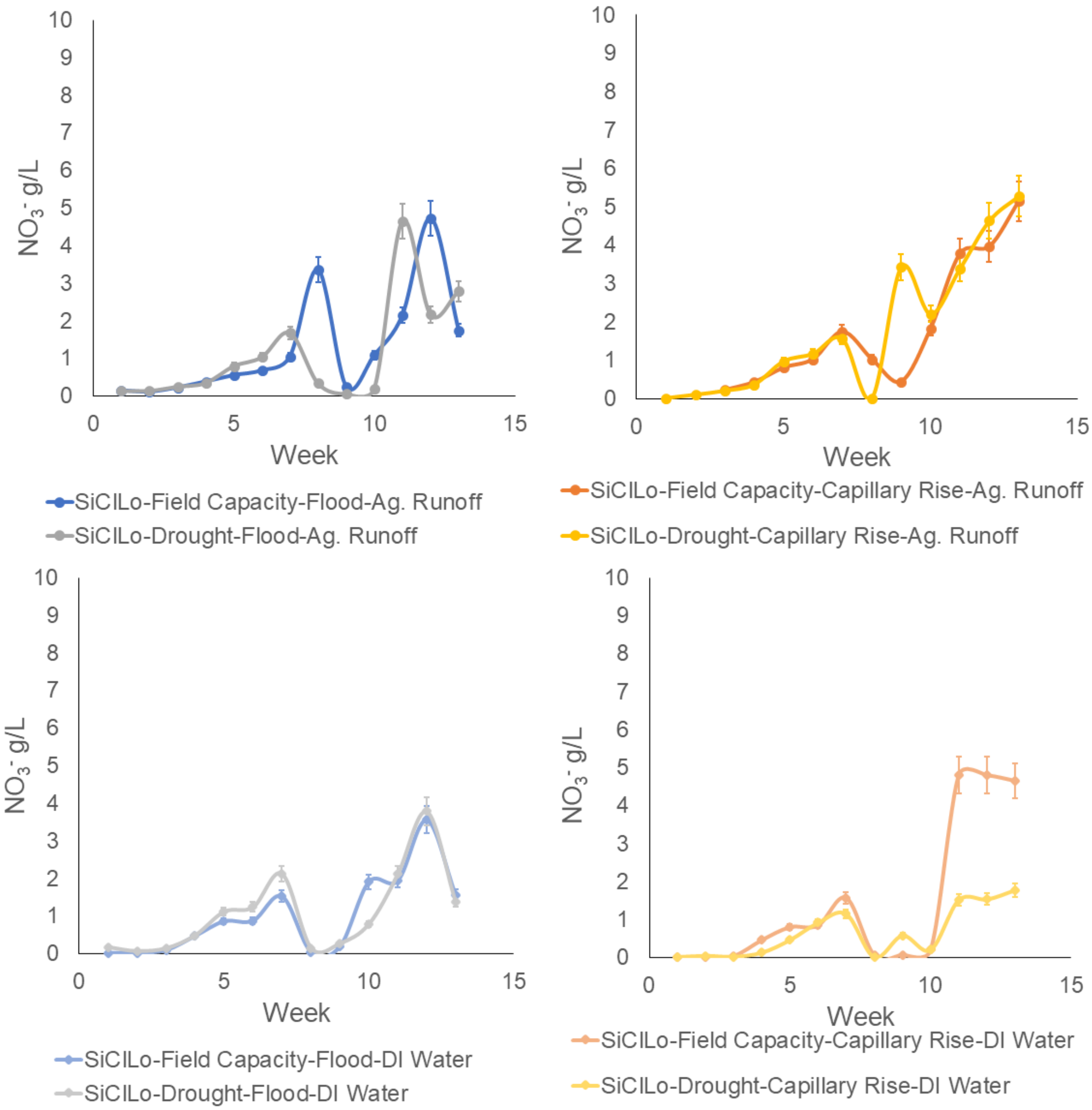

Supplemental Material F-18: Weekly Silty Clay Loam Porewater Nitrate Concentrations

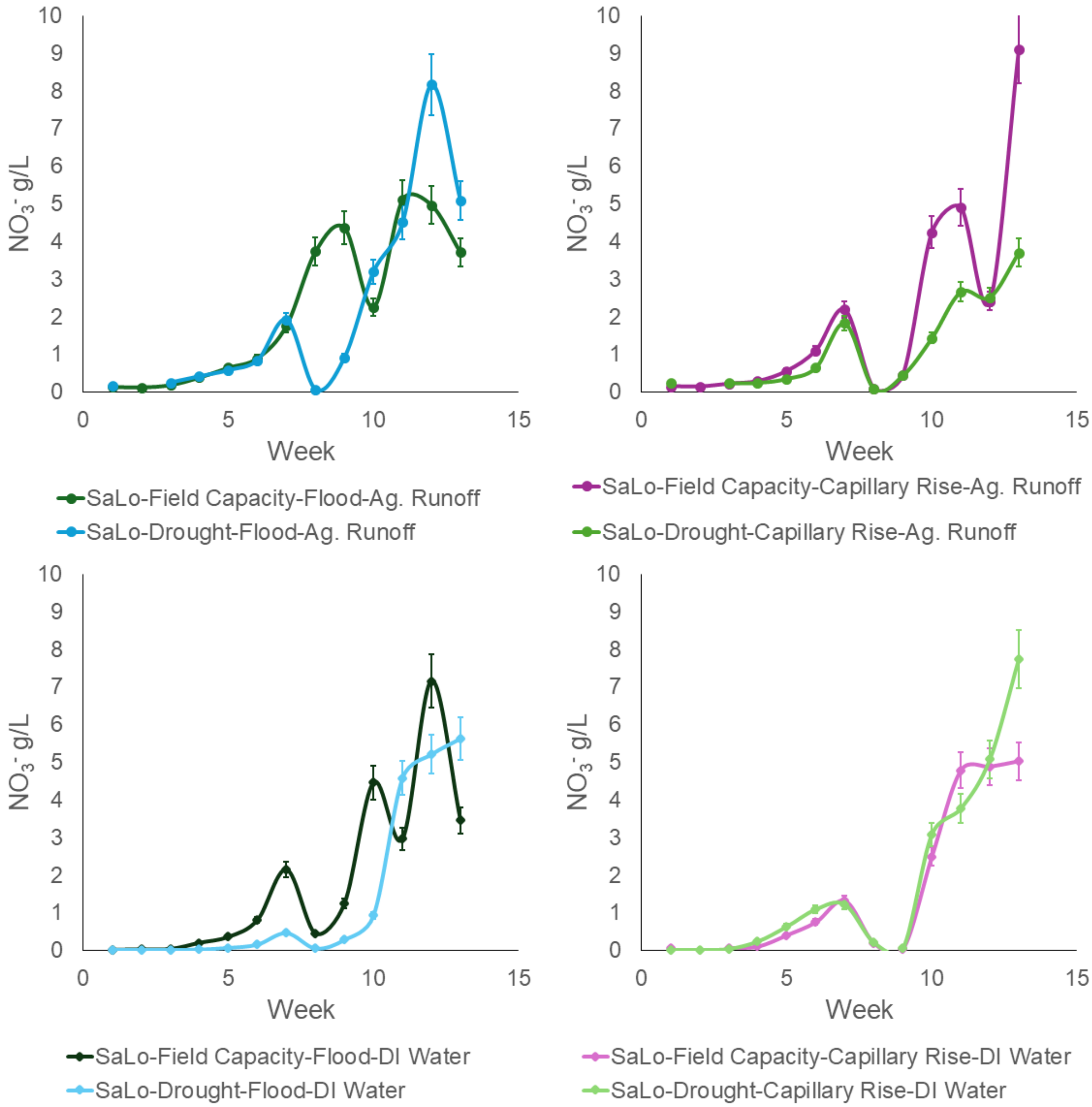

Supplemental Material F-19: Weekly Sandy Loam Porewater Nitrate Concentrations

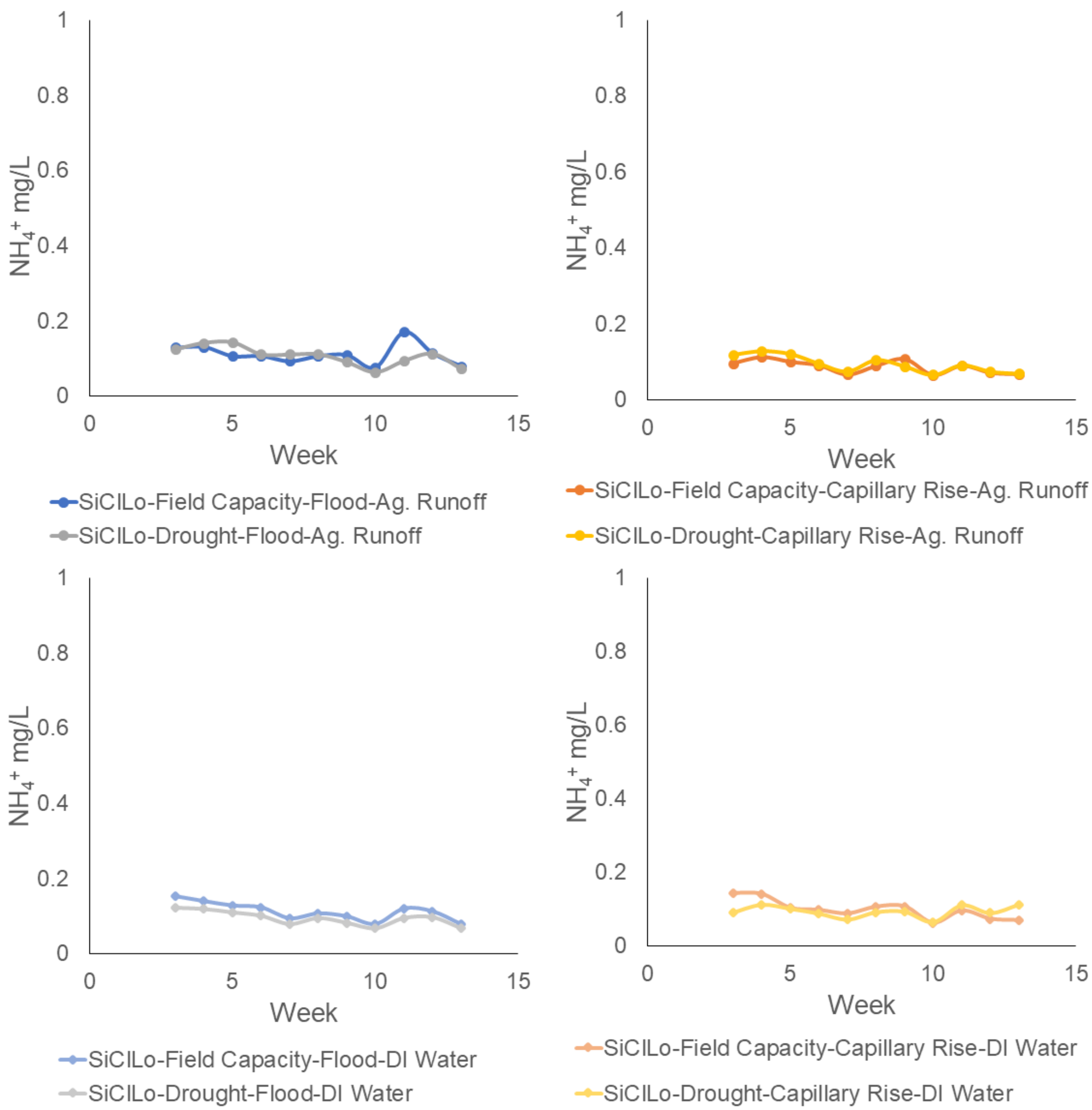

Supplemental Material F-20: Weekly Silty Clay Loam Porewater Ammonium Concentrations

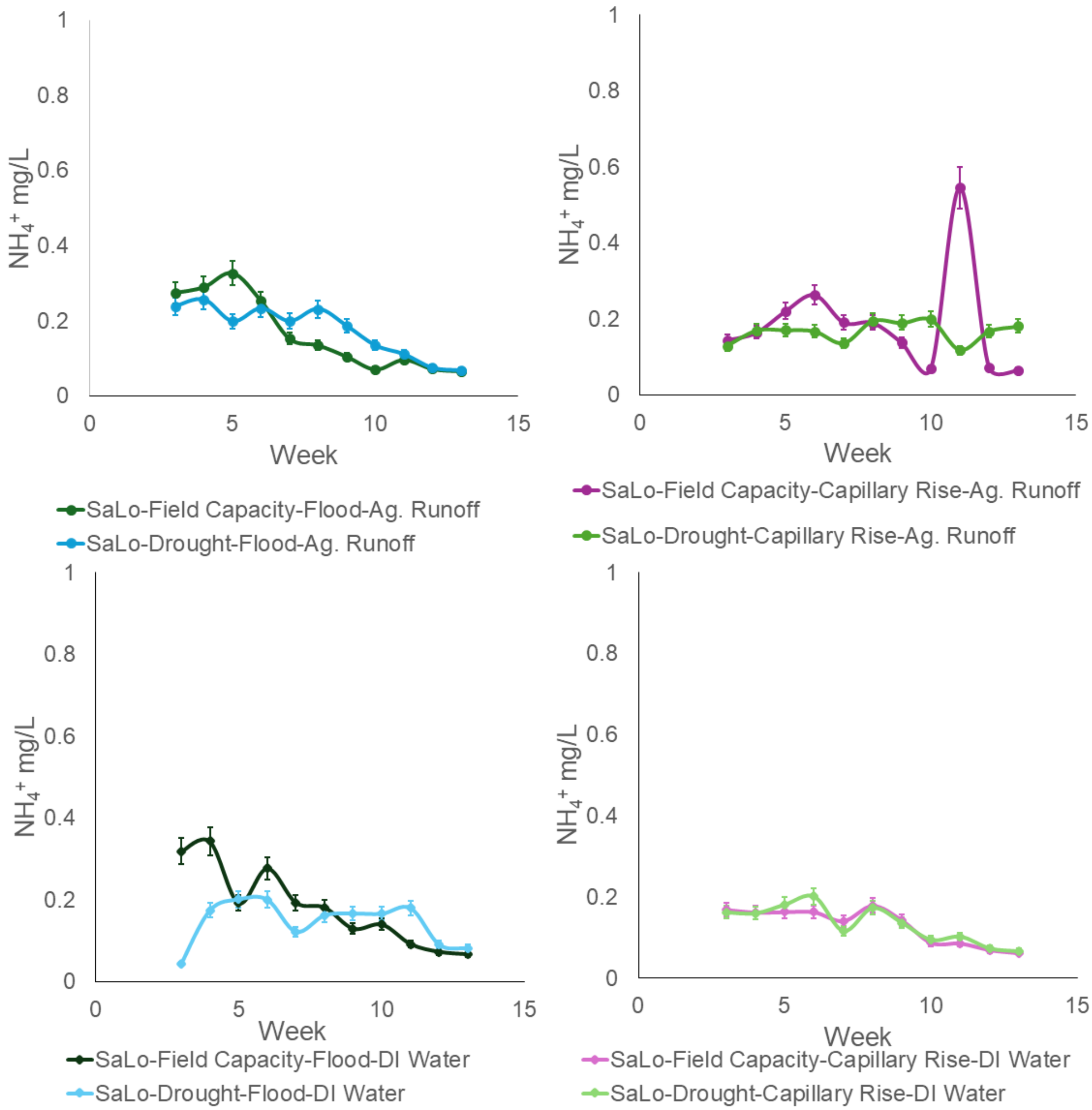

Supplemental Material F-21: Weekly Sandy Loam Porewater Ammonium Concentrations

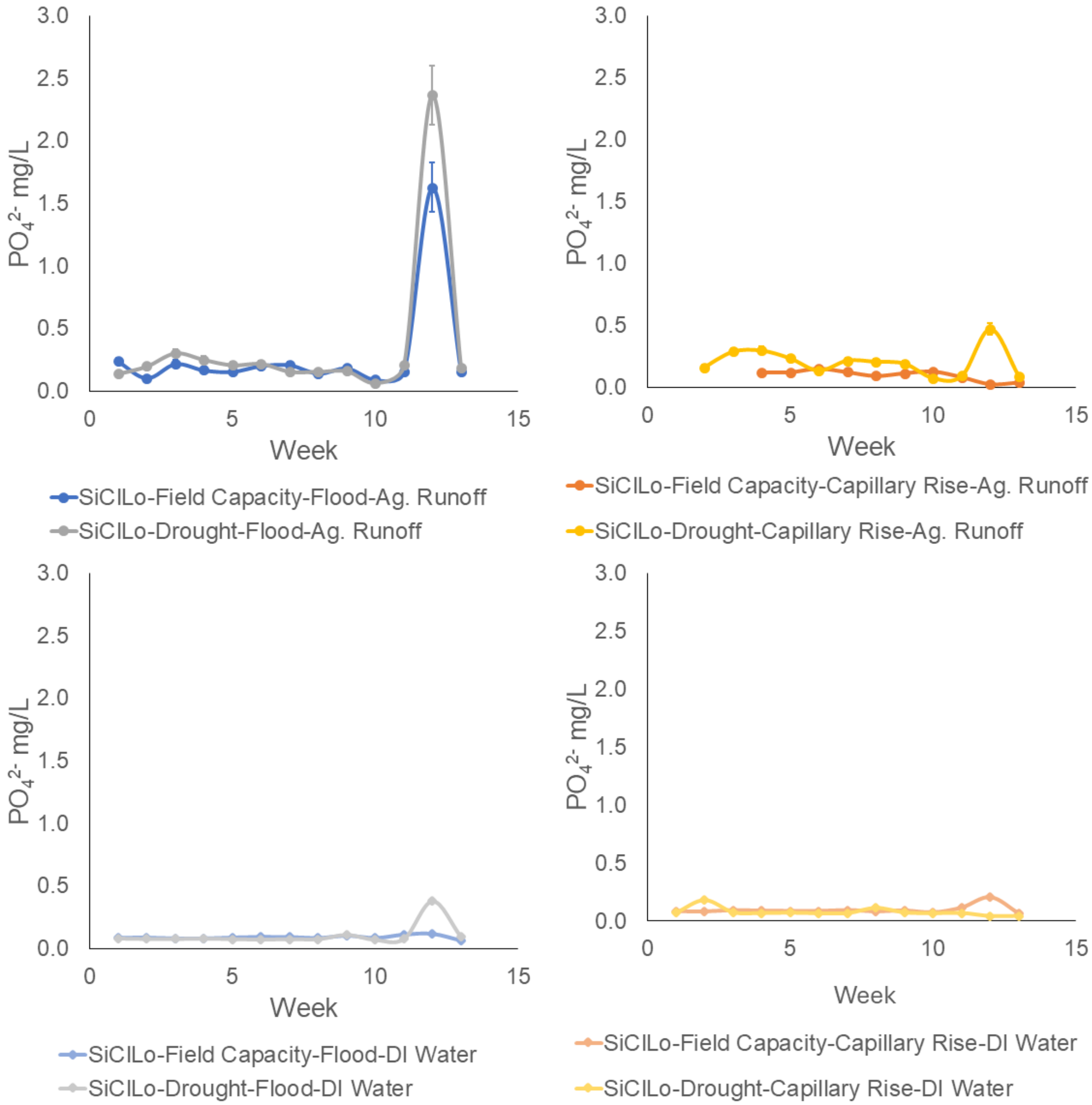

Supplemental Material F-22: Weekly Silty Clay Loam Porewater Phosphate Concentrations

Supplemental Material F-23: Weekly Sandy Loam Porewater Phosphate Concentrations

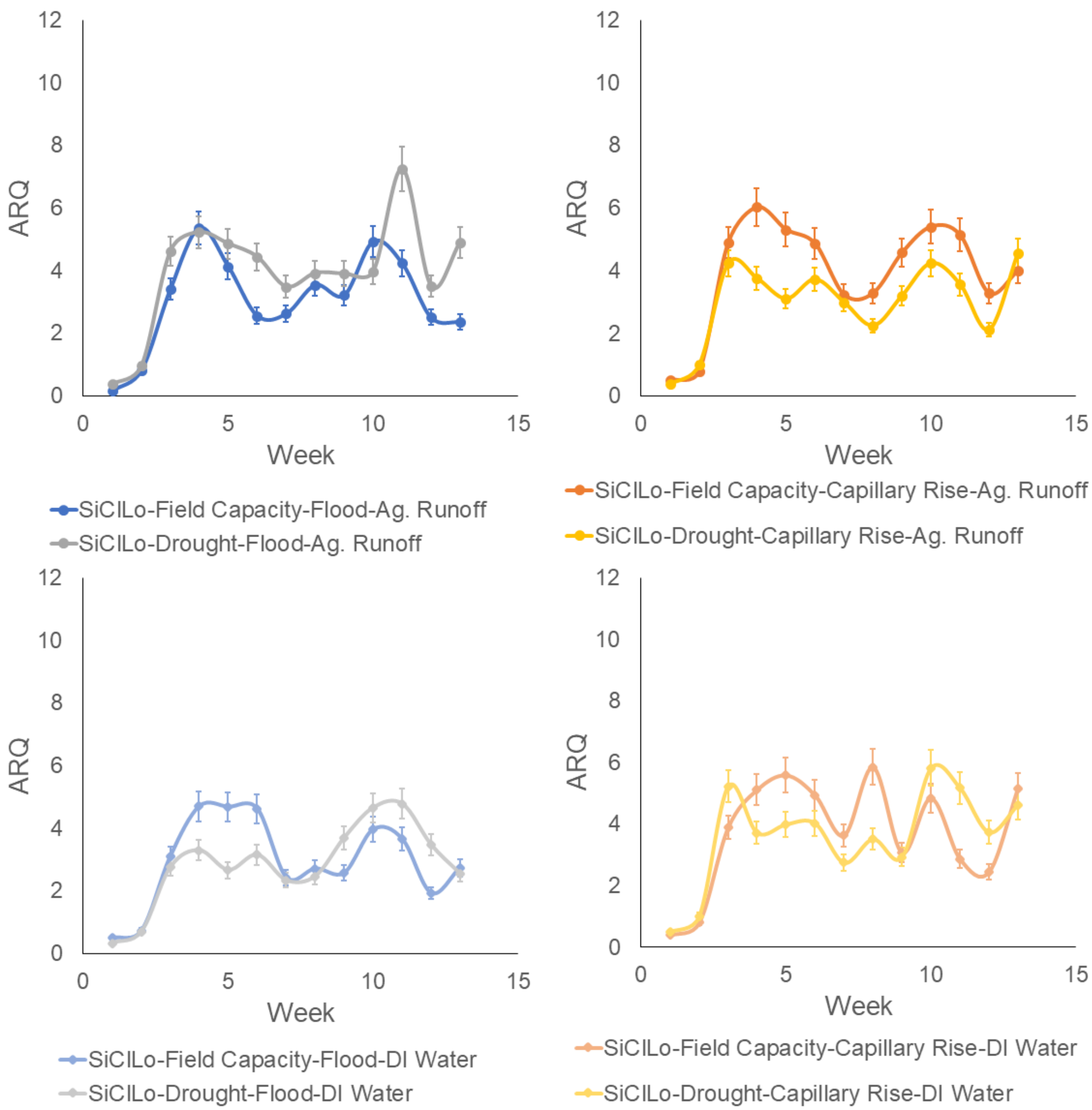

Supplemental Material F-24: Weekly Silty Clay Loam ARQ Values

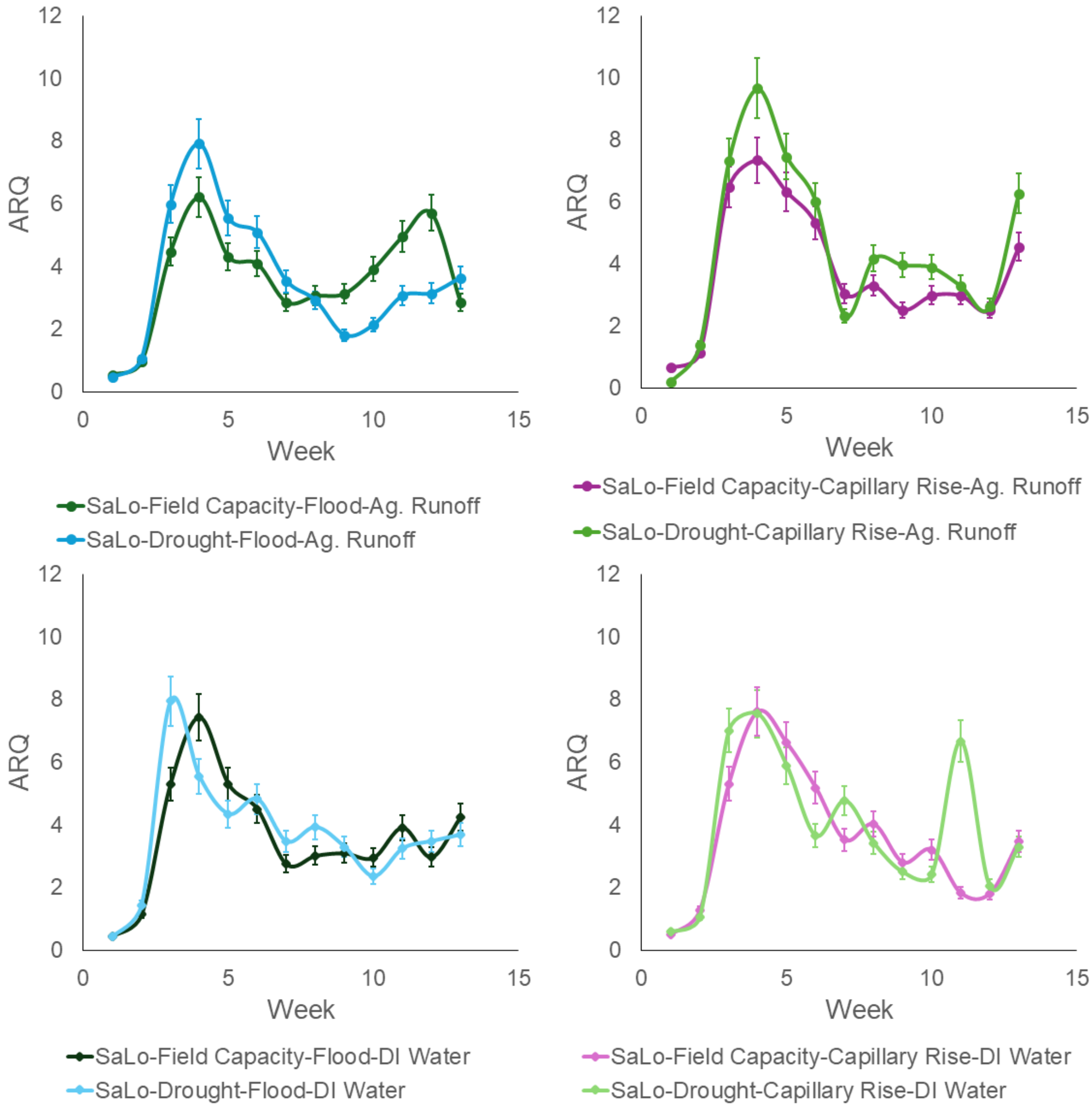

Supplemental Material F-25: Weekly Sandy Loam ARQ Values

8.02 Supplemental Material-Tables

	Comparison	Against	Estimate	SE	CI	T	p.value	Cluster	LowerCI	UpperCI
1	SiClLo.Drought.Capillary Rise.DI	SaLo.Drought.Flood.DI	-0.48064835	0.21088333	0.41333133	-2.279215	0.022654315	1	-0.8939796823	-0.0673170266
2	SiClLo.Drought.Capillary Rise.DI	SaLo.Field Capacity.Capillary Rise.DI	-0.47470058	0.21099250	0.41354531	-2.249846	0.024458742	1	-0.8882458835	-0.0611552701
3	SiClLo.Drought.Capillary Rise.DI	SaLo.Field Capacity.Flood.DI	-0.47100862	0.21106518	0.41368775	-2.231579	0.025642803	1	-0.8846963668	-0.0573208643
4	SiClLo.Drought.Capillary Rise.DI	SiClLo.Field Capacity.Capillary Rise.DI	-0.45971078	0.21131258	0.41417266	-2.175501	0.029592577	1	-0.8738834440	-0.0455381201
5	SiClLo.Drought.Flood.DI	SaLo.Field Capacity.Flood.DI	-0.20941671	0.08591438	0.16839219	-2.437505	0.014789026	2	-0.3778089000	-0.0410245131
6	SiClLo.Field Capacity.Flood.Ag	SaLo.Drought.Capillary Rise.DI	-0.18231188	0.06195087	0.12142370	-2.942846	0.003252099	3	-0.3037355826	-0.0608881802
7	SiClLo.Drought.Flood.Ag	SaLo.Drought.Capillary Rise.DI	-0.17197954	0.05866735	0.11498800	-2.931435	0.003373996	3	-0.2869675421	-0.0569915364
8	SaLo.Drought.Capillary Rise.Ag	SaLo.Drought.Flood.Ag	-0.16844282	0.05590900	0.10958164	-3.012803	0.002588467	3	-0.2780244644	-0.0588611785
9	SaLo.Drought.Capillary Rise.Ag	SaLo.Field Capacity.Capillary Rise.Ag	-0.16402005	0.05608965	0.10993572	-2.924248	0.003452896	3	-0.2739557717	-0.0540843306
10	SaLo.Drought.Capillary Rise.Ag	SaLo.Drought.Capillary Rise.DI	-0.16368986	0.05610370	0.10996326	-2.917630	0.003527022	3	-0.2736531197	-0.0537266060
11	SiClLo.Field Capacity.Flood.Ag	SaLo.Drought.Flood.DI	-0.15481159	0.06328506	0.12403872	-2.446258	0.014434765	4	-0.2788503113	-0.0307728694
12	SiClLo.Field Capacity.Flood.Ag	SaLo.Field Capacity.Capillary Rise.DI	-0.14886381	0.06365224	0.12475838	-2.338705	0.019350696	4	-0.2736221937	-0.0241054317
13	SiClLo.Field Capacity.Flood.Ag	SaLo.Field Capacity.Flood.DI	-0.14517185	0.06389553	0.12523523	-2.272019	0.023085361	4	-0.2704070826	-0.0199366203
14	SiClLo.Drought.Flood.Ag	SaLo.Drought.Flood.DI	-0.14447925	0.06007525	0.11774749	-2.404971	0.016173740	4	-0.2622267395	-0.0267317570
15	SiClLo.Drought.Flood.Ag	SaLo.Field Capacity.Capillary Rise.DI	-0.13853147	0.06046208	0.11850569	-2.291212	0.021951139	4	-0.2570371564	-0.0200257848
16	SaLo.Drought.Capillary Rise.Ag	SaLo.Drought.Flood.DI	-0.13618957	0.05757496	0.11284692	-2.365431	0.018009113	4	-0.2490364882	-0.0233426554
17	SiClLo.Drought.Flood.Ag	SaLo.Field Capacity.Flood.DI	-0.13483951	0.06071826	0.11900780	-2.220741	0.026368540	4	-0.2538473056	-0.0158317130
18	SiClLo.Field Capacity.Flood.Ag	SiClLo.Field Capacity.Capillary Rise.DI	-0.13387402	0.06471667	0.12684467	-2.068617	0.038582017	4	-0.2607186883	-0.0070293475
19	SaLo.Drought.Capillary Rise.Ag	SaLo.Field Capacity.Capillary Rise.DI	-0.13024179	0.05797861	0.11363809	-2.246376	0.024679907	4	-0.2438798793	-0.0166037089
20	SaLo.Drought.Capillary Rise.Ag	SaLo.Field Capacity.Flood.DI	-0.12654983	0.05824581	0.11416178	-2.172686	0.029803976	4	-0.2407116119	-0.0123880538
21	SiClLo.Drought.Flood.Ag	SaLo.Field Capacity.Flood.Ag	-0.12456585	0.06149870	0.12053744	-2.025504	0.042815640	4	-0.2451032945	-0.0040284095
22	SiClLo.Drought.Flood.Ag	SiClLo.Field Capacity.Capillary Rise.DI	-0.12354168	0.06158210	0.12070092	-2.006130	0.044842431	4	-0.2442425988	-0.0028407528
23	SaLo.Drought.Capillary Rise.Ag	SiClLo.Drought.Capillary Rise.Ag	-0.11786719	0.05892632	0.11549559	-2.000247	0.045473621	4	-0.2333627796	-0.0023715958
24	SaLo.Drought.Capillary Rise.Ag	SaLo.Field Capacity.Flood.Ag	-0.11627618	0.05905916	0.11575596	-1.968808	0.048975094	4	-0.2320321324	-0.0005202186
25	SiClLo.Field Capacity.Capillary Rise.Ag	SaLo.Drought.Flood.Ag	-0.06293574	0.02903302	0.05690473	-2.167729	0.030179285	5	-0.1198404622	-0.0060310109
26	SiClLo.Field Capacity.Capillary Rise.Ag	SaLo.Drought.Capillary Rise.DI	-0.05818278	0.02940911	0.05764186	-1.978393	0.047884404	5	-0.1158246381	-0.0005409178
27	SaLo.Field Capacity.Capillary Rise.Ag	SiClLo.Field Capacity.Capillary Rise.Ag	0.05851297	0.02938210	0.05758892	1.991449	0.046431504	6	0.0009240491	0.1161018835
28	SiClLo.Drought.Capillary Rise.Ag	SiClLo.Drought.Flood.Ag	0.12615686	0.06137117	0.12028750	2.055637	0.039817503	7	0.0058693649	0.2464443634
29	SaLo.Field Capacity.Flood.Ag	SiClLo.Field Capacity.Flood.Ag	0.13489819	0.06463733	0.12668917	2.087001	0.036888022	7	0.0082090217	0.2615873665
30	SiClLo.Drought.Capillary Rise.Ag	SiClLo.Field Capacity.Flood.Ag	0.13648921	0.06451606	0.12645147	2.115585	0.034380116	7	0.0100377330	0.2629406796
31	SaLo.Field Capacity.Capillary Rise.Ag	SiClLo.Drought.Flood.Ag	0.17230973	0.05865392	0.11496168	2.937736	0.003306185	8	0.0573480434	0.2872714118
32	SaLo.Drought.Flood.Ag	SiClLo.Drought.Flood.Ag	0.17673250	0.05848129	0.11462332	3.022035	0.002510815	8	0.0621091763	0.2913558195
33	SaLo.Field Capacity.Capillary Rise.Ag	SiClLo.Field Capacity.Flood.Ag	0.18264207	0.06193816	0.12139879	2.948781	0.003190300	8	0.0612432756	0.3040408639
34	SiClLo.Field Capacity.Capillary Rise.Ag	SiClLo.Field Capacity.Flood.DI	0.18486551	0.08584761	0.16826132	2.153415	0.031286099	9	0.0166041928	0.3531268321
35	SaLo.Drought.Flood.Ag	SiClLo.Field Capacity.Flood.Ag	0.18706484	0.06177482	0.12107864	3.028173	0.002460371	8	0.0659861993	0.3081434807
36	SiClLo.Field Capacity.Capillary Rise.Ag	SiClLo.Drought.Flood.DI	0.18837396	0.08712852	0.17077190	2.162024	0.030616319	9	0.0176020604	0.3591458567
37	SiClLo.Field Capacity.Capillary Rise.DI	SiClLo.Field Capacity.Flood.DI	0.19461043	0.08523541	0.16706140	2.283211	0.022417942	9	0.0275490226	0.3616718312
38	SaLo.Field Capacity.Flood.Ag	SiClLo.Field Capacity.Flood.DI	0.19563460	0.08517531	0.16694361	2.296846	0.021627534	9	0.0286909954	0.3625782107
39	SiClLo.Drought.Capillary Rise.Ag	SiClLo.Field Capacity.Flood.DI	0.19722562	0.08508350	0.16676366	2.318024	0.020448007	9	0.0304619511	0.3639892794
40	SiClLo.Field Capacity.Capillary Rise.DI	SiClLo.Drought.Flood.DI	0.19811887	0.08652545	0.16958987	2.289718	0.022037668	9	0.0285289986	0.3677087474
41	SaLo.Field Capacity.Flood.Ag	SiClLo.Drought.Flood.DI	0.19914305	0.08646625	0.16947385	2.303130	0.021271506	9	0.0296692006	0.3686168977
42	SiClLo.Drought.Capillary Rise.Ag	SiClLo.Drought.Flood.DI	0.20073406	0.08637582	0.16929662	2.323961	0.020127575	9	0.0314374463	0.3700306765
43	SaLo.Field Capacity.Flood.DI	SiClLo.Field Capacity.Flood.DI	0.20590826	0.08461496	0.16584532	2.433474	0.014954728	9	0.0400629434	0.3717535774
44	SaLo.Field Capacity.Capillary Rise.DI	SiClLo.Field Capacity.Flood.DI	0.20960022	0.08443182	0.16548637	2.482479	0.013047176	9	0.0441138521	0.3750865912
45	SaLo.Field Capacity.Capillary Rise.DI	SiClLo.Drought.Flood.DI	0.21310867	0.08573405	0.16803873	2.485695	0.012929884	9	0.0450699343	0.3811474013
46	SaLo.Drought.Flood.DI	SiClLo.Field Capacity.Flood.DI	0.21554800	0.08415604	0.16494583	2.561290	0.010428431	9	0.0506021703	0.3804938283
47	SaLo.Drought.Flood.DI	SiClLo.Drought.Flood.DI	0.21905645	0.08546250	0.16750650	2.563188	0.010371592	9	0.0515499424	0.3865629485
48	SaLo.Drought.Capillary Rise.DI	SiClLo.Field Capacity.Flood.DI	0.24304829	0.08316040	0.16299439	2.922644	0.003470726	10	0.0800538995	0.4060426813
49	SaLo.Field Capacity.Capillary Rise.Ag	SiClLo.Field Capacity.Flood.DI	0.24337848	0.08315097	0.16297591	2.926947	0.003423073	10	0.0804025735	0.4063543839
50	SaLo.Drought.Capillary Rise.DI	SiClLo.Drought.Flood.DI	0.24655674	0.08448243	0.16558557	2.918438	0.003517900	10	0.0809711647	0.4121423082
51	SaLo.Field Capacity.Capillary Rise.Ag	SiClLo.Drought.Flood.DI	0.24688692	0.08447315	0.16556738	2.922667	0.003470471	10	0.0813195457	0.4124543040
52	SaLo.Drought.Flood.Ag	SiClLo.Field Capacity.Flood.DI	0.24780125	0.08302984	0.16273848	2.984484	0.002840567	10	0.0850627715	0.4105397265
53	SaLo.Drought.Flood.Ag	SiClLo.Drought.Flood.DI	0.25130970	0.08435394	0.16533372	2.979229	0.002889748	10	0.0859759726	0.4166434176
54	SiClLo.Field Capacity.Capillary Rise.Ag	SiClLo.Drought.Capillary Rise.DI	0.44996587	0.21155840	0.41465447	2.126911	0.033427491	11	0.0353113943	0.8646203409
55	SaLo.Field Capacity.Flood.Ag	SiClLo.Drought.Capillary Rise.DI	0.46073496	0.21128854	0.41412554	2.180596	0.029213308	11	0.0466094160	0.8748605004
56	SiClLo.Drought.Capillary Rise.Ag	SiClLo.Drought.Capillary Rise.DI	0.46232597	0.21125185	0.41405362	2.188506	0.028632754	11	0.0482723463	0.8763795945
57	SaLo.Drought.Capillary Rise.DI	SiClLo.Drought.Capillary Rise.DI	0.50814865	0.21049245	0.41256521	2.414094	0.015774377	12	0.0955834361	0.9207138549
58	SaLo.Field Capacity.Capillary Rise.Ag	SiClLo.Drought.Capillary Rise.DI	0.50847883	0.21048878	0.41255800	2.415705	0.015704771	12	0.0959208300	0.9210368377
59	SaLo.Drought.Flood.Ag	SiClLo.Drought.Capillary Rise.DI	0.51290160	0.21044161	0.41246556	2.437263	0.014798903	12	0.1004360391	0.9253671691

Supplemental Material T-1: Post Hoc Wald Test Results Featuring statistically significant Pore Water Nitrate Comparisons grouped into statistically different clusters composed of statistically similar comparisons of effects on porewater nitrate concentrations.

	Comparison	Against	Estimate	SE	CI	T	p.value	LowerCI	UpperCI	Cluster
1	SiClLo.Field Capacity.Capillary Rise.Ag	SaLo.Field Capacity.Flood.DI	-6.196247	1.8283446	3.583555	-3.388993	0.0007014980	-9.77980244	-2.612691649	1
2	SiClLo.Field Capacity.Capillary Rise.Ag	SaLo.Field Capacity.Flood.Ag	-5.938845	1.8349808	3.596562	-3.236462	0.0012102143	-9.53540779	-2.342282910	2
3	SiClLo.Drought.Capillary Rise.DI	SaLo.Field Capacity.Flood.DI	-5.874440	1.7238021	3.378652	-3.407839	0.0006547949	-9.25309224	-2.495788095	2
4	SiClLo.Field Capacity.Capillary Rise.Ag	SaLo.Drought.Flood.Ag	-5.749534	1.8406580	3.607690	-3.123630	0.0017863523	-9.35722312	-2.141843917	2
5	SiClLo.Drought.Flood.DI	SaLo.Field Capacity.Flood.DI	-5.443108	1.5886589	3.113771	-3.426228	0.0006120259	-8.55687929	-2.329336506	3
6	SiClLo.Drought.Capillary Rise.Ag	SaLo.Field Capacity.Flood.DI	-5.287366	1.5412740	3.020897	-3.430517	0.0006024326	-8.30826338	-2.266469348	3
7	SiClLo.Drought.Capillary Rise.Ag	SaLo.Field Capacity.Flood.Ag	-5.029965	1.5491617	3.036357	-3.246895	0.0011667161	-8.06632161	-1.993607734	4
8	SiClLo.Drought.Capillary Rise.Ag	SaLo.Drought.Flood.Ag	-4.840653	1.5558972	3.049558	-3.111165	0.0018635079	-7.89021132	-1.791094367	4
9	SiClLo.Field Capacity.Capillary Rise.DI	SaLo.Field Capacity.Flood.DI	-4.697028	1.3685328	2.682324	-3.432163	0.0005987867	-7.37935236	-2.014703851	5
10	SiClLo.Drought.Capillary Rise.Ag	SaLo.Field Capacity.Capillary Rise.Ag	-4.510634	1.5697037	3.076619	-2.873557	0.0040587735	-7.58725289	-1.434014386	5
11	SiClLo.Field Capacity.Flood.Ag	SaLo.Field Capacity.Flood.DI	-4.143332	1.2165364	2.384411	-3.405843	0.0006596009	-6.52774346	-1.758920712	6
12	SiClLo.Drought.Flood.Ag	SaLo.Field Capacity.Flood.DI	-4.096418	1.2041105	2.360057	-3.402028	0.0006688769	-6.45647483	-1.736361564	6
13	SiClLo.Field Capacity.Capillary Rise.Ag	SaLo.Drought.Capillary Rise.DI	-4.077838	1.9276809	3.778255	-2.115411	0.0343949190	-7.85609221	-0.299583133	7
14	SiClLo.Field Capacity.Capillary Rise.Ag	SaLo.Drought.Flood.DI	-4.049146	1.9298574	3.782520	-2.098158	0.0358911567	-7.83166691	-0.266625973	7
15	SiClLo.Field Capacity.Capillary Rise.Ag	SaLo.Field Capacity.Capillary Rise.DI	-3.889839	1.9424216	3.807146	-2.002572	0.0452232395	-7.69698548	-0.082692921	7
16	SiClLo.Drought.Flood.Ag	SaLo.Field Capacity.Flood.Ag	-3.839017	1.2142318	2.379894	-3.161683	0.0015685999	-6.21891079	-1.459122213	6
17	SiClLo.Drought.Capillary Rise.DI	SaLo.Drought.Flood.DI	-3.727340	1.8311648	3.589083	-2.035502	0.0418003909	-7.31642258	-0.138256544	7
18	SaLo.Field Capacity.Capillary Rise.DI	SaLo.Field Capacity.Flood.DI	-2.306408	0.7851236	1.538842	-2.937636	0.0033072461	-3.84525020	-0.767565492	8
19	SaLo.Drought.Flood.DI	SaLo.Field Capacity.Flood.DI	-2.147101	0.7532941	1.476456	-2.850282	0.0043680485	-3.62355704	-0.670644166	8
20	SaLo.Drought.Capillary Rise.DI	SaLo.Field Capacity.Flood.DI	-2.118409	0.7476620	1.465418	-2.833378	0.0046058845	-3.58382696	-0.652991783	8
21	SaLo.Drought.Capillary Rise.Ag	SaLo.Field Capacity.Flood.DI	-1.560697	0.6444462	1.263115	-2.421765	0.0154453415	-2.82381185	-0.297582617	9
22	SaLo.Drought.Capillary Rise.Ag	SaLo.Field Capacity.Flood.Ag	-1.303296	0.6633827	1.300230	-1.964621	0.0494581290	-2.60352564	-0.003065438	9
23	SaLo.Drought.Flood.Ag	SaLo.Drought.Capillary Rise.DI	1.671696	0.7777063	1.524304	2.149521	0.0315931426	0.14739149	3.196000212	10
24	SaLo.Drought.Flood.Ag	SaLo.Drought.Flood.DI	1.700387	0.7831183	1.534912	2.171303	0.0299082891	0.16547512	3.235299045	10
25	SaLo.Drought.Flood.Ag	SaLo.Field Capacity.Capillary Rise.DI	1.859694	0.8137613	1.594972	2.285307	0.0222948365	0.26472219	3.454666452	10
26	SaLo.Field Capacity.Flood.Ag	SaLo.Drought.Capillary Rise.DI	1.861008	0.7639956	1.497431	2.435888	0.0148552916	0.36357621	3.358439148	10
27	SaLo.Field Capacity.Flood.Ag	SaLo.Drought.Flood.DI	1.889699	0.7695058	1.508231	2.455731	0.0140598537	0.38146753	3.397930288	10
28	SaLo.Field Capacity.Flood.Ag	SaLo.Field Capacity.Capillary Rise.DI	2.049006	0.8006787	1.569330	2.559087	0.0104947599	0.47967587	3.618336425	10
29	SaLo.Drought.Capillary Rise.Ag	SiClLo.Field Capacity.Flood.Ag	2.582635	1.3082255	2.564122	1.974151	0.0483645528	0.01851296	5.146756738	11
30	SaLo.Field Capacity.Capillary Rise.Ag	SiClLo.Field Capacity.Flood.DI	2.981444	1.1557344	2.265239	2.579696	0.0098887184	0.71620457	5.246683536	12
31	SaLo.Drought.Capillary Rise.Ag	SiClLo.Field Capacity.Capillary Rise.DI	3.136331	1.4505538	2.843085	2.162161	0.0306057697	0.29324539	5.979416356	12
32	SaLo.Drought.Flood.Ag	SiClLo.Field Capacity.Flood.DI	3.311463	1.1368421	2.228211	2.912861	0.0035813379	1.08325270	5.539673818	13
33	SaLo.Field Capacity.Capillary Rise.Ag	SiClLo.Drought.Flood.Ag	3.319685	1.2404105	2.431205	2.676280	0.0074444494	0.88848085	5.750890089	13
34	SaLo.Field Capacity.Capillary Rise.Ag	SiClLo.Field Capacity.Flood.Ag	3.366599	1.2524713	2.454844	2.687965	0.0071888890	0.91175553	5.821443174	13
35	SaLo.Field Capacity.Flood.Ag	SiClLo.Field Capacity.Flood.DI	3.500775	1.1275645	2.210026	3.104723	0.0019045753	1.29074864	5.710801542	13
36	SaLo.Drought.Flood.Ag	SiClLo.Drought.Flood.Ag	3.649705	1.2228427	2.396772	2.984607	0.0028394311	1.25293291	6.046476440	14
37	SaLo.Drought.Flood.Ag	SiClLo.Field Capacity.Flood.Ag	3.696619	1.2350772	2.420751	2.993026	0.0027622593	1.27586725	6.117369873	14
38	SaLo.Drought.Capillary Rise.Ag	SiClLo.Drought.Capillary Rise.Ag	3.726669	1.6144615	3.164345	2.308305	0.0209821955	0.56232453	6.891013733	15
39	SaLo.Drought.Capillary Rise.DI	SiClLo.Drought.Capillary Rise.DI	3.756031	1.8288703	3.584586	2.053744	0.0400005123	0.17144493	7.340616664	15
40	SaLo.Field Capacity.Flood.DI	SiClLo.Field Capacity.Flood.DI	3.758177	1.1166437	2.188622	3.365601	0.0007637720	1.56955511	5.946798462	14
41	SaLo.Drought.Capillary Rise.Ag	SiClLo.Drought.Flood.DI	3.882411	1.6597384	3.253087	2.339170	0.0193266229	0.62932345	7.135497875	15
42	SaLo.Field Capacity.Flood.Ag	SiClLo.Field Capacity.Flood.Ag	3.885930	1.2265534	2.404045	3.168171	0.0015340147	1.48188575	6.289975025	14
43	SaLo.Field Capacity.Capillary Rise.Ag	SiClLo.Field Capacity.Capillary Rise.DI	3.920295	1.4005230	2.745025	2.799165	0.0051234887	1.17527039	6.665320359	14
44	SaLo.Drought.Flood.Ag	SiClLo.Field Capacity.Capillary Rise.DI	4.250315	1.3850104	2.714620	3.068796	0.0021492321	1.53569417	6.964934993	16
45	SaLo.Drought.Capillary Rise.Ag	SiClLo.Drought.Capillary Rise.DI	4.313743	1.7894726	3.507366	2.410623	0.0159253218	0.80637664	7.821109230	17
46	SaLo.Field Capacity.Flood.Ag	SiClLo.Field Capacity.Capillary Rise.DI	4.439626	1.3774273	2.699757	3.223129	0.0012679824	1.73986895	7.139383875	16
47	SaLo.Drought.Capillary Rise.Ag	SiClLo.Field Capacity.Capillary Rise.Ag	4.635550	1.8903539	3.705094	2.452213	0.0141980698	0.93045623	8.340643390	18
48	SaLo.Field Capacity.Capillary Rise.Ag	SiClLo.Drought.Flood.DI	4.666375	1.6162446	3.167839	2.887171	0.0038872241	1.49853576	7.834214577	18
49	SaLo.Drought.Flood.Ag	SiClLo.Drought.Flood.DI	4.996394	1.6028435	3.141573	3.117207	0.0018257353	1.85482116	8.137967588	19
50	SaLo.Field Capacity.Capillary Rise.Ag	SiClLo.Drought.Capillary Rise.DI	5.097707	1.7492316	3.428494	2.914255	0.0035653817	1.66921354	8.526201331	19
51	SaLo.Field Capacity.Flood.Ag	SiClLo.Drought.Flood.DI	5.185706	1.5963088	3.128765	3.248561	0.0011599037	2.05694105	8.314471353	19
52	SaLo.Field Capacity.Capillary Rise.Ag	SiClLo.Field Capacity.Capillary Rise.Ag	5.419514	1.8523218	3.630551	2.925795	0.0034357705	1.78896352	9.050065108	20
53	SaLo.Drought.Flood.Ag	SiClLo.Drought.Capillary Rise.DI	5.427727	1.7368678	3.404261	3.125009	0.0017779991	2.02346578	8.831987512	20
54	SaLo.Field Capacity.Flood.Ag	SiClLo.Drought.Capillary Rise.DI	5.617038	1.7308457	3.392457	3.245257	0.0011734479	2.22458099	9.009495954	20

Supplemental Material T-2: Post Hoc Wald Test Results Featuring statistically significant Pore Water Ammonium Comparisons grouped into statistically different clusters composed of statistically similar comparisons of effects on porewater ammonium concentrations.

	Comparison	Against	Estimate	SE	CI	T	p.value	LowerCI	UpperCI	Cluster
1	SaLo.Drought.Flood.DI	SiClLo.Drought.Flood.DI	-7.4163256	2.58718029	5.07087337	-2.866567	4.149503e-03	-12.4871990	-2.3454522	1
2	SaLo.Field Capacity.Capillary Rise.DI	SiClLo.Drought.Flood.DI	-7.1999161	2.57679531	5.05051881	-2.794136	5.203862e-03	-12.2504349	-2.1493973	1
3	SiClLo.Field Capacity.Capillary Rise.Ag	SiClLo.Drought.Flood.Ag	-7.1957038	1.60917830	3.15398947	-4.471663	7.761350e-06	-10.3496933	-4.0417144	1
4	SiClLo.Field Capacity.Capillary Rise.Ag	SiClLo.Field Capacity.Flood.Ag	-7.0026401	1.60922096	3.15407308	-4.351572	1.351652e-05	-10.1567131	-3.8485670	1
5	SiClLo.Drought.Capillary Rise.DI	SiClLo.Drought.Flood.DI	-6.2161902	2.17442625	4.26187545	-2.858773	4.252835e-03	-10.4780657	-1.9543148	1
6	SaLo.Drought.Capillary Rise.DI	SiClLo.Drought.Flood.DI	-5.9641449	2.09200171	4.10032335	-2.850927	4.359192e-03	-10.0644683	-1.8638216	1
7	SiClLo.Field Capacity.Capillary Rise.Ag	SaLo.Drought.Flood.Ag	-4.9927758	1.62842398	3.19171101	-3.066017	2.169309e-03	-8.1844868	-1.8010648	2
8	SiClLo.Field Capacity.Capillary Rise.Ag	SaLo.Field Capacity.Flood.Ag	-4.6887537	1.63753337	3.20956541	-2.863303	4.192498e-03	-7.8983191	-1.4791883	2
9	SiClLo.Field Capacity.Capillary Rise.Ag	SiClLo.Drought.Flood.DI	-4.0290747	1.66642397	3.26619097	-2.417797	1.561479e-02	-7.2952656	-0.7628837	2
10	SaLo.Field Capacity.Flood.Ag	SiClLo.Field Capacity.Flood.Ag	-2.3138863	0.31406712	0.61557156	-7.367490	1.738708e-13	-2.9294579	-1.6983148	3
11	SaLo.Drought.Flood.Ag	SiClLo.Drought.Flood.Ag	-2.2029280	0.25980770	0.50922310	-8.479071	2.269986e-17	-2.7121511	-1.6937049	3
12	SiClLo.Field Capacity.Capillary Rise.DI	SiClLo.Drought.Flood.DI	-2.1379941	1.03004907	2.01889617	-2.075624	3.792878e-02	-4.1568903	-0.1190980	3
13	SaLo.Drought.Flood.Ag	SiClLo.Field Capacity.Flood.Ag	-2.0098643	0.26013905	0.50987254	-7.726115	1.108784e-14	-2.5197368	-1.4999917	3
14	SaLo.Drought.Capillary Rise.Ag	SiClLo.Drought.Flood.Ag	-1.9567032	0.21739589	0.42609595	-9.000645	2.243963e-19	-2.3827991	-1.5306072	3
15	SaLo.Drought.Capillary Rise.Ag	SiClLo.Field Capacity.Flood.Ag	-1.7636394	0.21779897	0.42688599	-8.097556	5.607430e-16	-2.1905254	-1.3367534	3
16	SiClLo.Drought.Capillary Rise.Ag	SiClLo.Drought.Flood.Ag	-1.5127811	0.14842325	0.29090956	-10.192346	2.145232e-24	-1.8036907	-1.2218716	3
17	SaLo.Field Capacity.Capillary Rise.Ag	SiClLo.Drought.Flood.Ag	-1.3569911	0.12623070	0.24741217	-10.750088	5.920507e-27	-1.6044033	-1.1095790	3
18	SiClLo.Drought.Capillary Rise.Ag	SiClLo.Field Capacity.Flood.Ag	-1.3197173	0.14903182	0.29210236	-8.855272	8.347970e-19	-1.6118197	-1.0276150	3
19	SaLo.Field Capacity.Capillary Rise.Ag	SiClLo.Field Capacity.Flood.Ag	-1.1639273	0.12694937	0.24882077	-9.168437	4.799264e-20	-1.4127481	-0.9151066	3
20	SaLo.Drought.Capillary Rise.Ag	SaLo.Field Capacity.Capillary Rise.Ag	-0.5997120	0.25020114	0.49039424	-2.396920	1.653355e-02	-1.0901063	-0.1093178	4
21	SiClLo.Drought.Flood.Ag	SiClLo.Field Capacity.Flood.Ag	0.1930638	0.01725068	0.03381133	11.191663	4.479524e-29	0.1592525	0.2268751	4
22	SiClLo.Drought.Capillary Rise.Ag	SaLo.Drought.Flood.Ag	0.6901469	0.29791596	0.58391529	2.316583	2.052648e-02	0.1062316	1.2740622	5
23	SaLo.Field Capacity.Capillary Rise.Ag	SaLo.Drought.Flood.Ag	0.8459369	0.28762393	0.56374291	2.941121	3.270263e-03	0.2821940	1.4096798	5
24	SiClLo.Drought.Capillary Rise.Ag	SaLo.Field Capacity.Flood.Ag	0.9941690	0.34570705	0.67758583	2.875756	4.030617e-03	0.3165832	1.6717548	5
25	SaLo.Field Capacity.Capillary Rise.Ag	SaLo.Field Capacity.Flood.Ag	1.1499590	0.33691831	0.66035989	3.413169	6.421222e-04	0.4895991	1.8103189	5
26	SaLo.Drought.Capillary Rise.Ag	SiClLo.Drought.Flood.DI	1.2099260	0.49168060	0.96369399	2.460797	1.386289e-02	0.2462320	2.1736200	5
27	SiClLo.Drought.Capillary Rise.Ag	SiClLo.Drought.Flood.DI	1.6538481	0.46622374	0.91379853	3.547327	3.891612e-04	0.7400495	2.5676466	5
28	SaLo.Field Capacity.Capillary Rise.Ag	SiClLo.Drought.Flood.DI	1.8096381	0.45978685	0.90118223	3.935820	8.291327e-05	0.9084558	2.7108203	5
29	SiClLo.Drought.Flood.Ag	SaLo.Field Capacity.Flood.Ag	2.5069501	0.31380055	0.61504908	7.988992	1.360464e-15	1.8919010	3.1219992	6
30	SaLo.Field Capacity.Flood.Ag	SiClLo.Field Capacity.Capillary Rise.DI	2.7976732	0.98249147	1.92568329	2.847529	4.406004e-03	0.8719899	4.7233565	6
31	SiClLo.Field Capacity.Flood.Ag	SiClLo.Drought.Flood.DI	2.9735654	0.44366306	0.86957959	6.702306	2.051564e-11	2.1039858	3.8431450	6
32	SaLo.Drought.Flood.Ag	SiClLo.Field Capacity.Capillary Rise.DI	3.1016953	0.96737602	1.89605700	3.206297	1.344549e-03	1.2056383	4.9977523	6
33	SiClLo.Drought.Flood.Ag	SiClLo.Drought.Flood.DI	3.1666292	0.44348416	0.86922895	7.140343	9.309800e-13	2.2974002	4.0358581	6
34	SaLo.Drought.Capillary Rise.Ag	SiClLo.Field Capacity.Capillary Rise.DI	3.3479202	0.95730037	1.87630872	3.497252	4.700784e-04	1.4716114	5.2242289	6
35	SiClLo.Drought.Capillary Rise.Ag	SiClLo.Field Capacity.Capillary Rise.DI	3.7918422	0.94479590	1.85179996	4.013398	5.985081e-05	1.9400422	5.6436422	6
36	SiClLo.Drought.Flood.DI	SiClLo.Field Capacity.Flood.DI	3.8033819	1.44723510	2.83658079	2.628033	8.588013e-03	0.9668011	6.6399627	6
37	SaLo.Field Capacity.Capillary Rise.Ag	SiClLo.Field Capacity.Capillary Rise.DI	3.9476322	0.94168853	1.84570951	4.192078	2.764104e-05	2.1019227	5.7933417	6
38	SaLo.Field Capacity.Flood.Ag	SiClLo.Field Capacity.Flood.DI	4.4630610	1.41397065	2.77138247	3.156403	1.597281e-03	1.6916785	7.2344435	7
39	SaLo.Drought.Flood.Ag	SiClLo.Field Capacity.Flood.DI	4.7670831	1.40362748	2.75110987	3.396259	6.831358e-04	2.0159732	7.5181929	7
40	SaLo.Drought.Capillary Rise.Ag	SiClLo.Field Capacity.Flood.DI	5.0133079	1.39676433	2.73765809	3.589230	3.316566e-04	2.2756499	7.7509660	7
41	SiClLo.Field Capacity.Flood.Ag	SiClLo.Field Capacity.Capillary Rise.DI	5.1115595	0.93433215	1.83129101	5.470816	4.479674e-08	3.2802685	6.9428505	7
42	SaLo.Drought.Capillary Rise.Ag	SiClLo.Field Capacity.Capillary Rise.Ag	5.2390007	1.62250599	3.18011174	3.228956	1.242429e-03	2.0588889	8.4191124	7
43	SiClLo.Drought.Flood.Ag	SiClLo.Field Capacity.Capillary Rise.DI	5.3046233	0.93425846	1.83114659	5.677897	1.363608e-08	3.4734767	7.1357699	7
44	SiClLo.Drought.Capillary Rise.Ag	SiClLo.Field Capacity.Flood.DI	5.4572300	1.38832502	2.72111703	3.930801	8.466317e-05	2.7361130	8.1783470	7
45	SaLo.Field Capacity.Capillary Rise.Ag	SiClLo.Field Capacity.Flood.DI	5.6130200	1.38622993	2.71701065	4.049126	5.140921e-05	2.8960093	8.3300306	7
46	SiClLo.Drought.Capillary Rise.Ag	SiClLo.Field Capacity.Capillary Rise.Ag	5.6829227	1.61521668	3.16582469	3.518366	4.342138e-04	2.5170980	8.8487474	7
47	SaLo.Field Capacity.Capillary Rise.Ag	SiClLo.Field Capacity.Capillary Rise.Ag	5.8387127	1.61347914	3.16241911	3.618710	2.960755e-04	2.6762936	9.0011318	7
48	SiClLo.Drought.Flood.DI	SaLo.Field Capacity.Flood.DI	6.4809961	2.26262161	4.43473835	2.864375	4.178334e-03	2.0462578	10.9157345	8
49	SaLo.Field Capacity.Flood.Ag	SaLo.Drought.Capillary Rise.DI	6.6238240	2.06923747	4.05570544	3.201094	1.369068e-03	2.5681186	10.6795295	8
50	SiClLo.Field Capacity.Flood.Ag	SiClLo.Field Capacity.Flood.DI	6.7769473	1.38137387	2.70749278	4.905947	9.297752e-07	4.0694545	9.4844401	8
51	SaLo.Field Capacity.Flood.Ag	SiClLo.Drought.Capillary Rise.DI	6.8758693	2.15254326	4.21898479	3.194300	1.401703e-03	2.6568845	11.0948541	8
52	SaLo.Drought.Flood.Ag	SaLo.Drought.Capillary Rise.DI	6.9278461	2.06225107	4.04201210	3.359361	7.812290e-04	2.8858340	10.9698582	8
53	SiClLo.Drought.Flood.Ag	SiClLo.Field Capacity.Flood.DI	6.9700111	1.38132751	2.70740193	5.045879	4.514417e-07	4.2626092	9.6774130	8
54	SaLo.Field Capacity.Flood.Ag	SaLo.Field Capacity.Flood.DI	7.1406752	2.24160877	4.39355318	3.185514	1.444973e-03	2.7471220	11.5342284	8
55	SaLo.Drought.Capillary Rise.Ag	SaLo.Drought.Capillary Rise.DI	7.1740710	2.05762046	4.03293609	3.486586	4.892278e-04	3.1411349	11.2070071	8
56	SaLo.Drought.Flood.Ag	SiClLo.Drought.Capillary Rise.DI	7.1798914	2.14583396	4.20583456	3.345968	8.199591e-04	2.9740568	11.3857259	8
57	SaLo.Drought.Capillary Rise.Ag	SiClLo.Drought.Capillary Rise.DI	7.4261162	2.14138704	4.19711859	3.467900	5.245423e-04	3.2289977	11.6232348	9
58	SaLo.Drought.Flood.Ag	SaLo.Field Capacity.Flood.DI	7.4446973	2.23517244	4.38093799	3.330704	8.662673e-04	3.0637593	11.8256353	9
59	SiClLo.Drought.Capillary Rise.Ag	SaLo.Drought.Capillary Rise.DI	7.6179930	2.05195553	4.02183284	3.712553	2.051793e-04	3.5961602	11.6398258	9
60	SaLo.Drought.Capillary Rise.Ag	SaLo.Field Capacity.Flood.DI	7.6909222	2.23090643	4.37257660	3.447443	5.659204e-04	3.3183456	12.0634988	9
61	SaLo.Field Capacity.Capillary Rise.Ag	SaLo.Drought.Capillary Rise.DI	7.7737830	2.05054886	4.01907576	3.791074	1.499971e-04	3.7547072	11.7928588	9
62	SaLo.Field Capacity.Flood.Ag	SaLo.Field Capacity.Capillary Rise.DI	7.8595952	2.55834930	5.01436463	3.072135	2.125334e-03	2.8452306	12.8739598	9
63	SiClLo.Drought.Capillary Rise.Ag	SiClLo.Drought.Capillary Rise.DI	7.8700383	2.13594885	4.18645976	3.684563	2.290953e-04	3.6835785	12.0564980	9
64	SaLo.Field Capacity.Capillary Rise.Ag	SiClLo.Drought.Capillary Rise.DI	8.0258283	2.13459844	4.18381294	3.759877	1.699967e-04	3.8420153	12.2096412	9
65	SaLo.Field Capacity.Flood.Ag	SaLo.Drought.Flood.DI	8.0760047	2.56884855	5.03494315	3.143823	1.667564e-03	3.0410616	13.1109479	9
66	SiClLo.Drought.Capillary Rise.Ag	SaLo.Field Capacity.Flood.DI	8.1348442	2.22569134	4.36235503	3.654974	2.572079e-04	3.7724892	12.4971992	9
67	SaLo.Drought.Flood.Ag	SaLo.Field Capacity.Capillary Rise.DI	8.1636173	2.55261618	5.00312772	3.198137	1.383184e-03	3.1604895	13.1667450	9
68	SaLo.Field Capacity.Capillary Rise.Ag	SaLo.Field Capacity.Flood.DI	8.2906342	2.22439628	4.35981671	3.727139	1.936656e-04	3.9308175	12.6504509	9
69	SaLo.Drought.Flood.Ag	SaLo.Drought.Flood.DI	8.3800268	2.56324954	5.02396910	3.269298	1.078147e-03	3.3560577	13.4039959	9
70	SaLo.Drought.Capillary Rise.Ag	SaLo.Field Capacity.Capillary Rise.DI	8.4098421	2.54889540	4.99583499	3.299407	9.688949e-04	3.4140071	13.4056771	9
71	SaLo.Drought.Capillary Rise.Ag	SaLo.Drought.Flood.DI	8.6262516	2.55953813	5.01669473	3.370238	7.510340e-04	3.6095569	13.6429464	9
72	SiClLo.Drought.Capillary Rise.Ag	SaLo.Field Capacity.Capillary Rise.DI	8.8537642	2.54440006	4.98702412	3.479706	5.019643e-04	3.8667401	13.8407883	10
73	SiClLo.Field Capacity.Flood.Ag	SaLo.Drought.Capillary Rise.DI	8.9377104	2.04734004	4.01278648	4.365523	1.268189e-05	4.9249239	12.9504968	10
74	SaLo.Field Capacity.Capillary Rise.Ag	SaLo.Field Capacity.Capillary Rise.DI	9.0095542	2.54326203	4.98479359	3.542519	3.963248e-04	4.0247606	13.9943478	10
75	SiClLo.Drought.Capillary Rise.Ag	SaLo.Drought.Flood.DI	9.0701737	2.55500576	5.00781130	3.549962	3.852866e-04	4.0623624	14.0779850	10
76	SiClLo.Drought.Flood.Ag	SaLo.Drought.Capillary Rise.DI	9.1307741	2.04731060	4.01272878	4.459887	8.200284e-06	5.1180454	13.1435029	10
77	SiClLo.Field Capacity.Flood.Ag	SiClLo.Drought.Capillary Rise.DI	9.1897556	2.13152212	4.17778335	4.311358	1.622547e-05	5.0119723	13.3675390	10
78	SaLo.Field Capacity.Capillary Rise.Ag	SaLo.Drought.Flood.DI	9.2259637	2.55388012	5.00560503	3.612528	3.032262e-04	4.2203587	14.2315687	10
79	SiClLo.Drought.Flood.Ag	SiClLo.Drought.Capillary Rise.DI	9.3828194	2.13149399	4.17772823	4.401992	1.072615e-05	5.2050912	13.5605476	10
80	SiClLo.Field Capacity.Flood.Ag	SaLo.Field Capacity.Flood.DI	9.4545615	2.22145001	4.35404202	4.256032	2.080873e-05	5.1005195	13.8086036	10
81	SiClLo.Drought.Flood.Ag	SaLo.Field Capacity.Flood.DI	9.6476253	2.22142316	4.35398940	4.342993	1.405546e-05	5.2936359	14.0016147	10
82	SiClLo.Field Capacity.Flood.Ag	SaLo.Field Capacity.Capillary Rise.DI	10.1734815	2.54068048	4.97973373	4.004235	6.221851e-05	5.1937478	15.1532152	11
83	SiClLo.Drought.Flood.Ag	SaLo.Field Capacity.Capillary Rise.DI	10.3665453	2.54065699	4.97968769	4.080262	4.498503e-05	5.3868576	15.3462330	11
84	SiClLo.Field Capacity.Flood.Ag	SaLo.Drought.Flood.DI	10.3898910	2.55132985	5.00060652	4.072343	4.654251e-05	5.3892845	15.3904975	11
85	SiClLo.Drought.Flood.Ag	SaLo.Drought.Flood.DI	10.5829548	2.55130687	5.00056147	4.148052	3.353155e-05	5.5823933	15.5835163	11

Supplemental Material T-3: Post Hoc Wald Test Results Featuring statistically significant Pore Water Phosphate Comparisons grouped into statistically different clusters composed of statistically similar comparisons of effects on porewater phosphate concentrations.

	Comparison	Against	Estimate	SE	CI	p.value	LowerCI	UpperCI	Cluster
1	SiClLo.Field Capacity.Flood.Ag	SaLo.Drought.Capillary Rise.Dl	-1.5349611	0.2687518	0.5267536	1.120211e-08	-2.061714672	-1.008207555	1
2	SiClLo.Field Capacity.Flood.Ag	SaLo.Field Capacity.Flood.Dl	-1.4892334	0.2695731	0.5283632	3.305866e-08	-2.017596636	-0.960870148	1
3	SiClLo.Drought.Flood.Dl	SaLo.Field Capacity.Flood.Dl	-1.2558573	0.2643494	0.5181248	2.026657e-06	-1.773982120	-0.737732495	2
4	SiClLo.Field Capacity.Capillary Rise.Ag	SaLo.Drought.Capillary Rise.Dl	-1.1377246	0.2598715	0.5093482	1.197585e-05	-1.647072866	-0.628376422	3
5	SiClLo.Field Capacity.Capillary Rise.Ag	SaLo.Field Capacity.Flood.Ag	-1.1334069	0.2599516	0.5095051	1.300212e-05	-1.642912000	-0.623901818	3
6	SiClLo.Field Capacity.Capillary Rise.Ag	SaLo.Drought.Flood.Ag	-1.1263657	0.2639652	0.5173718	1.980309e-05	-1.643737421	-0.608993917	3
7	SiClLo.Drought.Capillary Rise.Ag	SaLo.Field Capacity.Capillary Rise.Ag	-1.0971786	0.2788764	0.5465977	8.344534e-05	-1.643776294	-0.550580933	3
8	SiClLo.Field Capacity.Capillary Rise.Ag	SaLo.Field Capacity.Flood.Dl	-1.0919969	0.2607209	0.5110129	2.809587e-05	-1.603009869	-0.580983976	3
9	SiClLo.Field Capacity.Flood.Ag	SaLo.Drought.Flood.Dl	-1.0583651	0.2818257	0.5523785	1.730730e-04	-1.610743553	-0.505986637	4
10	SiClLo.Drought.Capillary Rise.Ag	SaLo.Drought.Capillary Rise.Dl	-1.0535489	0.2676458	0.5245857	8.272853e-05	-1.578134589	-0.528963115	4
11	SiClLo.Drought.Capillary Rise.Ag	SaLo.Field Capacity.Flood.Ag	-1.0492311	0.2677233	0.5247377	8.888472e-05	-1.573968778	-0.524493456	4
12	SiClLo.Drought.Capillary Rise.Ag	SaLo.Drought.Flood.Ag	-1.0421899	0.2717175	0.5325664	1.252767e-04	-1.574756245	-0.509623509	4
13	SiClLo.Drought.Capillary Rise.Ag	SaLo.Field Capacity.Flood.Dl	-1.0078211	0.2684685	0.5261982	1.740593e-04	-1.534019303	-0.481622958	4
14	SiClLo.Field Capacity.Flood.Ag	SaLo.Field Capacity.Capillary Rise.Dl	-0.9970464	0.2786481	0.5461502	3.460263e-04	-1.543196679	-0.450896203	4
15	SiClLo.Drought.Flood.Ag	SaLo.Drought.Capillary Rise.Dl	-0.8971064	0.2639750	0.5173910	6.776829e-04	-1.414497370	-0.379715421	5
16	SiClLo.Drought.Flood.Ag	SaLo.Field Capacity.Flood.Ag	-0.8927887	0.2640536	0.5175450	7.219915e-04	-1.410333679	-0.375243641	5
17	SiClLo.Drought.Flood.Ag	SaLo.Field Capacity.Flood.Dl	-0.8513787	0.2648091	0.5190258	1.304147e-03	-1.370404519	-0.332352829	5
18	SiClLo.Field Capacity.Capillary Rise.Dl	SaLo.Field Capacity.Flood.Dl	-0.8503481	0.2647851	0.5189788	1.320600e-03	-1.369326950	-0.331369333	5
19	SiClLo.Drought.Capillary Rise.Dl	SaLo.Field Capacity.Flood.Dl	-0.7995661	0.2738849	0.5368145	3.507615e-03	-1.336380576	-0.262751660	5
20	SiClLo.Field Capacity.Flood.Ag	SiClLo.Drought.Capillary Rise.Dl	-0.6896673	0.3020572	0.5920321	2.241658e-02	-1.281699342	-0.097635206	6
21	SiClLo.Field Capacity.Capillary Rise.Ag	SaLo.Drought.Flood.Dl	-0.6611286	0.2733623	0.5357901	1.558435e-02	-1.196918736	-0.125338516	6
22	SiClLo.Field Capacity.Flood.Ag	SiClLo.Field Capacity.Capillary Rise.Dl	-0.6388853	0.2938542	0.5759543	2.969335e-02	-1.214839565	-0.062930935	6
23	SiClLo.Field Capacity.Capillary Rise.Ag	SaLo.Field Capacity.Capillary Rise.Dl	-0.5998100	0.2700945	0.5293852	2.636850e-02	-1.129195206	-0.070424738	7
24	SiClLo.Drought.Capillary Rise.Ag	SaLo.Drought.Flood.Dl	-0.5769528	0.2808377	0.5504418	3.993701e-02	-1.127394632	-0.026511036	7
25	SaLo.Drought.Capillary Rise.Ag	SaLo.Field Capacity.Capillary Rise.Ag	-0.5581492	0.2597774	0.5091638	3.166876e-02	-1.067312999	-0.048985399	7
26	SaLo.Drought.Capillary Rise.Ag	SaLo.Drought.Capillary Rise.Dl	-0.5145194	0.2463474	0.4828409	3.674439e-02	-0.997360374	-0.031678501	7
27	SaLo.Drought.Capillary Rise.Ag	SaLo.Field Capacity.Flood.Ag	-0.5102017	0.2464319	0.4830065	3.841901e-02	-0.993208155	-0.027195250	7
28	SaLo.Drought.Capillary Rise.Ag	SaLo.Drought.Flood.Ag	-0.5031605	0.2506445	0.4912632	4.469998e-02	-0.994423626	-0.011897299	7
29	SaLo.Field Capacity.Capillary Rise.Dl	SaLo.Field Capacity.Flood.Dl	-0.4921870	0.2477395	0.4855695	4.695438e-02	-0.977756409	-0.006617493	7
30	SaLo.Field Capacity.Capillary Rise.Ag	SaLo.Drought.Flood.Dl	0.5202258	0.2637453	0.5169408	4.855766e-02	0.003285017	1.037166542	8
31	SaLo.Drought.Flood.Ag	SaLo.Field Capacity.Capillary Rise.Dl	0.5265557	0.2511346	0.4922237	3.601948e-02	0.034331963	1.018779431	8
32	SaLo.Field Capacity.Flood.Ag	SaLo.Field Capacity.Capillary Rise.Dl	0.5335969	0.2469296	0.4839820	3.070094e-02	0.049614946	1.017578929	8
33	SaLo.Drought.Capillary Rise.Dl	SaLo.Field Capacity.Capillary Rise.Dl	0.5379147	0.2468453	0.4838168	2.932001e-02	0.054097862	1.021731483	8
34	SaLo.Drought.Flood.Dl	SiClLo.Field Capacity.Flood.Dl	0.5444145	0.2709154	0.5309943	4.448028e-02	0.013420180	1.075408728	8
35	SaLo.Field Capacity.Capillary Rise.Ag	SaLo.Field Capacity.Capillary Rise.Dl	0.5815444	0.2602490	0.5100880	2.544564e-02	0.071456394	1.091632473	9
36	SaLo.Drought.Capillary Rise.Ag	SiClLo.Field Capacity.Capillary Rise.Ag	0.6232052	0.2696397	0.5284938	2.081896e-02	0.094711379	1.151699034	9
37	SiClLo.Drought.Flood.Ag	SiClLo.Field Capacity.Flood.Ag	0.6378547	0.2938759	0.5759967	2.996972e-02	0.061858032	1.213851404	9
38	SaLo.Field Capacity.Capillary Rise.Dl	SiClLo.Drought.Flood.Dl	0.7636704	0.2735983	0.5362527	5.251135e-03	0.227417701	1.299923011	10
39	SaLo.Drought.Capillary Rise.Ag	SiClLo.Drought.Flood.Dl	0.7870656	0.2731493	0.5353727	3.958528e-03	0.251692871	1.322438312	10
40	SaLo.Drought.Flood.Dl	SiClLo.Drought.Flood.Dl	0.8249890	0.2768286	0.5425841	2.881135e-03	0.282404890	1.367573131	10
41	SaLo.Drought.Flood.Ag	SiClLo.Drought.Capillary Rise.Dl	0.8339349	0.2771506	0.5432151	2.621439e-03	0.290719761	1.377149967	10
42	SaLo.Field Capacity.Flood.Ag	SiClLo.Drought.Capillary Rise.Dl	0.8409761	0.2731554	0.5353845	2.078734e-03	0.305591611	1.376360597	10
43	SaLo.Drought.Capillary Rise.Dl	SiClLo.Drought.Capillary Rise.Dl	0.8452938	0.2730795	0.5352358	1.965388e-03	0.310058082	1.380529597	10
44	SaLo.Drought.Flood.Ag	SiClLo.Field Capacity.Capillary Rise.Dl	0.8847169	0.2680747	0.5254265	9.659460e-04	0.359290392	1.410143384	11
45	SaLo.Drought.Flood.Ag	SiClLo.Drought.Flood.Ag	0.8857474	0.2680985	0.5254730	9.537918e-04	0.360274411	1.411220429	11
46	SaLo.Field Capacity.Capillary Rise.Ag	SiClLo.Drought.Capillary Rise.Dl	0.8889236	0.2842631	0.5571558	1.765307e-03	0.331767849	1.446079353	11
47	SaLo.Field Capacity.Flood.Ag	SiClLo.Field Capacity.Capillary Rise.Dl	0.8917581	0.2640295	0.5174978	7.314952e-04	0.374260281	1.409255975	11
48	SaLo.Drought.Capillary Rise.Dl	SiClLo.Field Capacity.Capillary Rise.Dl	0.8960759	0.2639509	0.5173438	6.866421e-04	0.378732074	1.413419652	11
49	SaLo.Field Capacity.Capillary Rise.Ag	SiClLo.Field Capacity.Capillary Rise.Dl	0.9397056	0.2753313	0.5396493	6.425189e-04	0.400056369	1.479354880	11
50	SaLo.Field Capacity.Capillary Rise.Ag	SiClLo.Drought.Flood.Ag	0.9407362	0.2753543	0.5396945	6.344177e-04	0.401041653	1.480430661	11
51	SaLo.Field Capacity.Flood.Dl	SiClLo.Field Capacity.Flood.Dl	0.9752828	0.2581570	0.5059877	1.581774e-04	0.469295040	1.481270462	11
52	SaLo.Drought.Flood.Ag	SiClLo.Field Capacity.Flood.Dl	1.0096515	0.2614301	0.5124030	1.124478e-04	0.497248457	1.522054537	12
53	SaLo.Field Capacity.Flood.Ag	SiClLo.Field Capacity.Flood.Dl	1.0166927	0.2573800	0.5044648	7.809820e-05	0.512227962	1.521157511	12
54	SaLo.Drought.Capillary Rise.Ag	SiClLo.Field Capacity.Flood.Ag	1.0204417	0.2782073	0.5452863	2.445333e-04	0.475155350	1.565728001	12
55	SaLo.Drought.Capillary Rise.Dl	SiClLo.Field Capacity.Flood.Dl	1.0210105	0.2572991	0.5043063	7.242228e-05	0.516704141	1.525316804	12
56	SaLo.Field Capacity.Capillary Rise.Ag	SiClLo.Field Capacity.Flood.Dl	1.0646402	0.2701727	0.5295385	8.128085e-05	0.535101783	1.594178684	12
57	SaLo.Field Capacity.Capillary Rise.Ag	SiClLo.Field Capacity.Capillary Rise.Ag	1.1813544	0.2726210	0.5343371	1.468763e-05	0.647017282	1.715691529	13
58	SaLo.Drought.Flood.Ag	SiClLo.Drought.Flood.Dl	1.2902261	0.2675536	0.5244051	1.419065e-06	0.765820930	1.814631177	13
59	SaLo.Field Capacity.Flood.Ag	SiClLo.Drought.Flood.Dl	1.2972673	0.2635907	0.5166378	8.587406e-07	0.780629500	1.813905087	13
60	SaLo.Drought.Capillary Rise.Dl	SiClLo.Drought.Flood.Dl	1.3015850	0.2635118	0.5164831	7.837107e-07	0.785101930	1.818068128	13
61	SaLo.Field Capacity.Capillary Rise.Ag	SiClLo.Drought.Flood.Dl	1.3452148	0.2760896	0.5411357	1.102596e-06	0.804079085	1.886350495	13
62	SaLo.Drought.Flood.Ag	SiClLo.Field Capacity.Flood.Ag	1.5236021	0.2727212	0.5345336	2.314711e-08	0.989068569	2.058135707	14
63	SaLo.Field Capacity.Flood.Ag	SiClLo.Field Capacity.Flood.Ag	1.5306434	0.2688292	0.5269052	1.242868e-08	1.003738151	2.057548605	14
64	SaLo.Field Capacity.Capillary Rise.Ag	SiClLo.Field Capacity.Flood.Ag	1.5785909	0.2810906	0.5509376	1.954851e-08	1.027653263	2.129528486	14

Supplemental Material T-4: Post Hoc Wald Test Results Featuring statistically significant Pore Water pH Comparisons grouped into statistically different clusters composed of statistically similar comparisons of effects on porewater phosphate concentrations.

	Comparison	Against	Estimate	SE	CI	p.value	LowerCI	UpperCI	Cluster
1	SiClLo.Drought.Capillary Rise.Ag	SiClLo.Drought.Flood.Ag	-0.06864426	0.02733481	0.05357622	0.0120307899	-0.1222204838	-0.015068037	1
2	SiClLo.Drought.Capillary Rise.Ag	SiClLo.Field Capacity.Capillary Rise.Ag	-0.06831048	0.02735130	0.05360856	0.0125064759	-0.1219190382	-0.014701924	1
3	SiClLo.Drought.Capillary Rise.Ag	SaLo.Drought.Capillary Rise.DI	-0.06658656	0.02743673	0.05377598	0.0152278891	-0.1203625431	-0.012810576	1
4	SiClLo.Drought.Flood.DI	SaLo.Field Capacity.Flood.DI	-0.06650974	0.02942369	0.05767042	0.0237955055	-0.1241801662	-0.008839317	1
5	SiClLo.Field Capacity.Flood.Ag	SaLo.Drought.Capillary Rise.DI	-0.06078308	0.02706840	0.05305406	0.0247337079	-0.1138371381	-0.007729017	2
6	SiClLo.Drought.Capillary Rise.Ag	SaLo.Field Capacity.Capillary Rise.Ag	-0.05898537	0.02781762	0.05452254	0.0339696562	-0.1135079089	-0.004462828	2
7	SiClLo.Drought.Capillary Rise.Ag	SiClLo.Field Capacity.Capillary Rise.DI	-0.05616894	0.02796047	0.05480252	0.0445509501	-0.1109714528	-0.001366421	2
8	SaLo.Drought.Capillary Rise.Ag	SaLo.Field Capacity.Capillary Rise.DI	0.04526662	0.02286398	0.04481340	0.0477234956	0.0004532175	0.090080024	3
9	SaLo.Drought.Capillary Rise.Ag	SaLo.Field Capacity.Flood.Ag	0.04549200	0.02287848	0.04484183	0.0467654417	0.0006501686	0.090333822	3
10	SaLo.Drought.Capillary Rise.Ag	SaLo.Field Capacity.Flood.DI	0.04556725	0.02288333	0.04485132	0.0464494353	0.0007159316	0.090418570	3
11	SaLo.Drought.Capillary Rise.Ag	SiClLo.Drought.Capillary Rise.DI	0.04583569	0.02290060	0.04488519	0.0453379353	0.0009505024	0.090720873	3
12	SaLo.Drought.Capillary Rise.Ag	SaLo.Drought.Flood.Ag	0.04966040	0.02314730	0.04536871	0.0319202613	0.0042916889	0.095029114	3
13	SaLo.Drought.Flood.DI	SiClLo.Field Capacity.Flood.DI	0.05922756	0.02845530	0.05577239	0.0373950843	0.0034551656	0.114999945	4
14	SiClLo.Field Capacity.Capillary Rise.DI	SiClLo.Field Capacity.Flood.DI	0.06191313	0.02832002	0.05550724	0.0288012125	0.0064058969	0.117420373	4
15	SaLo.Drought.Flood.Ag	SiClLo.Drought.Flood.DI	0.06241659	0.02962816	0.05807119	0.0351466723	0.0043453989	0.120487784	4
16	SiClLo.Field Capacity.Capillary Rise.Ag	SiClLo.Field Capacity.Flood.Ag	0.06250700	0.02698178	0.05288430	0.0205235139	0.0096227026	0.115391296	4
17	SiClLo.Drought.Flood.Ag	SiClLo.Field Capacity.Flood.Ag	0.06284078	0.02696506	0.05285151	0.0197822536	0.0099892693	0.115692288	4
18	SaLo.Field Capacity.Capillary Rise.Ag	SiClLo.Field Capacity.Flood.DI	0.06472957	0.02817903	0.05523091	0.0216140587	0.0094986615	0.119960472	4
19	SiClLo.Drought.Capillary Rise.DI	SiClLo.Drought.Flood.DI	0.06624131	0.02943704	0.05769660	0.0244317703	0.0085447083	0.123937902	4
20	SaLo.Field Capacity.Flood.Ag	SiClLo.Drought.Flood.DI	0.06658500	0.02941994	0.05766309	0.0236196355	0.0089219070	0.124248087	4
21	SaLo.Field Capacity.Capillary Rise.DI	SiClLo.Drought.Flood.DI	0.06681037	0.02940874	0.05764113	0.0230994267	0.0091692396	0.124451504	4
22	SaLo.Drought.Flood.DI	SiClLo.Drought.Flood.DI	0.07106063	0.02919854	0.05722913	0.0149451654	0.0138314958	0.128289758	5
23	SaLo.Drought.Capillary Rise.DI	SiClLo.Field Capacity.Flood.DI	0.07233076	0.02780319	0.05449426	0.0092809725	0.0178365017	0.126825013	5
24	SiClLo.Field Capacity.Capillary Rise.DI	SiClLo.Drought.Flood.DI	0.07374621	0.02906678	0.05697088	0.0111765290	0.0167753230	0.130717090	5
25	SiClLo.Field Capacity.Capillary Rise.Ag	SiClLo.Field Capacity.Flood.DI	0.07405468	0.02771892	0.05432909	0.0075484070	0.0197255881	0.128383770	5
26	SiClLo.Drought.Flood.Ag	SiClLo.Field Capacity.Flood.DI	0.07438846	0.02770265	0.05429720	0.0072476232	0.0200912631	0.128685654	5
27	SaLo.Field Capacity.Capillary Rise.Ag	SiClLo.Drought.Flood.DI	0.07656264	0.02892950	0.05670182	0.0081323521	0.0198608208	0.133264456	5
28	SaLo.Drought.Capillary Rise.DI	SiClLo.Drought.Flood.DI	0.08416383	0.02856373	0.05598491	0.0032136320	0.0281789212	0.140148737	6
29	SiClLo.Field Capacity.Capillary Rise.Ag	SiClLo.Drought.Flood.DI	0.08588775	0.02848176	0.05582424	0.0025652589	0.0300635064	0.141711995	6
30	SiClLo.Drought.Flood.Ag	SiClLo.Drought.Flood.DI	0.08622153	0.02846593	0.05579322	0.0024541517	0.0304283090	0.142014751	6
31	SaLo.Drought.Capillary Rise.Ag	SiClLo.Field Capacity.Flood.Ag	0.08869624	0.02571329	0.05039805	0.0005617677	0.0382981914	0.139094291	6
32	SaLo.Drought.Capillary Rise.Ag	SiClLo.Drought.Capillary Rise.Ag	0.09449972	0.02610126	0.05115846	0.0002940289	0.0433412599	0.145658186	7
33	SaLo.Drought.Capillary Rise.Ag	SiClLo.Field Capacity.Flood.DI	0.10024392	0.02648668	0.05191390	0.0001538993	0.0483300259	0.152157816	7
34	SaLo.Drought.Capillary Rise.Ag	SiClLo.Drought.Flood.DI	0.11207699	0.02728483	0.05347827	0.0000399677	0.0585987183	0.165555267	8

Supplemental Material T-5: Post Hoc Wald Test Results Featuring statistically significant ARQ Comparisons grouped into statistically different clusters composed of statistically similar comparisons of effects on porewater phosphate concentrations.

Acronym	Soil Texture	Moisture Regime	Water Application	Water Type
SiClLo-FC-F-Ag	Silty Clay Loam	Field Capacity	Flooding	Ag. Runoff
SiClLo-FC-F-DI	Silty Clay Loam	Field Capacity	Flooding	DI Water
SiClLo-FC-CR-Ag	Silty Clay Loam	Field Capacity	Capillary Rise	Ag. Runoff
SiClLo-FC-CR-DI	Silty Clay Loam	Field Capacity	Capillary Rise	DI Water
SiClLo-D-F-Ag	Silty Clay Loam	Drought	Flooding	Ag. Runoff
SiClLo-D-F-DI	Silty Clay Loam	Drought	Flooding	DI Water
SiClLo-D-CR-Ag	Silty Clay Loam	Drought	Capillary Rise	Ag. Runoff
SiClLo-D-CR-DI	Silty Clay Loam	Drought	Capillary Rise	DI Water
SaLo-FC-F-Ag	Sandy Loam	Field Capacity	Flooding	Ag. Runoff
SaLo-FC-F-DI	Sandy Loam	Field Capacity	Flooding	DI Water
SaLo-FC-CR-Ag	Sandy Loam	Field Capacity	Capillary Rise	Ag. Runoff
SaLo-FC-CR-DI	Sandy Loam	Field Capacity	Capillary Rise	DI Water
SaLo-D-F-Ag	Sandy Loam	Drought	Flooding	Ag. Runoff
SaLo-D-F-DI	Sandy Loam	Drought	Flooding	DI Water
SaLo-D-CR-Ag	Sandy Loam	Drought	Capillary Rise	Ag. Runoff
SaLo-D-CR-DI	Sandy Loam	Drought	Capillary Rise	DI Water

Supplemental Material T-6: Table showing what each treatment acronym means, including Soil Texture, Moisture Regime, Water Application, and Water Type.

8.03 Supplemental Material-Code

8.03.1 GAMM R Code (Supplemental Material C-1)

```
#install.packages("mgcv")
#install.packages("reshape2")
library(mgcv)
library(mgcViz)
GLMM.Table=read.csv("C:/Users/jacob/Documents/Research/GLMM.Table.2.csv", header=T)
attach(GLMM.Table)
names(GLMM.Table)
library(moments)
library(multcomp)
library(itsadug)
library(ggplot2)
library(tidyr)
library(dplyr)
library(purrr)
library(reshape2)
skewness(GLMM.Table$Nitrate, na.rm = TRUE)
skewness(GLMM.Table$Ammonium, na.rm = TRUE)
skewness(GLMM.Table$Phosphate, na.rm = TRUE)
skewness(GLMM.Table$Pore.Water.pH, na.rm = TRUE)
skewness(GLMM.Table$ARQ, na.rm = TRUE)

# Generate a simpler model without interaction terms
nitrate.gamm.1 <- gam(Nitrate ~ (Soil.Texture) + (Moisture.Regime) + (Water.Application) +
(Ag.DI)+
                    s(Week, bs = "ad", k=13),
                   family=gaussian(link="inverse"),
data = GLMM.Table, na.action=na.omit)
```

```
summary(nitrate.gamm.1)
#Add in Interactions
GLMM.Table$Soil.Texture <- as.factor(GLMM.Table$Soil.Texture)
GLMM.Table$Moisture.Regime <- as.factor(GLMM.Table$Moisture.Regime)
GLMM.Table$Water.Application <- as.factor(GLMM.Table$Water.Application)
GLMM.Table$Ag.DI <- as.factor(GLMM.Table$Ag.DI)


#Go to best model code.r for bs and k values
nitrate.gamm.2 <- gam(Nitrate ~ (Soil.Texture) * (Moisture.Regime) * (Water.Application) * (Ag.DI)+
                      s(Week, bs = "ad", k=13),
                     family=gaussian(link="inverse"),
                     data = GLMM.Table, na.action=na.omit)

# Summary of the model
summary(nitrate.gamm.2)
AIC(nitrate.gamm.2)
anova.nitrate=anova(nitrate.gamm.2)
print(anova.nitrate)
plot(nitrate.gamm.2, residuals=FALSE, pch=0.1, cex=0.1, shade=TRUE, shade.col="lightblue", seWithMean = TRUE, main="Nitrate GAM", cex.main=3, cex.lab=1.5, cex.axis=1.1)
concurvity(nitrate.gamm.2, full=TRUE)
k.check(nitrate.gamm.2)
gam.check(nitrate.gamm.2)
nitrate.plot.all=getViz(nitrate.gamm.2)
print(plot(nitrate.plot.all, allTerms=T, pages=1))
anova(nitrate.gamm.1, nitrate.gamm.2, test="Chisq")
wald_gam(nitrate.gamm.2, t.test=TRUE)
wald_nitrate_results <- wald_gam(nitrate.gamm.2, t.test=TRUE)
# Filter out only significant results (p < 0.05)
```

```
nitrate_significant_results <- wald_nitrate_results %>%
  filter(p.value < 0.05)  # Use p.value2 if appropriate
# Selecting and renaming columns for clarity
nitrate_significant_results_formatted <- nitrate_significant_results %>%
  select(Comparison = C1, Against = C2, Estimate, SE, CI, T = T, p.value)  # Adjust column names as needed

# View the formatted significant results
nitrate_significant_results_formatted
write.csv(nitrate_significant_results_formatted, "nitrate_significant_results_formatted.csv")

# Calculate Euclidean distance based on selected measures (e.g., Estimate and SE)
nitrate_distance_matrix <- dist(nitrate_significant_results_formatted[, c("Estimate", "SE")], method = "euclidean")
nitrate.hc <- hclust(nitrate_distance_matrix, method = "ward.D2")
# Choose a suitable number of clusters or cut height
nitrate.clusters <- cutree(nitrate.hc, k=12) # Or use a height threshold
nitrate_significant_results_formatted$Cluster <- nitrate.clusters
nitrate_grouped_summary <- nitrate_significant_results_formatted %>%
  group_by(Cluster) %>%
  summarize(MeanEstimate = mean(Estimate), MeanSE = mean(SE), .groups = 'drop')
print(nitrate_grouped_summary)
plot(nitrate.hc)



# Assuming 95% CI, which typically involves +/- 1.96 * SE for each estimate
# If CI bounds are already provided in your results, you can use those directly
nitrate_significant_results_formatted <- nitrate_significant_results_formatted %>%
  mutate(LowerCI = Estimate - 1.96 * SE,
         UpperCI = Estimate + 1.96 * SE)
```

```
# Creating the coefficient plot
ggplot(nitrate_significant_results_formatted, aes(x = reorder(Comparison, Estimate), y = Estimate)) +
  geom_point() + # Adds the point estimates
  geom_errorbar(aes(ymin = LowerCI, ymax = UpperCI), width = 0.2) + # Adds the CIs as error bars
  coord_flip() + # Flips the coordinates for horizontal bars
  labs(title = "Coefficient Plot of Wald Test Results",
      x = "Variable",
      y = "Estimate") +
  theme_minimal() # Using a minimal theme for clarity

ggplot(nitrate_significant_results_formatted, aes(x = Estimate, ymin = LowerCI, ymax = UpperCI, y = reorder(Comparison, Estimate))) +
  geom_point() + # Adds the point estimates as dots
  geom_errorbarh(aes(xmin = LowerCI, xmax = UpperCI), height = 0.2) + # Adds horizontal error bars for the CIs
  geom_vline(xintercept = 0, linetype = "dashed", color = "red") + # Optional: Add a line at x=0 for reference
  labs(title = "Forest Plot of Nitrate Wald Test Results",
      x = "Estimate",
      y = "Comparison") +
  theme_minimal() # Applying a minimal theme for clarity


# Assume Ammonium is your variable of interest

ammonium.gamm.1 <- gam(Ammonium ~ (Soil.Texture) + (Moisture.Regime) + (Water.Application) + (Ag.DI)+
                        s(Week, bs = "ps", k=4),
                      family=gaussian(link="inverse"),
```

```
                    data = GLMM.Table, na.action=na.omit)




ammonium.gamm.2 <- gam(Ammonium ~ (Soil.Texture) * (Moisture.Regime) *
(Water.Application) * (Ag.DI)+
                      s(Week, bs = "ps", k=4),
                     family=gaussian(link="inverse"),
                    data = GLMM.Table, na.action=na.omit)

# Summary of the model
summary(ammonium.gamm.2)

AIC(ammonium.gamm.2)
anova.ammonium=anova(ammonium.gamm.2)
print(anova.ammonium)
plot(ammonium.gamm.2, residuals=TRUE, pch=0.1, cex=0.1, shade=TRUE,
shade.col="lightblue", main="Ammonium GAM", cex.main=3, cex.lab=1.5, cex.axis=1.1)
concurvity(ammonium.gamm.2, full=TRUE)
k.check(ammonium.gamm.2)
gam.check(ammonium.gamm.2)
ammonium.plot.all=getViz(ammonium.gamm.2)
print(plot(ammonium.plot.all, allTerms=T, pages=1))
anova(ammonium.gamm.1, ammonium.gamm.2, test="Chisq")
wald_gam(ammonium.gamm.2, t.test=TRUE)
wald_ammonium_results <- wald_gam(ammonium.gamm.2, t.test=TRUE)
# Filter out only significant results (p < 0.05)
ammonium_significant_results <- wald_ammonium_results %>%
  filter(p.value < 0.05)  # Use p.value2 if appropriate
# Selecting and renaming columns for clarity
```

```
ammonium_significant_results_formatted <- ammonium_significant_results %>%
  select(Comparison = C1, Against = C2, Estimate, SE, CI, T = T, p.value)  # Adjust column names as needed

# View the formatted significant results
ammonium_significant_results_formatted
write.csv(ammonium_significant_results_formatted, "ammonium_significant_results_formatted.csv")
ammonium_significant_results_formatted <- ammonium_significant_results_formatted %>%
  mutate(LowerCI = Estimate - 1.96 * SE,
         UpperCI = Estimate + 1.96 * SE)

ggplot(ammonium_significant_results_formatted, aes(x = Estimate, ymin = LowerCI, ymax = UpperCI, y = reorder(Comparison, Estimate))) +
  geom_point() + # Adds the point estimates as dots
  geom_errorbarh(aes(xmin = LowerCI, xmax = UpperCI), height = 0.2) + # Adds horizontal error bars for the CIs
  geom_vline(xintercept = 0, linetype = "dashed", color = "red") + # Optional: Add a line at x=0 for reference
  labs(title = "Forest Plot of Ammonium Wald Test Results",
       x = "Estimate",
       y = "Comparison") +
  theme_minimal() # Applying a minimal theme for clarity

# Calculate Euclidean distance based on selected measures (e.g., Estimate and SE)
ammonium_distance_matrix <- dist(ammonium_significant_results_formatted[, c("Estimate", "SE")], method = "euclidean")
ammonium.hc <- hclust(ammonium_distance_matrix, method = "ward.D2")
plot(ammonium.hc)
# Choose a suitable number of clusters or cut height
ammonium.clusters <- cutree(ammonium.hc, k=20) # Or use a height threshold
ammonium_significant_results_formatted$Cluster <- ammonium.clusters
```

```
ammonium_grouped_summary <- ammonium_significant_results_formatted %>%
  group_by(Cluster) %>%
  summarize(MeanEstimate = mean(Estimate), MeanSE = mean(SE), .groups = 'drop')
print(ammonium_grouped_summary)


# Assume Phosphate is your variable of interest
phosphate.gamm.1 <- gam(Phosphate ~ (Soil.Texture) + (Moisture.Regime) +
(Water.Application) + (Ag.DI)+
                         s(Week, bs = "ps", k=9),
                       family=gaussian(link="inverse"),
                       data = GLMM.Table, na.action=na.omit)


phosphate.gamm.2 <- gam(Phosphate ~ (Soil.Texture) * (Moisture.Regime) *
(Water.Application) * (Ag.DI)+
                         s(Week, bs = "ps", k=9),
                        family=gaussian(link="inverse"),
                       data = GLMM.Table, na.action=na.omit)

anova(phosphate.gamm.1, phosphate.gamm.2, test="Chisq")
# Summary of the model
summary(phosphate.gamm.2)
AIC(phosphate.gamm.2)
anova.phosphate=anova.gam(phosphate.gamm.2)
print(anova.phosphate)
plot(phosphate.gamm.2, residuals=TRUE, pch=0.1, cex=0.1, shade=TRUE,
shade.col="lightblue", main="Phosphate GAM", cex.main=3, cex.lab=1.5, cex.axis=1.1)
concurvity(phosphate.gamm.2, full=TRUE)
gam.check(phosphate.gamm.2)
phosphate.plot.all=getViz(phosphate.gamm.2)
```

```
print(plot(phosphate.plot.all, allTerms=T, pages=1))
wald_gam(phosphate.gamm.2, t.test=TRUE)
wald_phosphate_results <- wald_gam(phosphate.gamm.2, t.test=TRUE)
# Filter out only significant results (p < 0.05)
phosphate_significant_results <- wald_phosphate_results %>%
  filter(p.value < 0.05)  # Use p.value2 if appropriate
# Selecting and renaming columns for clarity
phosphate_significant_results_formatted <- phosphate_significant_results %>%
  select(Comparison = C1, Against = C2, Estimate, SE, CI, T = T, p.value)  # Adjust column names as needed

# View the formatted significant results
phosphate_significant_results_formatted
write.csv(phosphate_significant_results_formatted, "phosphate_significant_results_formatted.csv")

phosphate_significant_results_formatted <- phosphate_significant_results_formatted %>%
  mutate(LowerCI = Estimate - 1.96 * SE,
         UpperCI = Estimate + 1.96 * SE)

ggplot(phosphate_significant_results_formatted, aes(x = Estimate, ymin = LowerCI, ymax = UpperCI, y = reorder(Comparison, Estimate))) +
  geom_point() + # Adds the point estimates as dots
  geom_errorbarh(aes(xmin = LowerCI, xmax = UpperCI), height = 0.2) + # Adds horizontal error bars for the CIs
  geom_vline(xintercept = 0, linetype = "dashed", color = "red") + # Optional: Add a line at x=0 for reference
  labs(title = "Forest Plot of Phosphate Wald Test Results",
       x = "Estimate",
       y = "Comparison") +
  theme_minimal() # Applying a minimal theme for clarity
# Calculate Euclidean distance based on selected measures (e.g., Estimate and SE)
```

```
phosphate_distance_matrix <- dist(phosphate_significant_results_formatted[, c("Estimate",
"SE")], method = "euclidean")
phosphate.hc <- hclust(phosphate_distance_matrix, method = "ward.D2")
plot(phosphate.hc)
# Choose a suitable number of clusters or cut height
phosphate.clusters <- cutree(phosphate.hc, h=2) # Or use a height threshold
phosphate_significant_results_formatted$Cluster <- phosphate.clusters
phosphate_grouped_summary <- phosphate_significant_results_formatted %>%
  group_by(Cluster) %>%
  summarize(MeanEstimate = mean(Estimate), MeanSE = mean(SE), .groups = 'drop')
print(phosphate_grouped_summary)




#Pore Water pH is variable of interest
pH.gamm.1 <- gam(Pore.Water.pH ~ (Soil.Texture) + (Moisture.Regime) + (Water.Application) +
(Ag.DI)+
                         s(Week, bs = "cc", k=11),
                       family=Gamma(link="identity"),
                       data = GLMM.Table, na.action=na.omit)


pH.gamm.2 <- gam(Pore.Water.pH ~ (Soil.Texture) * (Moisture.Regime) * (Water.Application) *
(Ag.DI)+
                         s(Week, bs = "cc", k=11),
                 family=Gamma(link="identity"),
                       data = GLMM.Table, na.action=na.omit)
```

```
anova(pH.gamm.1, pH.gamm.2, test="Chisq")
# Summary of the model
summary(pH.gamm.2)
AIC(pH.gamm.2)
anova.pH=anova.gam(pH.gamm.2)
print(anova.pH)
plot(pH.gamm.2, residuals=TRUE, pch=0.1, cex=0.1, shade=TRUE, shade.col="lightblue")
concurvity(pH.gamm.2, full=TRUE)
gam.check(pH.gamm.2)
pH.plot.all=getViz(pH.gamm.2)
print(plot(pH.plot.all, allTerms=T, pages=1))
wald_gam(pH.gamm.2, t.test=TRUE)
wald_pH_results <- wald_gam(pH.gamm.2, t.test=TRUE)
# Filter out only significant results (p < 0.05)
pH_significant_results <- wald_pH_results %>%
  filter(p.value < 0.05)
# Selecting and renaming columns for clarity
pH_significant_results_formatted = pH_significant_results %>%
  select(Comparison = C1, Against = C2, Estimate, SE, CI, p.value)  # Adjust column names as needed

# View the formatted significant results
pH_significant_results_formatted
write.csv(pH_significant_results_formatted, "pH_significant_results_formatted.csv")
pH_significant_results_formatted <- pH_significant_results_formatted %>%
  mutate(LowerCI = Estimate - 1.96 * SE,
         UpperCI = Estimate + 1.96 * SE)

ggplot(pH_significant_results_formatted, aes(x = Estimate, ymin = LowerCI, ymax = UpperCI, y = reorder(Comparison, Estimate))) +
  geom_point() + # Adds the point estimates as dots
```

```
  geom_errorbarh(aes(xmin = LowerCI, xmax = UpperCI), height = 0.2) + # Adds horizontal error bars for the CIs
  geom_vline(xintercept = 0, linetype = "dashed", color = "red") + # Optional: Add a line at x=0 for reference
  labs(title = "Forest Plot of Porewater pH Wald Test Results",
       x = "Estimate",
       y = "Comparison") +
  theme_minimal() # Applying a minimal theme for clarity

pH_distance_matrix <- dist(pH_significant_results_formatted[, c("Estimate", "SE")], method = "euclidean")
pH.hc <- hclust(pH_distance_matrix, method = "ward.D2")
plot(pH.hc)
# Choose a suitable number of clusters or cut height
pH.clusters <- cutree(pH.hc, k=14) # Or use a height threshold
pH_significant_results_formatted$Cluster <- pH.clusters
pH_grouped_summary <- pH_significant_results_formatted %>%
  group_by(Cluster) %>%
  summarize(MeanEstimate = mean(Estimate), MeanSE = mean(SE), .groups = 'drop')
print(pH_grouped_summary)


#ARQ is variable of interest and is  bounded on one end by 0
ARQ.gamm.1 <- gam(ARQ ~ (Soil.Texture) + (Moisture.Regime) + (Water.Application) + (Ag.DI)+
                   s(Week, bs = "tp", k=11),
                  family=Gamma(link="inverse"),
                  data = GLMM.Table, na.action=na.omit)
```

```
ARQ.gamm.2 <- gam(ARQ ~ (Soil.Texture) * (Moisture.Regime) * (Water.Application) * (Ag.DI)+
                   s(Week, bs = "tp", k=11),
                  family=Gamma(link="inverse"),
                 data = GLMM.Table, na.action=na.omit)


anova(ARQ.gamm.1, ARQ.gamm.2, test="Chisq")
# Summary of the model
summary(ARQ.gamm.2)
AIC(ARQ.gamm.2)
anova.ARQ=anova.gam(ARQ.gamm.2)
print(anova.ARQ)
plot(ARQ.gamm.2, residuals=FALSE, pch=0.1, cex=0.1, shade=TRUE, shade.col="lightblue", main="ARQ GAM", cex.main=3, cex.lab=1.5, cex.axis=1.1)
concurvity(ARQ.gamm.2, full=TRUE)
gam.check(ARQ.gamm.2)
ARQ.plot.all=getViz(ARQ.gamm.2)
print(plot(ARQ.plot.all, allTerms=T, pages=1))
wald_gam(ARQ.gamm.2, t.test=TRUE)
wald_ARQ_results <- wald_gam(ARQ.gamm.2, t.test=TRUE)
# Filter out only significant results (p < 0.05)
ARQ_significant_results <- wald_ARQ_results %>%
  filter(p.value < 0.05)
# Selecting and renaming columns for clarity
ARQ_significant_results_formatted = ARQ_significant_results %>%
  select(Comparison = C1, Against = C2, Estimate, SE, CI, p.value)  # Adjust column names as needed

# View the formatted significant results
ARQ_significant_results_formatted
write.csv(ARQ_significant_results_formatted, "ARQ_significant_results_formatted.csv")
```

```
ARQ_significant_results_formatted <- ARQ_significant_results_formatted %>%
  mutate(LowerCI = Estimate - 1.96 * SE,
         UpperCI = Estimate + 1.96 * SE)

ggplot(ARQ_significant_results_formatted, aes(x = Estimate, ymin = LowerCI, ymax = UpperCI, y = reorder(Comparison, Estimate))) +
  geom_point() + # Adds the point estimates as dots
  geom_errorbarh(aes(xmin = LowerCI, xmax = UpperCI), height = 0.2) + # Adds horizontal error bars for the CIs
  geom_vline(xintercept = 0, linetype = "dashed", color = "red") + # Optional: Add a line at x=0 for reference
  labs(title = "Forest Plot of ARQ Wald Test Results",
       x = "Estimate",
       y = "Comparison") +
  theme_minimal() # Applying a minimal theme for clarity

ARQ_distance_matrix <- dist(ARQ_significant_results_formatted[, c("Estimate", "SE")], method = "euclidean")
ARQ.hc <- hclust(ARQ_distance_matrix, method = "ward.D2")
plot(ARQ.hc)
# Choose a suitable number of clusters or cut height
ARQ.clusters <- cutree(ARQ.hc, k=8) # Or use a height threshold
ARQ_significant_results_formatted$Cluster <- ARQ.clusters
ARQ_grouped_summary <- ARQ_significant_results_formatted %>%
  group_by(Cluster) %>%
  summarize(MeanEstimate = mean(Estimate), MeanSE = mean(SE), .groups = 'drop')
print(ARQ_grouped_summary)
#Correlation Tables
GLMM.Table%>%
  group_by(Week) %>%
  summarize(correlation = cor(Nitrate, Ammonium))
```

```
GLMM.Table%>%
  group_by(Week) %>%
  summarize(correlation = cor(Nitrate, Phosphate))
GLMM.Table%>%
  group_by(Week) %>%
  summarize(correlation = cor(Nitrate, Pore.Water.pH))
GLMM.Table%>%
  group_by(Week) %>%
  summarize(correlation = cor(Nitrate, ARQ))
GLMM.Table%>%
  group_by(Week) %>%
  summarize(correlation = cor(Ammonium, Phosphate))
GLMM.Table%>%
  group_by(Week) %>%
  summarize(correlation = cor(Ammonium, Pore.Water.pH))
GLMM.Table%>%
  group_by(Week) %>%
  summarize(correlation = cor(Ammonium, ARQ))
GLMM.Table%>%
  group_by(Week) %>%
  summarize(correlation = cor(Phosphate, Pore.Water.pH))
GLMM.Table%>%
  group_by(Week) %>%
  summarize(correlation = cor(Phosphate, ARQ))
GLMM.Table%>%
  group_by(Week) %>%
  summarize(correlation = cor(Pore.Water.pH, ARQ))


# Define a function to calculate correlation
```

```
calc_correlation <- function(data, var1, var2) {
  data %>%
    group_by(Week) %>%
    summarize(correlation = cor(.data[[var1]], .data[[var2]]),
              variable_pair = paste(var1, var2, sep = "-")) %>%
    ungroup()
}

# List of variable pairs
var_pairs <- list(
  c("Nitrate", "Ammonium"),
  c("Nitrate", "Phosphate"),
  c("Nitrate", "Pore.Water.pH"),
  c("Nitrate", "ARQ"),
  c("Ammonium", "Phosphate"),
  c("Ammonium", "Pore.Water.pH"),
  c("Ammonium", "ARQ"),
  c("Phosphate", "Pore.Water.pH"),
  c("Phosphate", "ARQ"),
  c("Pore.Water.pH", "ARQ")
)

# Calculate correlations for all pairs
correlations <- map_df(var_pairs, ~calc_correlation(GLMM.Table, .x[1], .x[2]))

# Plotting
ggplot(correlations, aes(x = Week, y = correlation, color = variable_pair, group = variable_pair)) +
  geom_line() +
  labs(title = "Weekly Correlations", x = "Week", y = "Correlation") +
```

```
  theme_minimal() +
  theme(legend.position = "bottom") +
  guides(color = guide_legend(title = "Variable Pair"))
# Calculate Euclidean distance based on selected measures (e.g., Estimate and SE)
nitrate_distance_matrix <- dist(nitrate_significant_results_formatted[, c("Estimate", "SE")], method = "euclidean")
nitrate.hc <- hclust(nitrate_distance_matrix, method = "ward.D2")
# Choose a suitable number of clusters or cut height
nitrate.clusters <- cutree(nitrate.hc, k=12) # Or use a height threshold
nitrate_significant_results_formatted$Cluster <- nitrate.clusters
nitrate_grouped_summary <- nitrate_significant_results_formatted %>%
  group_by(Cluster) %>%
  summarize(MeanEstimate = mean(Estimate), MeanSE = mean(SE), .groups = 'drop')
print(nitrate_grouped_summary)
plot(nitrate.hc)



# Assuming 95% CI, which typically involves +/- 1.96 * SE for each estimate
# If CI bounds are already provided in your results, you can use those directly
nitrate_significant_results_formatted <- nitrate_significant_results_formatted %>%
  mutate(LowerCI = Estimate - 1.96 * SE,
         UpperCI = Estimate + 1.96 * SE)

# Creating the coefficient plot
ggplot(nitrate_significant_results_formatted, aes(x = reorder(Comparison, Estimate), y = Estimate)) +
  geom_point() + # Adds the point estimates
  geom_errorbar(aes(ymin = LowerCI, ymax = UpperCI), width = 0.2) + # Adds the CIs as error bars
  coord_flip() + # Flips the coordinates for horizontal bars
```

```
  labs(title = "Coefficient Plot of Wald Test Results",
       x = "Variable",
       y = "Estimate") +
  theme_minimal() # Using a minimal theme for clarity

ggplot(nitrate_significant_results_formatted, aes(x = Estimate, ymin = LowerCI, ymax = UpperCI, y = reorder(Comparison, Estimate))) +
  geom_point() + # Adds the point estimates as dots
  geom_errorbarh(aes(xmin = LowerCI, xmax = UpperCI), height = 0.2) + # Adds horizontal error bars for the CIs
  geom_vline(xintercept = 0, linetype = "dashed", color = "red") + # Optional: Add a line at x=0 for reference
  labs(title = "Forest Plot of Nitrate Wald Test Results",
       x = "Estimate",
       y = "Comparison") +
  theme_minimal() # Applying a minimal theme for clarity
# View the formatted significant results
ammonium_significant_results_formatted
write.csv(ammonium_significant_results_formatted, "ammonium_significant_results_formatted.csv")
ammonium_significant_results_formatted <- ammonium_significant_results_formatted %>%
  mutate(LowerCI = Estimate - 1.96 * SE,
         UpperCI = Estimate + 1.96 * SE)

ggplot(ammonium_significant_results_formatted, aes(x = Estimate, ymin = LowerCI, ymax = UpperCI, y = reorder(Comparison, Estimate))) +
  geom_point() + # Adds the point estimates as dots
  geom_errorbarh(aes(xmin = LowerCI, xmax = UpperCI), height = 0.2) + # Adds horizontal error bars for the CIs
  geom_vline(xintercept = 0, linetype = "dashed", color = "red") + # Optional: Add a line at x=0 for reference
  labs(title = "Forest Plot of Ammonium Wald Test Results",
```

```
      x = "Estimate",
      y = "Comparison") +
  theme_minimal() # Applying a minimal theme for clarity

# Calculate Euclidean distance based on selected measures (e.g., Estimate and SE)
ammonium_distance_matrix <- dist(ammonium_significant_results_formatted[, c("Estimate", "SE")], method = "euclidean")
ammonium.hc <- hclust(ammonium_distance_matrix, method = "ward.D2")
plot(ammonium.hc)
# Choose a suitable number of clusters or cut height
ammonium.clusters <- cutree(ammonium.hc, k=20) # Or use a height threshold
ammonium_significant_results_formatted$Cluster <- ammonium.clusters
ammonium_grouped_summary <- ammonium_significant_results_formatted %>%
  group_by(Cluster) %>%
  summarize(MeanEstimate = mean(Estimate), MeanSE = mean(SE), .groups = 'drop')
print(ammonium_grouped_summary)
phosphate_significant_results_formatted <- phosphate_significant_results_formatted %>%
  mutate(LowerCI = Estimate - 1.96 * SE,
         UpperCI = Estimate + 1.96 * SE)

ggplot(phosphate_significant_results_formatted, aes(x = Estimate, ymin = LowerCI, ymax = UpperCI, y = reorder(Comparison, Estimate))) +
  geom_point() + # Adds the point estimates as dots
  geom_errorbarh(aes(xmin = LowerCI, xmax = UpperCI), height = 0.2) + # Adds horizontal error bars for the CIs
  geom_vline(xintercept = 0, linetype = "dashed", color = "red") + # Optional: Add a line at x=0 for reference
  labs(title = "Forest Plot of Phosphate Wald Test Results",
      x = "Estimate",
      y = "Comparison") +
  theme_minimal() # Applying a minimal theme for clarity
```

```
# Calculate Euclidean distance based on selected measures (e.g., Estimate and SE)
phosphate_distance_matrix <- dist(phosphate_significant_results_formatted[, c("Estimate", "SE")], method = "euclidean")
phosphate.hc <- hclust(phosphate_distance_matrix, method = "ward.D2")
plot(phosphate.hc)
# Choose a suitable number of clusters or cut height
phosphate.clusters <- cutree(phosphate.hc, h=2) # Or use a height threshold
phosphate_significant_results_formatted$Cluster <- phosphate.clusters
phosphate_grouped_summary <- phosphate_significant_results_formatted %>%
  group_by(Cluster) %>%
  summarize(MeanEstimate = mean(Estimate), MeanSE = mean(SE), .groups = 'drop')
print(phosphate_grouped_summary)
pH_significant_results_formatted <- pH_significant_results_formatted %>%
  mutate(LowerCI = Estimate - 1.96 * SE,
         UpperCI = Estimate + 1.96 * SE)

ggplot(pH_significant_results_formatted, aes(x = Estimate, ymin = LowerCI, ymax = UpperCI, y = reorder(Comparison, Estimate))) +
  geom_point() + # Adds the point estimates as dots
  geom_errorbarh(aes(xmin = LowerCI, xmax = UpperCI), height = 0.2) + # Adds horizontal error bars for the CIs
  geom_vline(xintercept = 0, linetype = "dashed", color = "red") + # Optional: Add a line at x=0 for reference
  labs(title = "Forest Plot of Porewater pH Wald Test Results",
       x = "Estimate",
       y = "Comparison") +
  theme_minimal() # Applying a minimal theme for clarity

pH_distance_matrix <- dist(pH_significant_results_formatted[, c("Estimate", "SE")], method = "euclidean")
pH.hc <- hclust(pH_distance_matrix, method = "ward.D2")
plot(pH.hc)
```

```
# Choose a suitable number of clusters or cut height
pH.clusters <- cutree(pH.hc, k=14) # Or use a height threshold
pH_significant_results_formatted$Cluster <- pH.clusters
pH_grouped_summary <- pH_significant_results_formatted %>%
  group_by(Cluster) %>%
  summarize(MeanEstimate = mean(Estimate), MeanSE = mean(SE), .groups = 'drop')
print(pH_grouped_summary)
ARQ_significant_results_formatted
write.csv(ARQ_significant_results_formatted, "ARQ_significant_results_formatted.csv")
ARQ_significant_results_formatted <- ARQ_significant_results_formatted %>%
  mutate(LowerCI = Estimate - 1.96 * SE,
         UpperCI = Estimate + 1.96 * SE)

ggplot(ARQ_significant_results_formatted, aes(x = Estimate, ymin = LowerCI, ymax = UpperCI, y = reorder(Comparison, Estimate))) +
  geom_point() + # Adds the point estimates as dots
  geom_errorbarh(aes(xmin = LowerCI, xmax = UpperCI), height = 0.2) + # Adds horizontal error bars for the CIs
  geom_vline(xintercept = 0, linetype = "dashed", color = "red") + # Optional: Add a line at x=0 for reference
  labs(title = "Forest Plot of ARQ Wald Test Results",
       x = "Estimate",
       y = "Comparison") +
  theme_minimal() # Applying a minimal theme for clarity

ARQ_distance_matrix <- dist(ARQ_significant_results_formatted[, c("Estimate", "SE")], method = "euclidean")
ARQ.hc <- hclust(ARQ_distance_matrix, method = "ward.D2")
plot(ARQ.hc)
# Choose a suitable number of clusters or cut height
ARQ.clusters <- cutree(ARQ.hc, k=8) # Or use a height threshold
```

```
ARQ_significant_results_formatted$Cluster <- ARQ.clusters
ARQ_grouped_summary <- ARQ_significant_results_formatted %>%
  group_by(Cluster) %>%
  summarize(MeanEstimate = mean(Estimate), MeanSE = mean(SE), .groups = 'drop')
print(ARQ_grouped_summary)
```

8.03.2 Correlation and K-Means Clustering R Code (Supplemental Material C-2)

```
Initial.Final.data <- read.csv("Initial.Final.Table.csv", header=T)
attach(Initial.Final.data)
head(Initial.Final.data)
summary(Initial.Final.data)
# Convert categorical variables to factors
str(Initial.Final.data)
Initial.Final.data$Time <- as.factor(Initial.Final.data$Time)
Initial.Final.data$Land.Use <- as.factor(Initial.Final.data$Land.Use)
Initial.Final.data$Moisture.Regime <- as.factor(Initial.Final.data$Moisture.Regime)
Initial.Final.data$Water.Application <- as.factor(Initial.Final.data$Water.Application)
Initial.Final.data$Ag.DI <- as.factor(Initial.Final.data$Ag.DI)

cor_matrix <- cor(Initial.Final.data[, c("KCl.Nitrate", "KCl.Ammonium", "Fe2", "Fe3", "perC",
"perN", "perS", "Soil.pH")], use = "complete.obs")
corrplot::corrplot(cor_matrix, method = "circle", type="lower")

covmat <- cov(Initial.Final.data[, sapply(Initial.Final.data, is.numeric)], use="na.or.complete")
print(covmat)

#K-means clustering
# Load necessary packages
#install.packages("dplyr")
#install.packages("ggplot2")
library(dplyr)
library(ggplot2)
```

```
# Filter only numeric columns
numeric_data <- Initial.Final.data %>% select_if(is.numeric)

# Scale the data
scaled_data <- scale(numeric_data)
set.seed(123) # for reproducibility
wss <- (nrow(scaled_data)-1)*sum(apply(scaled_data,2,var))
for (i in 2:15) wss[i] <- sum(kmeans(scaled_data, centers=i)$tot.withinss)

# Plot the Elbow Curve
plot(1:15, wss, type="b", xlab="Number of Clusters", ylab="Within groups sum of squares")

set.seed(123) # for reproducibility
k_value <- 6  # or whatever value you chose based on the Elbow curve
kmeans_result <- kmeans(scaled_data, centers=k_value)
kmeans_result$Factor_Importance <- c("Land.Use", "Moisture.Regime", "Water.Application",
"Ag.DI")
# Print cluster assignments
print(kmeans_result$cluster)

# Attach cluster assignments to the original data
Initial.Final.data$cluster <- kmeans_result$cluster

# Check cluster centers
print(kmeans_result$centers)

# Perform PCA
pca_result <- prcomp(scaled_data)
```

```
# Plot clusters using the first two principal components
ggplot(as.data.frame(pca_result$x), aes(PC1, PC2, color=factor(kmeans_result$cluster))) +
  geom_point(alpha=0.6, size=8) +
  theme_minimal() +
  labs(color='Cluster')+
  theme(axis.text.x = element_text(size=20),  # Increase x-axis label size
        axis.text.y = element_text(size=20))  # Increase y-axis label size
scores <- pca_result$x
PC1_scores <- scores[,1]
PC2_scores <- scores[,2]
PC1_scores
PC2_scores

# Assuming you stored your k-means result in kmeans_result
cluster_assignments <- kmeans_result$cluster

# You can add this as a new column to your data for easier inspection
Initial.Final.data$Cluster <- cluster_assignments

# View the dataset with the cluster assignments
head(Initial.Final.data)
tail(Initial.Final.data)
Initial.Final.data
cluster1_data <- Initial.Final.data %>% filter(Cluster == 1)
cluster2_data <- Initial.Final.data %>% filter(Cluster == 2)
cluster3_data <- Initial.Final.data %>% filter(Cluster == 3)
cluster4_data <- Initial.Final.data %>% filter(Cluster == 4)
cluster5_data <- Initial.Final.data %>% filter(Cluster == 5)
cluster6_data <- Initial.Final.data %>% filter(Cluster == 6)
head(cluster1_data)
```

```
head(cluster2_data)
head(cluster3_data)
head(cluster4_data)
head(cluster5_data)
head(cluster6_data)
clusters_3_and_5_data <- Initial.Final.data %>% filter(Cluster %in% c(3, 5))
head(clusters_3_and_5_data)

#Parallel Coordinates Plot
install.packages("RColorBrewer")
library(RColorBrewer)

num_clusters <- length(unique(Initial.Final.data$cluster))
cluster_colors <- brewer.pal(num_clusters, "Set1")  # "Set1" is a palette with distinct colors. Adjust as needed.

#install.packages("GGally")
library(GGally)
Initial.Final.data$cluster <- kmeans_result$cluster
ggparcoord(Initial.Final.data, columns = 1:(ncol(Initial.Final.data)-1), groupColumn = ncol(Initial.Final.data), scale = "uniminmax") +
  theme_minimal() +
  labs(title = "Parallel Coordinates Plot for K-means Data", group="Cluster") +
  theme(legend.position="bottom")

# Get loadings for PC1 and PC2
loadings_pc1 <- pca_result$rotation[, "PC1"]
loadings_pc2 <- pca_result$rotation[, "PC2"]
sort(loadings_pc1, decreasing = TRUE)
sort(loadings_pc2, decreasing = TRUE)
```

```
# Assuming pca_result is the result of prcomp
summary_pca <- summary(pca_result)

# Variance explained by each principal component
explained_variance <- summary_pca$importance[2, ]

# Proportion of variance explained
proportion_explained <- explained_variance / sum(explained_variance)

# Percentage of variance explained by PC1 and PC2
percent_variance_PC1 <- proportion_explained[1] * 100
percent_variance_PC2 <- proportion_explained[2] * 100

# Output the variance explained by PC1 and PC2
cat("Percentage of variance explained by PC1:", percent_variance_PC1, "%\n")
cat("Percentage of variance explained by PC2:", percent_variance_PC2, "%\n")


#Hierarchical Clustering
numeric_data <- Initial.Final.data[sapply(Initial.Final.data, is.numeric)]
scaled_numeric_data <- scale(numeric_data)
dist_matrix <- dist(scaled_numeric_data, method = "euclidean")
hclust_result <- hclust(dist_matrix, method = "average")
# If for example, you want to use a column "Labels" as the labels on the dendrogram
rownames(scaled_data) <- Initial.Final.data$Labels
plot(hclust_result, hang = -1)
cluster_assignments <- cutree(hclust_result, k=6)
rect.hclust(hclust_result, k = 6, border = "red")
```

8.03.3 Random Forest R Code (Supplemental Material C-3)

```
#install.packages(c("randomForest", "ggplot2"))
```

```
library(randomForest)
library(ggplot2)
Initial.Final.data$Land.Use <- as.factor(Initial.Final.data$Land.Use)
Initial.Final.data$Moisture.Regime <- as.factor(Initial.Final.data$Moisture.Regime)
Initial.Final.data$Water.Application <- as.factor(Initial.Final.data$Water.Application)
Initial.Final.data$Ag.DI <- as.factor(Initial.Final.data$Ag.DI)

#Nitrate

rf.nitrate <- randomForest(KCl.Nitrate ~ Land.Use + Moisture.Regime + Water.Application +
Ag.DI, data=Initial.Final.data, ntree=500, mtry=2, importance=TRUE)
importance.nitrate <- importance(rf.nitrate)

importance.nitrate.df <- data.frame(
  Variable = rownames(importance.nitrate),
  Importance = importance.nitrate[,"IncNodePurity"]
)

ggplot(importance.nitrate.df, aes(x=reorder(Variable, Importance), y=Importance)) +
  geom_bar(stat="identity") +
  coord_flip() +
  labs(title="Feature Importance-Nitrate", x="Variables", y="Increase in Node Purity")

#Ammonium

rf.ammonium <- randomForest(KCl.Ammonium ~ Land.Use + Moisture.Regime +
Water.Application + Ag.DI, data=Initial.Final.data, ntree=500, mtry=2, importance=TRUE)
importance.ammonium <- importance(rf.ammonium)

importance.ammonium.df <- data.frame(
  Variable = rownames(importance.ammonium),
```

```
  Importance = importance.ammonium[,"IncNodePurity"]
)

ggplot(importance.ammonium.df, aes(x=reorder(Variable, Importance), y=Importance)) +
  geom_bar(stat="identity") +
  coord_flip() +
  labs(title="Feature Importance-Ammonium", x="Variables", y="Increase in Node Purity")


#Fe2
rf.Fe2 <- randomForest(Fe2 ~ Land.Use + Moisture.Regime + Water.Application + Ag.DI,
data=Initial.Final.data, ntree=500, mtry=2, importance=TRUE)
importance.Fe2 <- importance(rf.Fe2)

importance.Fe2.df <- data.frame(
  Variable = rownames(importance.Fe2),
  Importance = importance.Fe2[,"IncNodePurity"]
)

ggplot(importance.Fe2.df, aes(x=reorder(Variable, Importance), y=Importance)) +
  geom_bar(stat="identity") +
  coord_flip() +
  labs(title="Feature Importance-Fe2", x="Variables", y="Increase in Node Purity")

#Fe3
rf.Fe3 <- randomForest(Fe3 ~ Land.Use + Moisture.Regime + Water.Application + Ag.DI,
data=Initial.Final.data, ntree=500, mtry=2, importance=TRUE)
importance.Fe3 <- importance(rf.Fe3)

importance.Fe3.df <- data.frame(
  Variable = rownames(importance.Fe3),
```

```
  Importance = importance.Fe3[,"IncNodePurity"]
)

ggplot(importance.Fe3.df, aes(x=reorder(Variable, Importance), y=Importance)) +
  geom_bar(stat="identity") +
  coord_flip() +
  labs(title="Feature Importance-Fe3", x="Variables", y="Increase in Node Purity")

#perC
rf.perC <- randomForest(perC ~ Land.Use + Moisture.Regime + Water.Application + Ag.DI, data=Initial.Final.data, ntree=500, mtry=2, importance=TRUE)
importance.perC <- importance(rf.perC)

importance.perC.df <- data.frame(
  Variable = rownames(importance.perC),
  Importance = importance.perC[,"IncNodePurity"]
)

ggplot(importance.perC.df, aes(x=reorder(Variable, Importance), y=Importance)) +
  geom_bar(stat="identity") +
  coord_flip() +
  labs(title="Feature Importance-perC", x="Variables", y="Increase in Node Purity")

#perN
rf.perN <- randomForest(perN ~ Land.Use + Moisture.Regime + Water.Application + Ag.DI, data=Initial.Final.data, ntree=500, mtry=2, importance=TRUE)
importance.perN <- importance(rf.perN)

importance.perN.df <- data.frame(
  Variable = rownames(importance.perN),
  Importance = importance.perN[,"IncNodePurity"]
```

```
)

ggplot(importance.perN.df, aes(x=reorder(Variable, Importance), y=Importance)) +
  geom_bar(stat="identity") +
  coord_flip() +
  labs(title="Feature Importance-perN", x="Variables", y="Increase in Node Purity")

#perS
rf.perS <- randomForest(perS ~ Land.Use + Moisture.Regime + Water.Application + Ag.DI, data=Initial.Final.data, ntree=500, mtry=2, importance=TRUE)
importance.perS <- importance(rf.perS)

importance.perS.df <- data.frame(
  Variable = rownames(importance.perS),
  Importance = importance.perS[,"IncNodePurity"]
)

ggplot(importance.perS.df, aes(x=reorder(Variable, Importance), y=Importance)) +
  geom_bar(stat="identity") +
  coord_flip() +
  labs(title="Feature Importance-perS", x="Variables", y="Increase in Node Purity")

#Soil.pH
rf.Soil.pH <- randomForest(Soil.pH ~ Land.Use + Moisture.Regime + Water.Application + Ag.DI, data=Initial.Final.data, ntree=500, mtry=2, importance=TRUE)
importance.Soil.pH <- importance(rf.Soil.pH)

importance.Soil.pH.df <- data.frame(
  Variable = rownames(importance.Soil.pH),
  Importance = importance.Soil.pH[,"IncNodePurity"]
)
```

```
ggplot(importance.Soil.pH.df, aes(x=reorder(Variable, Importance), y=Importance)) +
  geom_bar(stat="identity") +
  coord_flip() +
  labs(title="Feature Importance-Soil pH", x="Variables", y="Increase in Node Purity")
```

8.03.4 Soil Texture Triangle R Code (Supplemental Material C-4)

```
library(soiltexture)
TT.plot( class.sys = "USDA.TT" )
natural.texture=data.frame(
  "CLAY"=c(33.16, 28.82, 2.25, 26.32, 8.22), "SILT"=c(50.91, 31.14, 36.89, 19.82, 21.39),
"SAND"=c(15.93, 40.04, 60.85, 53.85, 70.39)
)
TT.plot(
  class.sys = "USDA.TT",
  tri.data = natural.texture,
  main = "Uncultivated Soil Texture",
  cex.main=2,
  col="red",
  col.lab="black",
  class.lab.col = "beige",
  pch=4,
  class.p.bg.col=c("slategray2", "palegreen", "skyblue", "palegoldenrod", "coral", "palevioletred",
"seagreen1", "royalblue", "orchid", "peru", "salmon", "indianred")
)
chart.labels.uc=c("A-Bw1”, “Bw2", "C", "Ab", "2C")
TT.text(
  tri.data = natural.texture,
  geo = geo,
  labels = chart.labels.uc,
  font = 2,
  col = "black",
```

```
  adj=1,
  pos=1
)
TT.points.in.classes(
  tri.data = natural.texture[1:5,],
  class.sys = "USDA.TT"
)
library(soiltexture)
TT.plot( class.sys = "USDA.TT" )
cultivated.texture=data.frame(
  "CLAY"=c(5.17, 3.19, 4.16, 19.14, 37.45, 42.83, 39.38), "SILT"=c(41.05, 54.65, 57.53, 63.12, 50.2, 52.54, 41.39), "SAND"=c(53.78, 42.15, 38.31, 17.74, 12.35, 4.63, 19.22)
)
TT.plot(
  class.sys = "USDA.TT",
  tri.data = cultivated.texture,
  main = "Cultivated Soil Texture",
  cex.main=2,
  col="red",
  col.lab="black",
  class.lab.col = "beige",
  pch=4,
  class.p.bg.col=c("slategray2", "palegreen", "skyblue", "palegoldenrod", "coral", "palevioletred", "seagreen1", "royalblue", "orchid", "peru", "salmon", "indianred")
)
chart.labels=c("Ap", "A", "AB", "Bw", "Bk1", "Bk2", "C")
TT.text(
  tri.data = cultivated.texture,
  geo = geo,
  labels = chart.labels,
  font = 2,
```

```
  col = "black",
  adj=1,
  pos=1
)
TT.points.in.classes(
  tri.data = cultivated.texture[1:5,],
  class.sys = "USDA.TT"
)
```

8.03.5 Porewater Chemistry Boxplot Code

```
#install.packages("tidyverse")
library(tidyverse)
long_data <- GLMM.Table %>%
  gather(key = "Variable", value = "Value", Soil.Texture, Moisture.Regime,
Water.Application, Ag.DI)
ggplot(long_data, aes(x = Value, y = Nitrate, fill = Value)) +
  geom_boxplot() +
  facet_wrap(~ Variable, scales = "free_x") +  # Use facetting by Variable
  labs(title = "Effect of Variables on Nitrate Concentrations",
       x = "",
       y = "Nitrate Concentration") +
  theme_minimal()

# Create an interaction variable
GLMM.Table$interaction_term <- interaction(GLMM.Table$Soil.Texture,
GLMM.Table$Moisture.Regime, drop = TRUE, sep = " & ")
long_data <- GLMM.Table %>%
  gather(key = "Variable", value = "Value", Soil.Texture, Moisture.Regime,
Water.Application, Ag.DI, interaction_term)
p <- ggplot(long_data, aes(x = Value, y = Nitrate, fill = Value)) +
  geom_boxplot() +
```

```
  facet_wrap(~ Variable, scales = "free_x") +  # Use facetting by Variable
  labs(title = "Effect of Variables and Interactions on Nitrate Concentrations",
       x = "",
       y = "Nitrate Concentration") +
  theme_minimal()

print(p)

# Create interaction variables
GLMM.Table$int_Land_Moisture <- interaction(GLMM.Table$Soil.Texture,
GLMM.Table$Moisture.Regime, drop = TRUE, sep = " & ")
GLMM.Table$int_Land_WaterApp <- interaction(GLMM.Table$Soil.Texture,
GLMM.Table$Water.Application, drop = TRUE, sep = " & ")
GLMM.Table$int_Land_WaterType <- interaction(GLMM.Table$Soil.Texture,
GLMM.Table$Ag.DI, drop = TRUE, sep = " & ")
GLMM.Table$int_Moisture_WaterApp <- interaction(GLMM.Table$Moisture.Regime,
GLMM.Table$Water.Application, drop = TRUE, sep = " & ")
GLMM.Table$int_Moisture_WaterType <- interaction(GLMM.Table$Moisture.Regime,
GLMM.Table$Ag.DI, drop = TRUE, sep = " & ")
GLMM.Table$int_WaterApp_WaterType <- interaction(GLMM.Table$Water.Application,
GLMM.Table$Ag.DI, drop = TRUE, sep = " & ")

# Three-way interactions
GLMM.Table$int_Land_Moisture_WaterApp <- interaction(GLMM.Table$Soil.Texture,
GLMM.Table$Moisture.Regime, GLMM.Table$Water.Application, drop = TRUE, sep = "
& ")
GLMM.Table$int_Land_Moisture_WaterType <- interaction(GLMM.Table$Soil.Texture,
GLMM.Table$Moisture.Regime, GLMM.Table$Ag.DI, drop = TRUE, sep = " & ")
GLMM.Table$int_Land_WaterApp_WaterType <- interaction(GLMM.Table$Soil.Texture,
GLMM.Table$Water.Application, GLMM.Table$Ag.DI, drop = TRUE, sep = " & ")
```

```
GLMM.Table$int_Moisture_WaterApp_WaterType <-
interaction(GLMM.Table$Moisture.Regime, GLMM.Table$Water.Application,
GLMM.Table$Ag.DI, drop = TRUE, sep = " & ")

# Four-way interaction
GLMM.Table$int_Land_Moisture_WaterApp_WaterType <-
interaction(GLMM.Table$Soil.Texture, GLMM.Table$Moisture.Regime,
GLMM.Table$Water.Application, GLMM.Table$Ag.DI, drop = TRUE, sep = " & ")

# Gather into long format
long_data <- GLMM.Table %>%
  gather(key = "Variable", value = "Value",
         Soil.Texture, Moisture.Regime, Water.Application, Ag.DI,
         int_Land_Moisture, int_Land_WaterApp, int_Land_WaterType,
         int_Moisture_WaterApp, int_Moisture_WaterType, int_WaterApp_WaterType,
         int_Land_Moisture_WaterApp, int_Land_Moisture_WaterType,
         int_Land_WaterApp_WaterType, int_Moisture_WaterApp_WaterType,
         int_Land_Moisture_WaterApp_WaterType)
nitrate.p2 <- ggplot(long_data, aes(x = Value, y = Nitrate, fill = Value)) +
  geom_boxplot() +
  facet_wrap(~ Variable, scales = "free_x") +  # Use facetting by Variable
  labs(title = "Effect of Variables and Their Interactions on Nitrate Concentrations",
       x = "",
       y = "Nitrate Concentration g/L") +
  theme_minimal() +
  theme_minimal() +
  theme(axis.text.x = element_text(angle = 45, hjust = 1, size = 8),  # Adjust x-axis text
size
        axis.text.y = element_text(size = 10),                         # Adjust y-axis text size
        axis.title.x = element_text(size = 14),                        # Adjust x-axis title size
```

```
        axis.title.y = element_text(size = 14),                    # Adjust y-axis title size
        plot.title = element_text(size = 16))

print(nitrate.p2)
#install.packages("tidyverse")
library(tidyverse)
long_data <- GLMM.Table %>%
  gather(key = "Variable", value = "Value", Land.Use, Moisture.Regime, Water.Application, Ag.DI)
ggplot(long_data, aes(x = Value, y = Ammonium, fill = Value)) +
  geom_boxplot() +
  facet_wrap(~ Variable, scales = "free_x") +  # Use facetting by Variable
  labs(title = "Effect of Variables on Ammonium Concentrations",
       x = "",
       y = "Ammonium Concentration") +
  theme_minimal()

# Create an interaction variable
GLMM.Table$interaction_term <- interaction(GLMM.Table$Soil.Texture, GLMM.Table$Moisture.Regime, drop = TRUE, sep = " & ")
long_data <- GLMM.Table %>%
  gather(key = "Variable", value = "Value", Soil.Texture, Moisture.Regime, Water.Application, Ag.DI, interaction_term)
p <- ggplot(long_data, aes(x = Value, y = Nitrate, fill = Value)) +
  geom_boxplot() +
  facet_wrap(~ Variable, scales = "free_x") +  # Use facetting by Variable
  labs(title = "Effect of Variables and Interactions on Nitrate Concentrations",
       x = "",
       y = "Nitrate Concentration") +
```

```
  theme_minimal()

print(p)

# Create interaction variables
GLMM.Table$int_Land_Moisture <- interaction(GLMM.Table$Soil.Texture,
GLMM.Table$Moisture.Regime, drop = TRUE, sep = " & ")
GLMM.Table$int_Land_WaterApp <- interaction(GLMM.Table$Soil.Texture,
GLMM.Table$Water.Application, drop = TRUE, sep = " & ")
GLMM.Table$int_Land_WaterType <- interaction(GLMM.Table$Soil.Texture,
GLMM.Table$Ag.DI, drop = TRUE, sep = " & ")
GLMM.Table$int_Moisture_WaterApp <- interaction(GLMM.Table$Moisture.Regime,
GLMM.Table$Water.Application, drop = TRUE, sep = " & ")
GLMM.Table$int_Moisture_WaterType <- interaction(GLMM.Table$Moisture.Regime,
GLMM.Table$Ag.DI, drop = TRUE, sep = " & ")
GLMM.Table$int_WaterApp_WaterType <- interaction(GLMM.Table$Water.Application,
GLMM.Table$Ag.DI, drop = TRUE, sep = " & ")

# Three-way interactions
GLMM.Table$int_Land_Moisture_WaterApp <- interaction(GLMM.Table$Soil.Texture,
GLMM.Table$Moisture.Regime, GLMM.Table$Water.Application, drop = TRUE, sep = "
& ")
GLMM.Table$int_Land_Moisture_WaterType <- interaction(GLMM.Table$Soil.Texture,
GLMM.Table$Moisture.Regime, GLMM.Table$Ag.DI, drop = TRUE, sep = " & ")
GLMM.Table$int_Land_WaterApp_WaterType <- interaction(GLMM.Table$Soil.Texture,
GLMM.Table$Water.Application, GLMM.Table$Ag.DI, drop = TRUE, sep = " & ")
GLMM.Table$int_Moisture_WaterApp_WaterType <-
interaction(GLMM.Table$Moisture.Regime, GLMM.Table$Water.Application,
GLMM.Table$Ag.DI, drop = TRUE, sep = " & ")

# Four-way interaction
```

```
GLMM.Table$int_Land_Moisture_WaterApp_WaterType <-
interaction(GLMM.Table$Soil.Texture, GLMM.Table$Moisture.Regime,
GLMM.Table$Water.Application, GLMM.Table$Ag.DI, drop = TRUE, sep = " & ")

# Gather into long format
long_data <- GLMM.Table %>%
  gather(key = "Variable", value = "Value",
         Soil.Texture, Moisture.Regime, Water.Application, Ag.DI,
         int_Land_Moisture, int_Land_WaterApp, int_Land_WaterType,
         int_Moisture_WaterApp, int_Moisture_WaterType, int_WaterApp_WaterType,
         int_Land_Moisture_WaterApp, int_Land_Moisture_WaterType,
         int_Land_WaterApp_WaterType, int_Moisture_WaterApp_WaterType,
         int_Land_Moisture_WaterApp_WaterType)
ammonium.p2 <- ggplot(long_data, aes(x = Value, y = Ammonium, fill = Value)) +
  geom_boxplot() +
  facet_wrap(~ Variable, scales = "free_x") +  # Use facetting by Variable
  labs(title = "Effect of Variables and Their Interactions on Ammonium Concentrations",
       x = "",
       y = "Ammonium Concentration") +
  theme_minimal() +
  theme(axis.text.x = element_text(angle = 45, hjust = 1, size = 8),  # Adjust x-axis text
size
        axis.text.y = element_text(size = 10),                        # Adjust y-axis text size
        axis.title.x = element_text(size = 14),                       # Adjust x-axis title size
        axis.title.y = element_text(size = 14),                       # Adjust y-axis title size
        plot.title = element_text(size = 16))

print(ammonium.p2)
#install.packages("tidyverse")
```

```
library(tidyverse)
long_data <- GLMM.Table %>%
  gather(key = "Variable", value = "Value", Land.Use, Moisture.Regime, Water.Application, Ag.DI)
ggplot(long_data, aes(x = Value, y = Phosphate, fill = Value)) +
  geom_boxplot() +
  facet_wrap(~ Variable, scales = "free_x") +  # Use facetting by Variable
  labs(title = "Effect of Variables on Phosphate Concentrations",
       x = "",
       y = "Phosphate Concentration") +
  theme_minimal()

# Create interaction variables
GLMM.Table$int_Land_Moisture <- interaction(GLMM.Table$Soil.Texture, GLMM.Table$Moisture.Regime, drop = TRUE, sep = " & ")
GLMM.Table$int_Land_WaterApp <- interaction(GLMM.Table$Soil.Texture, GLMM.Table$Water.Application, drop = TRUE, sep = " & ")
GLMM.Table$int_Land_WaterType <- interaction(GLMM.Table$Soil.Texture, GLMM.Table$Ag.DI, drop = TRUE, sep = " & ")
GLMM.Table$int_Moisture_WaterApp <- interaction(GLMM.Table$Moisture.Regime, GLMM.Table$Water.Application, drop = TRUE, sep = " & ")
GLMM.Table$int_Moisture_WaterType <- interaction(GLMM.Table$Moisture.Regime, GLMM.Table$Ag.DI, drop = TRUE, sep = " & ")
GLMM.Table$int_WaterApp_WaterType <- interaction(GLMM.Table$Water.Application, GLMM.Table$Ag.DI, drop = TRUE, sep = " & ")

# Three-way interactions
GLMM.Table$int_Land_Moisture_WaterApp <- interaction(GLMM.Table$Soil.Texture, GLMM.Table$Moisture.Regime, GLMM.Table$Water.Application, drop = TRUE, sep = " & ")
GLMM.Table$int_Land_Moisture_WaterType <- interaction(GLMM.Table$Soil.Texture, GLMM.Table$Moisture.Regime, GLMM.Table$Ag.DI, drop = TRUE, sep = " & ")
```

```
GLMM.Table$int_Land_WaterApp_WaterType <- interaction(GLMM.Table$Soil.Texture,
GLMM.Table$Water.Application, GLMM.Table$Ag.DI, drop = TRUE, sep = " & ")
GLMM.Table$int_Moisture_WaterApp_WaterType <-
interaction(GLMM.Table$Moisture.Regime, GLMM.Table$Water.Application,
GLMM.Table$Ag.DI, drop = TRUE, sep = " & ")

# Four-way interaction
GLMM.Table$int_Land_Moisture_WaterApp_WaterType <-
interaction(GLMM.Table$Soil.Texture, GLMM.Table$Moisture.Regime,
GLMM.Table$Water.Application, GLMM.Table$Ag.DI, drop = TRUE, sep = " & ")

# Gather into long format
long_data <- GLMM.Table %>%
  gather(key = "Variable", value = "Value",
         Soil.Texture, Moisture.Regime, Water.Application, Ag.DI,
         int_Land_Moisture, int_Land_WaterApp, int_Land_WaterType,
         int_Moisture_WaterApp, int_Moisture_WaterType, int_WaterApp_WaterType,
         int_Land_Moisture_WaterApp, int_Land_Moisture_WaterType,
         int_Land_WaterApp_WaterType, int_Moisture_WaterApp_WaterType,
         int_Land_Moisture_WaterApp_WaterType)
phosphate.p2 <- ggplot(long_data, aes(x = Value, y = Phosphate, fill = Value)) +
  geom_boxplot() +
  facet_wrap(~ Variable, scales = "free_x") +  # Use facetting by Variable
  labs(title = "Effect of Variables and Their Interactions on Phosphate Concentrations",
       x = "",
       y = "Phosphate Concentration") +
  theme_minimal() +
  theme(axis.text.x = element_text(angle = 45, hjust = 1, size = 8),  # Adjust x-axis text
size
        axis.text.y = element_text(size = 10),                        # Adjust y-axis text size
```

```
        axis.title.x = element_text(size = 14),                 # Adjust x-axis title size
        axis.title.y = element_text(size = 14),                 # Adjust y-axis title size
        plot.title = element_text(size = 16))

print(phosphate.p2)
#install.packages("tidyverse")
library(tidyverse)
long_data <- GLMM.Table %>%
  gather(key = "Variable", value = "Value", Land.Use, Moisture.Regime, Water.Application, Ag.DI)
ggplot(long_data, aes(x = Value, y = Pore.Water.pH, fill = Value)) +
  geom_boxplot() +
  facet_wrap(~ Variable, scales = "free_x") +  # Use facetting by Variable
  labs(title = "Effect of Variables on Pore Water pH",
       x = "",
       y = "Pore Water pH") +
  theme_minimal()

# Create interaction variables
GLMM.Table$int_Land_Moisture <- interaction(GLMM.Table$Soil.Texture, GLMM.Table$Moisture.Regime, drop = TRUE, sep = " & ")
GLMM.Table$int_Land_WaterApp <- interaction(GLMM.Table$Soil.Texture, GLMM.Table$Water.Application, drop = TRUE, sep = " & ")
GLMM.Table$int_Land_WaterType <- interaction(GLMM.Table$Soil.Texture, GLMM.Table$Ag.DI, drop = TRUE, sep = " & ")
GLMM.Table$int_Moisture_WaterApp <- interaction(GLMM.Table$Moisture.Regime, GLMM.Table$Water.Application, drop = TRUE, sep = " & ")
GLMM.Table$int_Moisture_WaterType <- interaction(GLMM.Table$Moisture.Regime, GLMM.Table$Ag.DI, drop = TRUE, sep = " & ")
GLMM.Table$int_WaterApp_WaterType <- interaction(GLMM.Table$Water.Application, GLMM.Table$Ag.DI, drop = TRUE, sep = " & ")
```

```
# Three-way interactions
GLMM.Table$int_Land_Moisture_WaterApp <- interaction(GLMM.Table$Soil.Texture,
GLMM.Table$Moisture.Regime, GLMM.Table$Water.Application, drop = TRUE, sep = "
& ")
GLMM.Table$int_Land_Moisture_WaterType <- interaction(GLMM.Table$Soil.Texture,
GLMM.Table$Moisture.Regime, GLMM.Table$Ag.DI, drop = TRUE, sep = " & ")
GLMM.Table$int_Land_WaterApp_WaterType <- interaction(GLMM.Table$Soil.Texture,
GLMM.Table$Water.Application, GLMM.Table$Ag.DI, drop = TRUE, sep = " & ")
GLMM.Table$int_Moisture_WaterApp_WaterType <-
interaction(GLMM.Table$Moisture.Regime, GLMM.Table$Water.Application,
GLMM.Table$Ag.DI, drop = TRUE, sep = " & ")

# Four-way interaction
GLMM.Table$int_Land_Moisture_WaterApp_WaterType <-
interaction(GLMM.Table$Soil.Texture, GLMM.Table$Moisture.Regime,
GLMM.Table$Water.Application, GLMM.Table$Ag.DI, drop = TRUE, sep = " & ")

# Gather into long format
long_data <- GLMM.Table %>%
  gather(key = "Variable", value = "Value",
         Soil.Texture, Moisture.Regime, Water.Application, Ag.DI,
         int_Land_Moisture, int_Land_WaterApp, int_Land_WaterType,
         int_Moisture_WaterApp, int_Moisture_WaterType, int_WaterApp_WaterType,
         int_Land_Moisture_WaterApp, int_Land_Moisture_WaterType,
         int_Land_WaterApp_WaterType, int_Moisture_WaterApp_WaterType,
         int_Land_Moisture_WaterApp_WaterType)
pH.p2 <- ggplot(long_data, aes(x = Value, y = Pore.Water.pH, fill = Value)) +
  geom_boxplot() +
  facet_wrap(~ Variable, scales = "free_x") +  # Use facetting by Variable
  labs(title = "Effect of Variables and Their Interactions on Pore Water pH",
```

```
      x = "",
      y = "Pore Water pH") +
  theme_minimal() +
  theme(axis.text.x = element_text(angle = 45, hjust = 1, size = 8),  # Adjust x-axis text size
        axis.text.y = element_text(size = 10),                         # Adjust y-axis text size
        axis.title.x = element_text(size = 14),                        # Adjust x-axis title size
        axis.title.y = element_text(size = 14),                        # Adjust y-axis title size
        plot.title = element_text(size = 16))

print(pH.p2)
#install.packages("tidyverse")
library(tidyverse)
long_data <- GLMM.Table %>%
  gather(key = "Variable", value = "Value",Soil.Texture, Moisture.Regime, Water.Application, Ag.DI)
ggplot(long_data, aes(x = Value, y = ARQ, fill = Value)) +
  geom_boxplot() +
  facet_wrap(~ Variable, scales = "free_x") +  # Use facetting by Variable
  labs(title = "Effect of Variables on ARQ",
      x = "",
      y = "ARQ") +
  theme_minimal()

# Create interaction variables
GLMM.Table$int_Land_Moisture <- interaction(GLMM.Table$Soil.Texture, GLMM.Table$Moisture.Regime, drop = TRUE, sep = " & ")
GLMM.Table$int_Land_WaterApp <- interaction(GLMM.Table$Soil.Texture, GLMM.Table$Water.Application, drop = TRUE, sep = " & ")
```

```
GLMM.Table$int_Land_WaterType <- interaction(GLMM.Table$Soil.Texture,
GLMM.Table$Ag.DI, drop = TRUE, sep = " & ")
GLMM.Table$int_Moisture_WaterApp <- interaction(GLMM.Table$Moisture.Regime,
GLMM.Table$Water.Application, drop = TRUE, sep = " & ")
GLMM.Table$int_Moisture_WaterType <- interaction(GLMM.Table$Moisture.Regime,
GLMM.Table$Ag.DI, drop = TRUE, sep = " & ")
GLMM.Table$int_WaterApp_WaterType <- interaction(GLMM.Table$Water.Application,
GLMM.Table$Ag.DI, drop = TRUE, sep = " & ")

# Three-way interactions
GLMM.Table$int_Land_Moisture_WaterApp <- interaction(GLMM.Table$Soil.Texture,
GLMM.Table$Moisture.Regime, GLMM.Table$Water.Application, drop = TRUE, sep = "
& ")
GLMM.Table$int_Land_Moisture_WaterType <- interaction(GLMM.Table$Soil.Texture,
GLMM.Table$Moisture.Regime, GLMM.Table$Ag.DI, drop = TRUE, sep = " & ")
GLMM.Table$int_Land_WaterApp_WaterType <- interaction(GLMM.Table$Soil.Texture,
GLMM.Table$Water.Application, GLMM.Table$Ag.DI, drop = TRUE, sep = " & ")
GLMM.Table$int_Moisture_WaterApp_WaterType <-
interaction(GLMM.Table$Moisture.Regime, GLMM.Table$Water.Application,
GLMM.Table$Ag.DI, drop = TRUE, sep = " & ")

# Four-way interaction
GLMM.Table$int_Land_Moisture_WaterApp_WaterType <-
interaction(GLMM.Table$Soil.Texture, GLMM.Table$Moisture.Regime,
GLMM.Table$Water.Application, GLMM.Table$Ag.DI, drop = TRUE, sep = " & ")

# Gather into long format
long_data <- GLMM.Table %>%
  gather(key = "Variable", value = "Value",
         Soil.Texture, Moisture.Regime, Water.Application, Ag.DI,
         int_Land_Moisture, int_Land_WaterApp, int_Land_WaterType,
         int_Moisture_WaterApp, int_Moisture_WaterType, int_WaterApp_WaterType,
```

```
          int_Land_Moisture_WaterApp, int_Land_Moisture_WaterType,
          int_Land_WaterApp_WaterType, int_Moisture_WaterApp_WaterType,
          int_Land_Moisture_WaterApp_WaterType)
ARQ.p2 <- ggplot(long_data, aes(x = Value, y = ARQ, fill = Value)) +
  geom_boxplot() +
  facet_wrap(~ Variable, scales = "free_x") +  # Use facetting by Variable
  labs(title = "Effect of Variables and Their Interactions on ARQ",
       x = "",
       y = "ARQ") +
  theme_minimal() +
  theme(axis.text.x = element_text(angle = 45, hjust = 1, size = 8),  # Adjust x-axis text size
        axis.text.y = element_text(size = 10),                        # Adjust y-axis text size
        axis.title.x = element_text(size = 14),                       # Adjust x-axis title size
        axis.title.y = element_text(size = 14),                       # Adjust y-axis title size
        plot.title = element_text(size = 16))

print(ARQ.p2)
```